LI, TIANJIAO. Ph.D. Role of Adipose Triglyceride Lipase in Hepatic Lipid Homeostasis and Lipotoxicity in Alcohol-Related Liver Disease. (2022)
Directed by Dr. Zhanxiang Zhou. 123 pp.

Alcohol-related liver disease (ALD) is a significant contributor to the liver disease burden worldwide. Hepatic steatosis is the earliest and most common clinical manifestation of ALD and is characterized by excessive triglyceride (TG)-enriched lipid droplet (LD) accumulation in the liver. Studies have shown that the activity of adipose triglyceride lipase (ATGL), the rate limiting enzyme of TG hydrolysis, is negatively related to hepatic LD content; however, it is unclear whether ATGL plays a role in the pathogenesis of ALD.

While a previous study reported that patients with non-alcoholic fatty liver disease showed reduced hepatic ATGL expression, it remains unclear how alcohol affects hepatic ATGL expression and what role ATGL plays in hepatic lipid metabolism in ALD. Although much effort has been made, the role of ATGL in hepatic lipotoxicity and inflammation has not been established. Therefore, a mouse model with hepatocyte-specific deletion of ATGL was generated and subjected to chronic alcohol feeding for 8 wk. Data presented in this dissertation suggest that alcohol induces hepatic ATGL expression, accumulation of TGs and free fatty acids (FFAs), and liver injury. Hepatocyte-specific ATGL deletion in mice further exacerbated alcohol-induced hepatic steatosis, inflammation, as well as fibrosis. Moreover, hepatocyte-specific ATGL deletion suppressed TG-enriched very-low-density lipoprotein (VLDL) secretion through impairing long-chain acyl-CoA synthetase 5 (ACSL5)-mediated fatty acid oxidation and subsequent incorporation of FFAs into TGs by diacylglycerol O-acyltransferase 1 (DGAT1). In addition, we found that hepatocyte-specific ATGL deletion aggravated alcohol-induced liver inflammation by upregulating chemokine CXCL1 and cytokine LCN2 and promoting subsequent neutrophil infiltration.

Given the sophisticated structure of the liver and the properties of transmission electron microscope (TEM) in directly visualizing liver morphology under high magnification, we utilized

this unique technique to evaluate the subcellular and functional changes in various cells of the liver of mice. We observed that alcohol intoxication perturbs the normal structure and morphology of mouse hepatocytes, such as reduced number of mitochondria and glycogen storage, LD accumulation, ER dilation and fragmentation, and the accumulation of autolysosomes in the cytoplasm. We further found that hepatocyte ATGL deficiency aggravated alcohol-caused structural and morphological changes in hepatocytes, Kupffer cells, hepatic stellate cells, and cholangiocytes in mice.

Lipotoxicity and translocation of gut-derived endotoxin (lipopolysaccharides, LPS) to the liver have both been reported to be involved in ER stress-mediated hepatic cell death. In the last set of experiments, *in vitro* cell culture studies were conducted using AML12 cells. This study showed that TG/LD accumulation and LPS stimulation synergistically induced cell death, stimulated ER stress, and upregulated CXCL1 and LCN2 expression via IκB-ζ activation in hepatocytes.

Collectively, data presented in this dissertation revealed the molecular mechanisms by which hepatocyte ATGL deficiency exacerbated alcohol-induced hepatic steatosis, hepatocyte death, and liver inflammation in the pathogenesis of ALD, which may advance the development and optimization of innovative diagnostic and therapeutic strategies targeting lipotoxicity for ALD treatment.

ROLE OF ADIPOSE TRIGLYCERIDE LIPASE IN HEPATIC LIPID HOMEOSTASIS AND LIPOTOXICITY IN ALCOHOL-RELATED LIVER DISEASE

by

Tianjiao Li

A Dissertation

Submitted to

the Faculty of The Graduate School at

The University of North Carolina at Greensboro

in Partial Fulfillment

of the Requirements for the Degree

Doctor of Philosophy

Greensboro

2022

Approved by

Dr. Zhanxiang Zhou
Committee Chair

DEDICATION

This dissertation is dedicated to my parents, Lixun Li and Fengying Wang, who have always been loving and supporting me during the challenges of graduate school and life.

APPROVAL PAGE

This dissertation written by Tianjiao Li has been approved by the following committee of the Faculty of The Graduate School at The University of North Carolina at Greensboro.

Committee Chair

Dr. Zhanxiang Zhou

Committee Members

Dr. Wei Zhong

Dr. Steven C. Fordahl

Dr. Keith Erikson

March 2, 2022

Date of Acceptance by Committee

March 15, 2022

Date of Final Oral Examination

ACKNOWLEDGEMENTS

First of all, I would like to say thank you to my parents, who have always been there for me throughout these years, giving me so much love and support, both emotionally and finically. I would also like to say thank you to my fiancé, Brice, for loving me unconditionally, and always comforting me when I was struggling with research and dealing with self-doubt and anxiety, he made this journey easier and my life happier.

I would love to express my gratitude to my mentor Dr. Zhanxiang Zhou, for his support and guidance during the running of this project, and for keeping me accountable and always giving the best of myself. I would also love to say thank you to my committee member Dr. Wei Zhong, for her help with my project and for guiding me through the journey of my publication as first author. I would also love to express my gratitude to my committee member Dr. Keith Erikson and Dr. Steve Fordahl, for their support and reassurance.

I am grateful to have kind and generous colleagues who have offered me hands-on help on the experiments, Dr. Wei Guo, Dr. Haibo Dong, Dr. Ruichao Yue. I would like to say thank you to our research specialist Xinguo Sun for her technical support. I am grateful to have our wonderful business officer Wendy Helton, for providing excellent administrative support and for being a great friend. I would like to expend my gratitude to all the faculty, staff, and my fellow graduate students from the Department of Nutrition, I could not have done this without all of your help and support. I want to especially thank Doreen Larvie for her friendship and support since day one we met.

Last but not least, I am proud and grateful for who I have become today. I would like to let this dissertation and this journey serve as a reminder to myself and to anyone who comes across it that you should always pursue your biggest dream and have faith in yourself that you’re capable of achieving anything you set mind to.

TABLE OF CONTENTS

LIST OF TABLES

LIST OF FIGURES

CHAPTER I: INTRODUCTION

Significance of Research

Alcohol-related liver disease (ALD) is a major contributor to liver disease burden worldwide (Dang et al., 2020). In the United States, mortality from all ALD has risen to 13.1 per 100,000 in men and 5.6 per 100,000 in women in 2017 (Moon et al., 2020). Reported in 2016, ALD has surpassed hepatitis C virus infection, becoming the leading indication for liver transplantation in the US (Cholankeril & Ahmed, 2018). In the US alone, the estimated cost of alcohol use disorder is $166 billion per year (Nelson & Kolls, 2002). Hepatic steatosis (fatty liver disease) is the earliest and most common manifestation in ALD, characterized by excessive lipid droplet (LD) accumulation in hepatocytes (Arumugam et al., 2020). Triglyceride (TG) is the foremost neutral lipid found in LDs in hepatocellular cytoplasm; hence, the imbalance between TG synthesis and lipolysis plays a crucial part in the pathogenesis of hepatic steatosis. Adipose triglyceride lipase (ATGL) is the rate limiting enzyme catalyzing the first step of TG break down (Zimmermann et al., 2004). A few studies have been done to investigate the role of ATGL in non-alcohol-related fatty liver disease (NAFLD) (Fuchs et al., 2022; Jha et al., 2014; Wu et al., 2011); however, how ethanol affects hepatic ATGL expression and how ATGL mediates hepatic steatosis and liver lipotoxicity in ALD remains unclear, which will be determined in **Aim 1** of this project.

Ultrastructure changes of the cells are critical in the onset and the progression of ALD; However, it remains obscure whether hepatic ATGL alters the ultrastructure of the cells in the liver and whether a synergistic effect exists between hepatocyte ATGL and alcohol intoxication, which will be investigated in **Aim 2** of this study.

Previous study from our laboratory demonstrated that alcohol feeding induced accumulation of both LDs and FFAs in the livers of the mice. Historically, saturated FFAs are considered as ‘toxic lipid’ that promotes hepatic lipotoxicity, whereas TGs are recognized as

relatively benign to lipotoxicity. However, emerging evidence suggests that FFAs can reduce/prevent alcohol-induced liver injury by alleviating hepatic steatosis. Hence, **aim 3** of the study is to dissect the role of hepatic accumulation of TGs/LDs and FFAs in inducing hepatocyte death and ER stress. Alcohol-induced gut-derived endotoxins (Lipopolysaccharides, LPS) translocation to the liver promotes hepatic inflammatory responses by inducing chemokine/cytokine expression in ALD. **Aim 4** of the study is to determine whether, and if so how, the accumulation of TGs/LDs and LPS stimulation synergistically induce cell death and chemokine/cytokine expression in hepatocytes.

Our research advances the existing body of knowledge in LD/TG accumulation-induced lipotoxicity and liver inflammation, which will eventually contribute to the development of preventive and therapeutic strategies for the treatment of ALD.

Study Objectives

In **Chapter II**, we will utilize a hepatocyte-specific ATGL deletion mouse model to achieve the following objectives: (1) to determine how alcohol affects hepatic ATGL expression; (2) to investigate the role of hepatic ATGL in lipid homeostasis; (3) to explore the potential mechanisms by which ATGL deletion suppresses hepatic TG-enriched very-low-density lipoprotein (VLDL-TG) lipidation and secretion; (4) to identify the potential cellular signaling pathways that mediate ATGL deficiency-induced hepatic neutrophil infiltration in mice; (5) to describe the effect of ATGL deletion on the development of alcohol-induced liver fibrosis.

In **Chapter III**, we will employ the transmission electron microscope technique to achieve the following objectives: (1) to determine the ultrastructure changes by alcohol and hepatocyte-specific ATGL deletion in hepatocytes, Kupffer cells, bile duct lumens, sinusoids of the liver; (2) To investigate whether a synergistic effect exists between hepatic ATGL and alcohol intoxication in altering ultrastructure of the liver.

In **Chapter IV**, we aim to achieve the following objectives: (1) to dissect the role of LD/TG accumulation and FFA accumulation in inducing ER stress and cell death in hepatocytes; (2) to determine the role of ATGL in OA-induced hepatocellular cytotoxicity; (3) to identify the molecular mechanisms by which intracellular LD/TG accumulation and extracellular LPS stimulation synergistically induce hepatocyte injury and promote inflammatory chemokine/cytokine expression in hepatocytes.

Literature Review

Alcohol-related Liver Disease

Alcohol use disorder is a worldwide problem that represents the third largest risk factor among many types of diseases (Rocco, 2014). Reported in 2017, an increase in mortality from ALD was observed among men and women of almost every age and race in the United States except of non-Hispanic blacks since 2006 (Moon et al., 2020). As the major organ metabolizing alcohol, the liver has long been recognized as the main victim of excessive and prolonged alcohol consumption (Rocco, 2014). Ethanol and its bioactive metabolites, acetaldehyde, fatty acid ethyl esters, aldehyde-protein adducts, are all considered as hepatotoxins, which are associated with a spectrum of liver injuries that are designated as alcohol-related liver disease (ALD) (Crabb et al., 2020). ALD can progress from hepatic steatosis to more advanced phases, including alcoholic hepatitis (AH), alcoholic cirrhosis (AC), and eventually hepatocellular carcinoma (HCC) or even liver failure (Stickel et al., 2017). To date, there is no clear biomarker or unique clinical presentation that can be used for the definitive diagnosis of ALD, especially to distinguish ALD from other types of liver diseases (Crabb et al., 2020; Dang et al., 2020). Except from abstinence and lifestyle intervention, pharmacologic treatment for ALD has not been established. While ALD below the level of cirrhosis is normally reversible upon sobriety, decompensating cirrhosis and hepatocellular carcinoma have a grave prognosis (Stickel et al., 2017). The existing literature suggests significant clinical and economic impacts of ALD; hence,

comprehensive studies are needed to explore the pathogenesis and disease progression of ALD to develop better medical strategies and therapeutic interventions.

The Pathogenesis of ALD

The pathogenesis of ALD is a complex process that involves direct and indirect effects of ethanol and its derivatives on various types of cells in the liver. Hepatocytes are the primary parenchymal cells for ethanol metabolism in the liver. There are two steps in ethanol metabolism. Alcohol dehydrogenase (ADH) is the most catalytically efficient ethanol-metabolizing enzyme that catalyzes ethanol into acetaldehyde, a very reactive and toxic compound. To minimize its toxicity, hepatocytes rapidly metabolize acetaldehyde into acetate in mitochondria by aldehyde dehydrogenase 2 (ALDH2), then acetate is released into circulation (Osna et al., 2017). Aside from ADH, cytochrome P450 2E1 (CYP2E1) and catalase are two other enzymes that also process ethanol-metabolizing capacity. A high level of NADH is generated through this redox reaction process resulting in a reduction of cellular NAD^+/NADH ratio, which induces oxidative stress and cell dysfunction, and exerts detrimental effects on numerous metabolic process, including the development of hepatic steatosis (Mello, Ceni, et al., 2008).

Lipotoxicity in Hepatic Steatosis

According to the “second hit” or “multiple hit” theory, alcohol-induced hepatic lipid accumulation acts as the first hit, which predisposes the liver for a second hit or multiple hits that induce hepatic inflammation and fibrogenesis (Rada et al., 2020; Tsukamoto et al., 2009). Chronic alcohol consumption perturbs hepatic lipid homeostasis through adipose tissue-liver crosstalk (Steiner & Lang, 2017). Briefly, alcohol disturbs the balance between lipogenesis and lipolysis in adipose tissue, which leads to increased FFAs release. The released FFAs are transported into circulation and eventually deposited in non-adipose tissue, including the liver (Wei et al., 2013). It is historically accepted that hepatic lipotoxicity occurs when the liver’s capacity of utilizing, secreting, and storing FAs as TGs is overwhelmed by the massive flux of

FAs from circulation, as well as alcohol-induced increase in FA synthesis and alcohol-inhibited FA oxidation (Gao & Bataller, 2011; Rada et al., 2020). Free fatty acids (FFAs) and other intracellular metabolites, such as diacylglycerol, lysophosphatidylcholine, and ceramides, have long been considered as cytotoxic, playing important roles in hepatocyte cell death in the development of both liver inflammation and liver fibrosis both (Dahlquist et al., 2020; Malhi & Gores, 2008; Mavrelis et al., 1983). While TGs formation are historically considered as relatively benign that poses less liver lipotoxicity by sequestering cytotoxic FFAs, it is unestablished whether or how bulk TGs accumulation modulates downstream cellular signaling pathways to regulate hepatocyte cell death and inflammation (Mashek, 2021).

The Role of Endotoxin in ALD

Gram-negative bacteria-derived lipopolysaccharide (LPS), also known as endotoxin, has been reported to play a critical part in the pathogenesis of ALD (Szabo & Bala, 2010). Human studies have demonstrated that plasma endotoxin levels are significantly elevated in inpatients with ALD compared to healthy subjects (Hanck et al., 1998; Parlesak et al., 2000; Schäfer et al., 2002). Animal studies revealed that plasma endotoxin levels correlate with the severity of liver injury (Jokelainen et al., 2001; Mathurin et al., 2000; Nanji et al., 2001). Under physiological condition, only trace amount of LPS penetrate the intestinal barrier, enter the portal circulation, and then cleared by Kupffer cells (resident macrophages in the liver) by phagocytosis or by hepatocytes via autophagy in the liver (Chen et al., 2014; Rao, 2009). Upon excessive alcohol intoxication, acetaldehyde-mediated disruption of epithelial tight junctions and adherens junctions increases intestinal permeability and eventually leads to intestinal barrier dysfunction (Rao, 2009; Szabo & Bala, 2010). When the endotoxin level overwhelms the clearance capacity of the liver, endotoxin escapes and spills into systemic circulation, which leads to the production of pro-inflammatory cytokines and chemokines.

Chemokines and Cytokines in ALD

Chemokines are small chemotactic proteins (8-13 kDa) initially identified by their ability to release migratory signals and recruit inflammatory cell to infected sites (Saiman & Friedman, 2012). Current evidence suggests that chemokines are associated with the progression of ALD and liver-associated morbidity and mortality in patients with AH (Chang et al., 2015, p.; Poulsen et al., 2021). Hepatocyte is one of the primary sources of chemokines in the liver, which drives immune cell infiltration, cell death, and eventually fibrogenesis (Saiman & Friedman, 2012). C-X-C motif chemokine ligand 1 (CXCL1) is one of the seven members to the CXC chemokine family that acts as chemoattractant for immune cells during infection. (Schumacher et al., 1992). Clinical studies and animal studies have demonstrated that CXCL1 regulates host immune response by recruiting and activating neutrophils to the infected sites (Sawant et al., 2016). Dominguez *et al.* revealed that patients with AH express higher levels of IL-8 family in the liver compared with healthy controls (Dominguez et al., 2009). Chang *et al.* also reported that CXCL1 is associated with liver neutrophil recruitment and liver injury in mice fed with high-fat diet plus alcohol binge (Chang et al., 2015). As the rapid advances in chemokine biology, researchers have identified chemokine receptors on non-immune cells as well, which expands the functions of chemokines to non-inflammatory aspects of injury, including apoptotic cell death (Saiman & Friedman, 2012). However, the molecular basis of how hepatic TGs accumulation and CXCL1 synergistically orchestrate cell death in the liver is not well understand.

Cytokines are low-molecular weight peptides produced by different types of cells in the liver that mediate cellular communication (McClain et al., 1999). Various pro-inflammatory cytokines, such as necrosis factor-alfa (TNF-α) and IFN-γ, and anti-inflammatory cytokines, including interleukin 10 and interleukin 6, have been reported to be involved in alcoholic liver injury (An et al., 2012; Kawaratani et al., 2013). Lipocalin 2 (LCN2) is an acute phase protein expressed upon stress such as bacterial infection to recruit and activate immune cells to inhibit bacterial growth by limiting siderophore-mediated bacterial iron acquisition (Wieser et al., 2016).

Although LCN2 demonstrates a protective function against acute and chronic liver injury in many models, including MCD diet-induced NAFLD model (Asimakopoulou et al., 2014, p. 2; Borkham-Kamphorst et al., 2013; Xu et al., 2015), Wieser *et al.* revealed that elevated systemic LCN2 greatly promotes the development of ALD by governing neutrophil infiltration (Wieser et al., 2016). It is demonstrated that the liver is the primary source of systemic LCN2 (Xu et al., 2015). Studies have reported that hepatocyte is the primary cell type that produces LCN2 in the liver upon ethanol exposure (Cai et al., 2016; Zhong et al., 2020). Hence, further research is needed to elucidate the pro-inflammatory function of LCN2 in ethanol-induced liver injury, and the cellular signaling pathways by which LCN2 mediates neutrophil infiltration.

Adipose Triglyceride Lipase (ATGL)

Hepatic steatosis is one of the earliest events in ALD, characterized by the accumulation of lipid droplets (LDs) in hepatocellular cytoplasm (Schulze & Ding, 2019). LDs are spherical cellular organelles that comprise a hydrophobic core of neutral lipid and an amphipathic phospholipid monolayer (Li et al., 2021). While previously assumed inert storage depots for neutral lipid, growing evidence is suggesting that LDs are highly dynamic organelles that are extremely responsive to cellular environment. LDs have a wide range of impacts on cell metabolism, signaling and function (Gluchowski et al., 2017; Mashek, 2021; Nguyen & Olzmann, 2017). Upon times of nutrition deprivation or enhanced energy demand, stored TG in LDs is hydrolyzed by a group of hormonally regulated hydrolytic enzymes to generate FAs and glycerol for energy generation (Li et al., 2021). In 2004, ATGL was discovered as the rate-limiting enzyme that catalyze the first step of TG hydrolysis by three independent research teams (Jenkins et al., 2004; Villena et al., 2004; Zimmermann et al., 2004).

The Structure-function Relationship of ATGL

The gene of human ATGL is located on chromosome 11p15.5 and includes 10 exons that encodes a 504-amino acid protein (NP_065109). The murine gene of ATGL encodes a 486-amino acid protein (BAC27476) with a calculated molecular mass of 54

kDa, which shares an 86.8% sequence identity with its human orthologue. Sequence analysis revealed that a patatin-like phospholipase domain between Ile 10-Leu 178 is located on the N-terminal half of the protein (Fig.1.1), which groups ATGL into the patatin-like phospholipase domain-containing family (PNPLA). Mutation studies and cell culture studies have confirmed that Ser47 and Asp 166, within the patatin-like containing domain, constitute the putative catalytic dyad in ATGL (Fig.1.1). ATGL is synthesized in the endoplasmic reticulum (ER) and directly delivered to LDs by the Golgi-ER transport protein complex GBF1 (Golgi-specific brefeldin A resistance factor 1)-Arf1 (ADP-ribosylation factor 1)-COPI (coat protein complex I). It has been reported that ATGL traffics from ER to LDs through membrane bridges that are controlled by the Arf1/COPI machinery. ATGL is localized in cytoplasm, on LDs, and on plasma membranes.

The C-terminal region of ATGL, harboring the putative hydrophobic lipid-binding stretch (Val315 to Ile364) and two potential AMPK phosphorylation sites (Ser 404 and Ser 427) has been demonstrated to be responsible for the localization of the enzyme around LDs. (Li et al., 2021)

Figure 1.1 Schematic Representation of Predicted Structure and Domain Organizations of Human ATGL

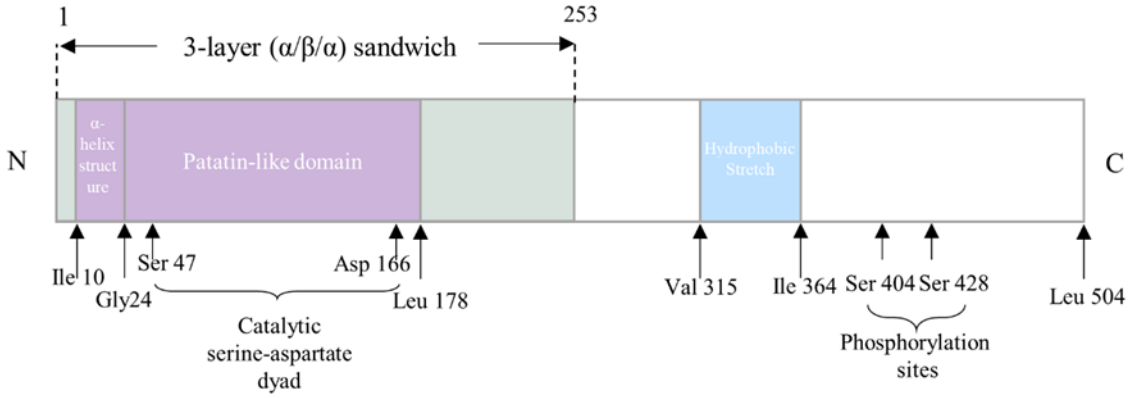

Note. Green: 3-layer (α/β/α) sandwich domain (residue 1-253). Purple: Patatin-like domain (residue 10-178), including the α-helix structure (residue 10-24) and the catalytic serine-

aspartate dyad (Ser 47 and Asp 166), which are essential in TG substrate binding and TG hydrolysis, respectively. Blue: putative hydrophobic lipid-binding stretch (residue 315-364), and two potential AMPK phosphorylation sites (Ser 404 and Ser 428), which are responsible for the localization of ATGL on LDs.

Regulatory Mechanisms of ATGL

The central role of ATGL in lipolysis makes its regulation crucial for maintaining a defined balance between lipid storage and breakdown. The expression and activity of ATGL are regulated at multiple levels, such as transcriptional and posttranslational regulations. The factors involved in transcriptional regulation of ATGL are summarized in Fig. 1.2 As a hormone-sensitive lipase, ATGL is activated by β-adrenergic activation (Schott et al., 2017). AMP-activated protein kinase (AMPK) could phosphorylate ATGL at Ser406, therefore active its enzymatic activity (Ahmadian et al., 2011). Insulin is a classic inhibitor of lipolysis. Studies revealed that insulin suppresses ATGL expression through upregulation of sirtuin 1 (SIRT1), which restrains the nuclear localization of forkhead box protein O1 (FoxO1) through deacetylation (Chakrabarti et al., 2011, p. 1). Insulin also inhibits ATGL expression through early growth response 1 (Egr1)- mechanistic target of rapamycin complex 1 (mTORC1) cell signaling pathway (Chakrabarti et al., 2010, 2013). The physical interaction between the master adipogenic transcriptional regulator peroxisome proliferator-activated receptor gamma (PPARγ) and Insulin responsive transcription factor specificity protein 1 (Sp1) is necessary for ATGL transactivation in mature adipocyte, while Sp1 alone suppresses ATGL expression in preadipocytes (Kim et al., 2006; Roy et al., 2017). Besides, tumor necrosis factor-alpha (TNF-α) is reported to stimulate lipolysis, partially through degrading ATGL's inhibitor G0/G1 switch gene 2 (G0S2) (Kralisch et al., 2005; Yang et al., 2011).

Figure 1.2 Simplified Overview of Regulation of ATGL Expression

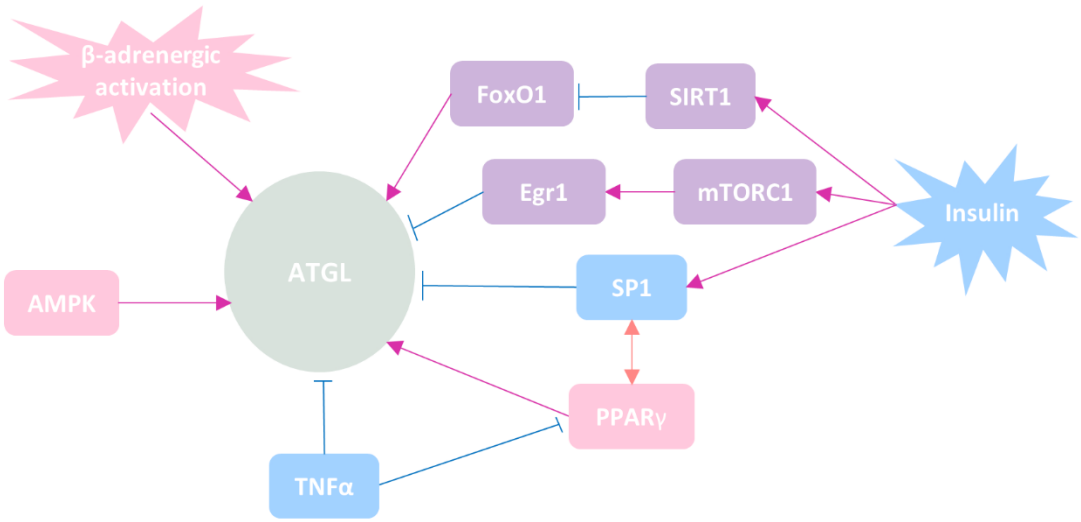

Note. ATGL is demonstrated to be activated by β-adrenergic activation. AMPK phosphorylates ATGL at Ser 406 therefore activates its enzymatic activities. Insulin inhibits ATGL expression through upregulating SIRT1, which restrains the nuclear localization of FoxO1 by deacetylating. Insulin also inhibits ATGL expression through Egr1-mTORC1 signaling pathway. Sp1 has an inhibitory control over ATGL in preadipocytes, while the functional interaction of PPARγ and Sp1 transactivates ATGL in mature adipocytes. TNF-α down-regulates ATGL mRNA level but does not alter its protein level.

Fig. 1.3 illustrates the regulation of ATGL at post-translational levels with a focus on the liver. Comparative gene identification-58 (CGI-58) is widely admitted as the primary co-activator of ATGL, which increase the TG hydrolase activity of ATGK by up to 20-fold (Lass et al., 2006). G0S2 is known as an endogenous inhibitor of ATGL even when CGI-58 is present (Lu et al., 2010; Schweiger et al., 2012). Perilipin family membranes are actively involved in regulating ATGL activity in a tissue-specific manner (Brasaemle, 2007). Perilipin 2 (Pln2) is the most expressed family member in the liver, promoting lipolysis through chaperone-mediated autophagy. Briefly, heat shock protein HSPA8/hsc70 mediates the degradation of Plin2 and Plin3 in lysosome and causes increased exposure of LDs surface to ATGL, thereby initiating the

first step of TG hydrolysis (Kaushik & Cuervo, 2015; Schweiger & Zechner, 2015). There are other protein interaction partners of ATGL, including Hypoxia-inducible lipid droplet-associated protein (HILPDA), E3 ubiquitin ligase COP1 (also called RFWD2), DEFA like effector C (CIDEC; also known as fat-specific protein 27, FSP27), pigment epithelium-derived factor (PEDF; also known as seeping family F member 1, SERPINF1) (Borg et al., 2011; Ghosh et al., 2016; Gimm et al., 2010, p.; Grahn et al., 2014; Niyogi et al., 2019).

Figure 1.3 Regulation of ATGL at Post Translational Level in the Liver

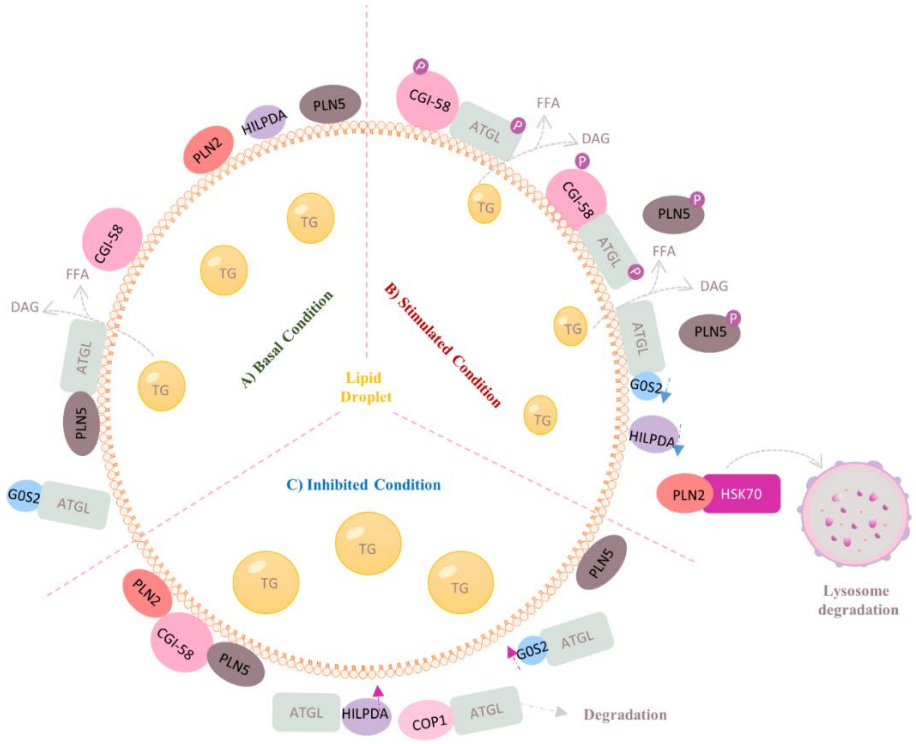

Note. A). In basal condition: LDs are coated with PLN2 and PLN5, which restrain the access of ATGL to the stored TGs. PLN5 also directly binds to ATGL, competing against CGI-58 for ATGL interaction. B). In stimulated condition, PKA-mediated phosphorylation of PLN5 results to the release of ATGL and subsequently the co-activation by CGI-58. PLN2 is degraded through chaperone-mediated autophagy, which exposes the surface of LDs to ATGL, therefore stimulating lipolysis. C). In inhibited condition: ATGL inhibitors HILPDA and G0S2 are

upregulated, which enhances the inhibitory control over ATGL. E3 ubiquitin ligase COP1-mediated proteasomal degradation reduces the protein levels of ATGL, hence inhibits lipolysis.

ATGL in Hepatic Lipid Metabolism

Emerging evidence suggest that the physiological function of ATGL is not restricted to adipose tissue but is also crucially important in many non-adipose tissues, such as the liver. ATGL is expressed in hepatocytes, hepatic stellate cells (HSC), and macrophages (Kupffer cells) (Eichmann et al., 2015, p. 58; Mello, Nakatsuka, et al., 2008; Zimmermann et al., 2004). Neutral lipid storage disease (NLSD) with myopathy (NLSD-M) is a rare autosomal recessive disorder caused by ATGL mutations. NLSD-M is characterized by excessive, non-lysosomal accumulation of TG-rich cytosolic LDs in non-adipocytes, including hepatocytes (Missaglia et al., 2019; Zhou et al., 2016). Mutations in ATGL lead to either its inactivation or compromised lipid droplet binding ability (Schweiger et al., 2008). Studies investigating the clinical, molecular, and cellular phenotypes in these patients illustrate an essential role of ATGL in maintaining systemic lipid homeostasis and multi-organ functions, including the liver (Fischer et al., 2007; Tavian et al., 2012). Liver damage was observed in half of NLSD-M patients, manifesting as mild to severe hepatic steatosis and elevated blood aminotransferase levels, including alanine aminotransferase (ALT) and aspartate aminotransferase (AST) (Missaglia et al., 2019; Pegoraro et al., 2020; Yavuz et al., 2020). The liver biopsy results of a 63-year-old female patient with NLSD-M revealed significant hepatic cytosolic lipid deposition, indicating impaired hepatic TG turnover (Schweiger et al., 2008). A 33-year-old Turkish patient with NLSD-M presented Grade 2 macrovesicular steatosis and hepatomegaly, which contributed to the unfortunate death of the patient (Yavuz et al., 2020). Studies using transgenic animal models showed that ATGL expression is inversely associated with hepatic LDs size and TG content (Reid et al., 2008; Turpin et al., 2011; Wu et al., 2011). In accordance with LDs accumulation and elevated hepatic TG contents, TG hydrolase activities in the livers of ATGL deficiency mice were dramatically decreased compared to their controls (Haemmerle et al., 2006; Ong et al., 2011; Reid et al.,

2008). In contrast, studies have shown that hepatic ATGL expression is positively correlated with hepatic FA β-oxidation (Ong et al., 2011; Reid et al., 2008). While decreased TG hydrolase activity accounts for the LDs accumulation in the livers of hepatic ATGL deficiency mice, the mechanisms by which ATGL mediate FA oxidation remains unclear. It is widely accepted that FA is a strong endogenous ligand that activates peroxisome proliferator activated receptor alpha (PPARα), a master regulator in FA β-oxidation (Chakravarthy et al., 2009; Pawlak et al., 2015). Given the fact that ATGL promotes the production of TG-derived FAs, it is assumed that ATGL might affect PPARα expression therefore influence its downstream target genes that are involved in FA β-oxidation. Indeed, hepatic PPARα expression is remarkably downregulated in ATGL deficiency mice (Jha et al., 2014; Ong et al., 2011). *Wu et al.* reported that PPARα agonist fenofibrate failed to normalize high-fat diet-induced elevated liver TG content in ATGL shRNA-treated mice, suggesting that ATGL regulates PPARα through a ligand-independent manner (Wu et al., 2011). Conversely, *Jha et al.* reported that fenofibrate supplementation completely normalized methionine-choline-deficient (MCD)-induced steatosis in mice (Jha et al., 2014). The discrepancies of how ATGL-deficient mice response to fenofibrate supplementation could be due to the various doses of fenofibrate, fasting status while mice sacrificed, as well as the different mechanisms underlying hepatic steatosis in two animal models. Future research is needed to further elucidate the molecular mechanisms underlying ATGL-mediated hepatic FA β-oxidation.

Inhibition of ATGL by Atglistatin

Atglistatin is a synthetic inhibitor of ATGL that selectively inhibits the activity of ATGL in a competitive manner both in vitro and in vivo (Mayer et al., 2013). Mayer et al. reported that short-term oral gavage of Atglistatin to mice markedly reduced plasma TG and lipolytic parameters FA and glycerol without inducing TG accumulation in all tissues investigated except liver. However, it did not significantly affect blood glucose, total cholesterol, ketone bodies, and insulin levels. Atglistatin distributes differently among various tissues with the highest concentration in the liver,

followed by white and brown adipose tissues, which might explain TG accumulation in the liver after administration of Atglistatin. However, Atglistatin failed to inhibit neither ATGL activity nor FAs release in human adipocyte (Mayer et al., 2013).

Role of ATGL in Hepatic Inflammation

Lipotoxicity occurs when excess lipids accumulate in the liver, which may lead to hepatic inflammation. It is clinically important to investigate the role of ATGL in the pathogenesis of hepatic inflammation, which is one of the most important characteristics in both non-alcoholic fatty liver disease (NAFLD) and ALD (Johnston et al., 2020). *Jha et al.* reported that ATGL KO mice fed with MCD diet developed more severe inflammation in the liver compared to their WT counterparts, as evidenced by increased expression of inflammatory markers, such as TNF-α, inducible nitric oxide synthase (iNOS), monocyte chemotactic protein-1 (MCP-1), and interleukin-1beta (IL-1β), as well as increased infiltration of mononuclear inflammatory cells in the liver. For the LPS model, mice were intraperitoneally injected with a single dose of LPS for 12 h at non-fasted state. Compared with WT mice, ATGL deficiency mice exhibited marked hepatic inflammation, as indicated by the significant upregulation of TNF-α, iNOS, MCP-1, and IL-6, along with elevated serum levels of TNF-α and IL-6. They further demonstrated that the anti-inflammatory effect of ATGL in the liver was partially achieved through PPARα signaling pathway (Jha et al., 2014). Blood ALT levels have been used as a surrogate marker for liver injuries (Pearce et al., 2013). *Wu et al.* reported that ATGL-KO mice had higher plasma ALT levels and ALT/AST ratio but no significant differences in hepatic macrophage infiltration compared with WT controls (Wu et al., 2011). It is worth noting that the absence of ATGL protected mice from tunicamycin-induced acute hepatic ER stress (Fuchs et al., 2012).

Given the current evidence, ATGL seems to play a protective role against hepatic inflammation in steatohepatitis. More studies using hepatocyte-specific ATGL knockout animal models are needed to further elucidate the clinical relevance of ATGL as a therapeutic target in the progression of metabolic liver diseases.

CHAPTER II: HEPATOCYTE-SPECIFIC DELETION OF ATGL EXACERBATES HEPATIC STEATOSIS, LIVER INFLAMMATION, AND FIBROSIS IN MOUSE MODEL OF ALD

Abstract

Hepatic steatosis is the earliest clinical manifestation in the progression of alcohol-related liver disease (ALD) and is characterized by excessive triglyceride (TG)-enriched lipid droplet accumulation in hepatocytes. Adipose triglyceride lipase (ATGL), the rate limiting enzyme of TG hydrolysis, has been reported to be down-regulated in patients with non-alcoholic fatty liver disease (NAFLD) and play critical roles in regulating hepatic TG content, LD accumulation, and hepatic inflammation. However, it remains unclear how alcohol affects hepatic ATGL expression. Although earlier evidence shows that chronic alcohol feeding resulted in hepatic accumulation of both TGs and free fatty acids (FFAs), it is still under debate whether the accumulated TGs or/and FFAs play a role in inducing hepatic lipotoxicity, and how ATGL regulates hepatic LDs and free fatty acid (FFAs) metabolism in ALD. In this study, we generated a mouse model of hepatocyte-specific ATGL deletion to address the above questions. We found that hepatic ATGL was upregulated by alcohol exposure, along with TG accumulation/LD expansion, FFA accumulation, and liver injury, which were further exacerbated by hepatocyte-specific ATGL deletion. Next, we demonstrated that hepatocyte-specific ATGL deletion partially reduced hepatic fatty acid oxidation and TG synthesis and suppressed VLDL-TG secretion. Moreover, we speculated that ATGL deficiency suppressed VLDL-TG secretion through impairing ACSL5-mediated fatty acid oxidation and their subsequent incorporation into TGs by DGAT1. In addition, hepatocyte-specific ATGL deletion aggravated alcohol-induced liver injury and inflammation by upregulating chemokine CXCL1 and cytokine LCN2 and subsequent neutrophil infiltration in the liver. Moreover, CHOP-related hepatocyte death may be associated with ATGL deficiency-enhanced hepatic inflammation. Last, we demonstrated that alcohol-

induced hepatic fibrosis was exacerbated by hepatocyte-specific deletion of ATGL. Taken together, these data suggest that hepatocyte-specific ATGL deletion exacerbates alcohol-induced hepatic steatosis, inflammation, and fibrogenesis in the mouse model of ALD.

Introduction

Alcohol misuse is the 7th leading risk factor for both deaths and disability-adjusted life-years worldwide (Griswold et al., 2018). Alcohol-related liver disease (ALD) has been reported to be a major contributor to the decreased life expectancy of Americans in 2017 (Moon et al., 2020). The overall weighted ALD prevalence has been stable since 2001-2002 to 2015-2016 at 8.8% and 8.1%, respectively (Dang et al., 2020). ALD now has overpassed HCV to become the leading indication for liver transplantation in the US (Dang et al., 2020). In 2015, healthcare cost for all-cause cirrhosis was $9.5 billion dollars in the US, 53% of which was associated with ALD (Mellinger et al., 2018). To date, there is no FDA-approved targeted therapy for ALD. The high morbidity and mortality, as well as economic burden of ALD emphasize the importance of better understanding the pathogenesis of ALD for the development of preventive and therapeutic pharmacological strategies.

Hepatic steatosis (fatty liver disease) is the earliest manifestation to chronic alcohol drinking in the progression of ALD and is characterized by triglyceride accumulation in hepatocytes (Donohue, 2007; Osna et al., 2017). The pathogenesis of ALD is a complex process orchestrated by a closely regulated network of cell signaling pathways. The ‘second hit hypothesis’ is generally recognized by many researchers where steatosis is considered as the first hit. Steatosis then sensitizes the liver to be susceptible to a second hit such as endotoxins, chemokine and cytokine production, mitochondrial dysfunction, and oxidative stress, which in turn leads to alcohol-related steatohepatitis (ASH) and/or fibrosis (Donohue, 2007). Alcohol consumption increases the levels of hepatic free fatty acids (FFAs) and subsequent TG formation. Accumulation of excessive lipids in non-adipose tissues leads to cell dysfunction and

cell death, a phenomenon referred to as lipotoxicity (Listenberger et al., 2003). There are three mechanisms involved in the elevation of FFAs in hepatic steatosis. First, ethanol and acetaldehyde oxidations generate a high level of NADH therefore reduce the cellular NAD^+/NADH ratio, which perturbs the cellular redox potential resulting in enhanced lipogenesis. Second, ethanol disrupts lipid homeostasis leading to increased TG break down in adipose tissues, which causes enhanced FFAs influx into the liver (Kang et al., 2007). Third, ethanol and acetaldehyde decelerate FFAs break down in the liver by damaging mitochondrial β-oxidation, as well as lysosome degradation by autophagy (Kharbanda et al., 1995, 1996; Zhong et al., 2014). Accumulation of saturated FFAs has been reported to induce apoptotic cell death in various types of cells, whereas unsaturated FFAs effectively rescued saturated FFAs-induced lipoapoptosis (Cnop et al., 2001; de Vries et al., 1997; Listenberger et al., 2001; Maedler et al., 2001). *Listenberger et al.* proposed that unsaturated FFAs are less toxic due to their higher ability to be incorporated into TGs compared to saturated FFAs, suggesting that hepatic TG formation upon FFAs overload is an initial protective cellular mechanism against FFAs-induced cytotoxicity, and therefore promoting cell viability (Listenberger et al., 2003).

In hepatic steatosis, accumulated TGs are deposited into lipid droplet (LD), a spherical cellular organelle that comprises a hydrophobic core of neutral lipid and an amphipathic phospholipid monolayer (Olzmann & Carvalho, 2019). While LDs are historically considered as inert organelles, recent evidence suggests that cellular LD and subsequent LD-derived metabolites play critical roles in the metabolic state of cell (Mashek, 2021; Schulze & Ding, 2019). Among all the lipases that contribute to hepatic LD catabolism-a process also known as lipolysis where TG is broken down into glycerol and FFAs-adipose triglyceride lipase (ATGL) has drawn the most attention. Patients with neutral lipid storage disease with myopathy (NLSD-M), a rare autosomal recessive disorder caused by ATGL mutations, develop excessive, non-lysosomal accumulation of TG-enriched cytosolic LDs in non-adipocytes, including hepatocytes (Missaglia et al., 2019). Liver damage is observed in half of NLSD-M patients, manifesting as

mild to severe hepatic steatosis and elevated blood aminotransferase levels, including alanine aminotransferase (ALT) and aspartate aminotransferase (AST) (Li et al., 2021). Liver-specific deletion of ATGL leads to increased hepatic TG content and LD accumulation but reduced fatty acid β-oxidation, while hepatic overexpression of ATGL attenuates hepatic steatosis and increases fatty acid oxidation (Ong et al., 2011; Reid et al., 2008; Wu et al., 2011). Given the fact that ATGL catalyzes the generation of FFAs during TG lipolysis, several studies have been conducted to investigate the role of ATGL in hepatic lipotoxicity and liver inflammation and the results are contradictory. *Jha et al.* demonstrated that ATGL ablation causes severe inflammation in the livers of mice fed with methionine-choline deficient (MCD) diet, a classical dietary model of non-alcohol associated steatohepatitis (NASH), as well as in mice challenged with endotoxins (Jha et al., 2014). *Wu et al.* reported that liver-specific deletion of ATGL leads to liver injury as shown by elevated plasma ALT levels and ALT/AST ratio (Wu et al., 2011). However, *Fuchs at el.* concluded that liver-specific inhibition of ATGL decelerates disease progression of dietary-induced nonalcoholic fatty liver disease (NAFLD) (Fuchs et al., 2022). Of note, the same research group has previously reported that global ATGL ablation protects mice from acute hepatic ER stress (Fuchs et al., 2012). Therefore, further studies are warranted to investigate the role of ATGL in hepatic steatosis, cell death, liver inflammation, and fibrosis, especially under stress circumstance such as alcohol exposure.

Previous study from our lab shows that chronic alcohol feeding induces both LD and FFA accumulation in the livers of mice (Guo et al., 2021). However, it is still obscure that whether it is accumulated hepatic LDs or FFAs that induce the lipotoxicity in ALD. Although an earlier study reported that patients with NAFLD show reduced hepatic ATGL expression (Kato et al., 2008), it is still unclear how alcohol affects hepatic ATGL expression, as well as how ATGL affects hepatic LD and FFA metabolism in ALD. Here, we demonstrate that hepatic ATGL is increased by chronic alcohol exposure and hepatocyte-specific deletion of ATGL exacerbates alcohol-induced hepatic steatosis by suppressing TG-enriched very low-density

lipoprotein (VLDL-TG) secretion and decreasing fatty acid oxidation. Increased hepatic steatosis due to ATGL deletion in hepatocytes aggravates alcohol-induced hepatic cell death, inflammation, and fibrosis in our mouse model.

Materials and Methods

Mice

C57BL/6J wild-type (WT), ATGL floxed mice ($ATGL^{flox/flox}$, stock no. 024218) and albumin-Cre mice (Alb-Cre, stock no. 003574) were purchased from the Jackson Laboratory (Bar Harbor, ME). The breeding strategy for the generation of hepatocyte-specific ATGL knockout mice is shown in Fig. 2.1 $ATGL^{flox/flox}$ mice were crossed bred with Alb-Cre mice to generate hepatocyte-specific ATGL knockout ($ATGL^{\triangle hep}$) mice. Mice were handled and all experiments were performed in accordance with the protocol approved by the North Carolina Research Campus Institutional Animal Care and Use Committee.

Figure 2.1 Breeding Strategy for the Generation of Hepatocyte-specific ATGL Knockout mice (ATGL$^{\triangle hep}$)

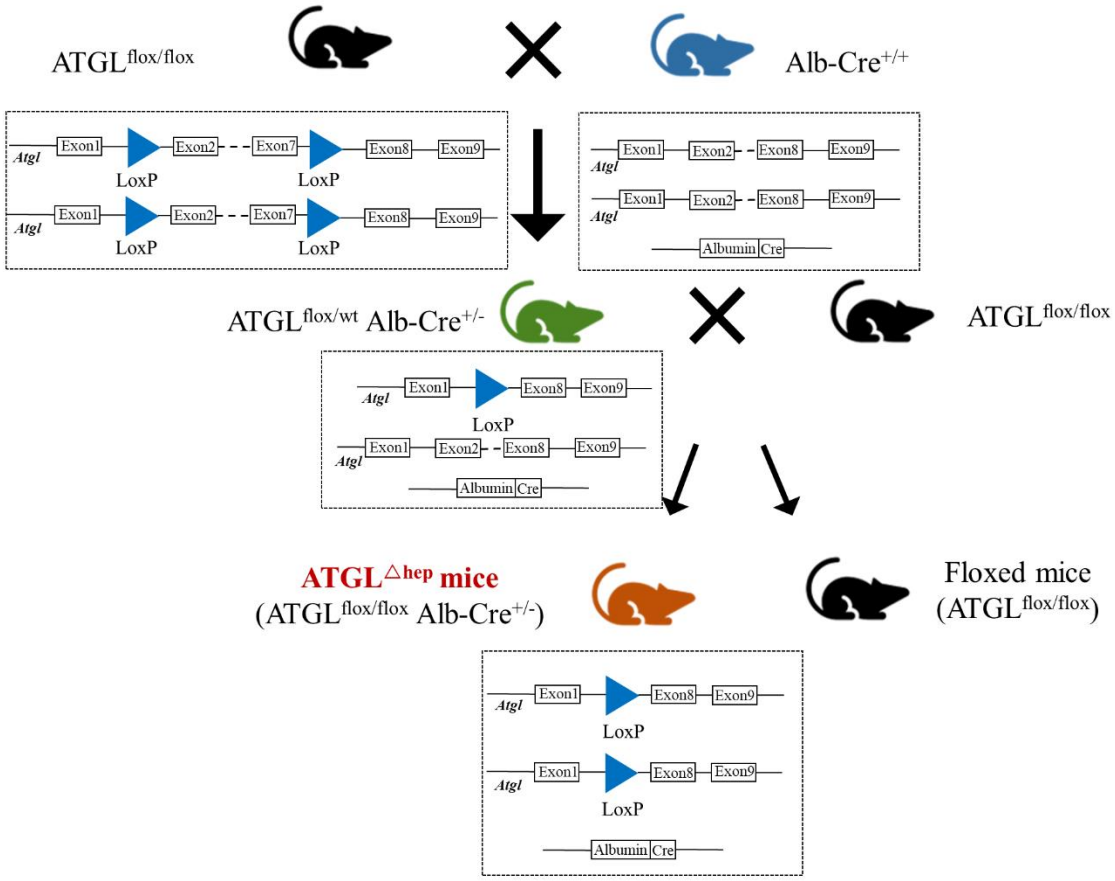

Note. Homozygous ATGL floxed mice (ATGL$^{flox/flox}$) were cross bred with Alb-Cre$^{+/+}$ mice. Offspring carrying floxed ATGL allele and Alb-Cre allele were crossed back with ATGL$^{flox/flox}$ mice. This led to the generation of ATGL$^{\triangle hep}$ mice, which harbors homozygous ATGL floxed alleles and Alb-Cre recombinase. Their littermates carrying homozygous floxed ATGL alleles, but no Alb-Cre recombinase were designated as wild type (ATGL$^{flox/flox}$) mice, which were used as controls in the study.

Chronic Alcohol Feeding and Treatment

Mice were maintained on a 12h light/ 12h dark cycle. There are two sets of mice with alcohol feeding. First, to investigate how alcohol affects hepatic ATGL expression, C57BL/6J male mice at 12 weeks old were randomly subjected to either an ethanol-containing Lieber-

DeCarli liquid diet (alcohol-fed, AF; n=5) or an isocaloric control (pair-fed, PF; n=5) liquid diet for 8 weeks as previously described (29). Second, to investigate the role of ATGL in ALD, male ATGL□hep mice at 12 weeks old were randomly subjected to AF or PF liquid diet for 8 weeks as previously described (29). Littermates of Alb-Cre negative ATGLflox/flox (WT) mice were used as controls. Briefly, ethanol content (%, w/v) in alcohol diet was gradually increased from 4.00%, to 4.14%, 4.28%, and 4.42% every 2 weeks. The AF mice were fed ad libitum, while PF mice were fed with the control diet as the same amount consumed by AF mice in the previous day. All ingredients used in the liquid diets were obtained from Dyets (Bethlehem, PA) except for ethanol (Sigma-Aldrich, St Louis, MO). At the end of 8 weeks of feeding, mice were anesthetized with inhalational isoflurane. Livers, epididymal white adipose tissues, blood of the mice were collected and stored at -80°C for future use.

Western Blot

Whole protein lysates from the mouse liver were extracted using T-PER tissue extraction reagent (Thermo Scientific) supplemented with protease and phosphatase inhibitors (Sigma-Aldrich, St. Louis, MO). Aliquots containing 30 mg of proteins were subjected to sodium dodecyl sulfate-polyacrylamide gel (8-15%) electrophoresis, transblotted onto polyvinylidene difluoride membranes (Bio-Rad, Hercules, CA), blocked with 5% nonfat dry milk in phosphate-buffered saline solution containing 1% Tween-20, and then probed overnight with the following antibodies, including anti-DGAT1, antiApoB100, anti-CYP4A1, anti-FABP1, anti-FATP2 (Santa Cruz Biotechnology, Dallas, TX), anti-MTP (BD Biosciences, San Jose, CA), anti-Tm6sf2 (MyBioSource Inc, San Diego, CA), anti-ATGL, anti-HSL, anti-p-HSL, anti-ACSL1, anti-ATF4, anti-ATF6, anti-CHOP (Cell Signaling Technology, Danvers, MA), anti-CPT1A, anti-ACADL, anti-ACOX1 (Proteintech Group, Inc, Rosemont, IL), anti-ACADM, anti-ACSL5 (Novus Biologicals, Littleton, CO), anti-MGL, anti-GAPDH, and anti-ACSL4 (Abcam, Cambridge, MA), respectively. Membranes were then washed and incubated with horseradish peroxidase conjugated goat anti-mouse immunoglobulin G or goat anti-rabbit immunoglobulin G (Thermo

Fisher Scientific, Rockford, IL). The bound complexes were detected with enhanced chemiluminescence (Thermo Fisher Scientific) and quantified by densitometry analysis.

Histopathological Examination

Histopathological examination was performed as previously described (30). Briefly, liver from each mouse was rapidly removed and fixed in 10% neutral buffered formalin and processed for paraffin embedding. Sections were cut into 5 μm thickness and processed with H&E staining. All sections were examined by light microscope.

Immunofluorescence

The immunofluorescence studies were performed as described previously (27). Cryostat sections of mouse liver were incubated with anti-MPO, anti-F4/80^{+} followed by Alexa Fluor 594-conjuated donkey anti-rat IgG (Jackson ImmunoResearch Laboratories, West Grove, PA, United States). The nuclei were counterstained by 4',6-diamidino-2-phenylindole (DAPI; Thermo Fisher Scientific)

Plasma ALT and AST Levels

Plasma ALT and AST levels were colorimetrically measured by Infinity ALT Reagent and Infinity AST Reagent (Thermo Fisher Scientific), respectively.

RNA Isolation and Quantitative Polymerase Chain Reaction (qPCR)

Total RNA was extracted from mouse liver using TRIzol™ reagent (Thermo Fisher Scientific) according to the manufacturer's instruction. Complimentary DNA (cDNA) was generated using TaqMan Reverse Transcription Reagents (Thermo Fisher Scientific). Real-time PCR was performed with SYBR green PCR master mix (Qiagen, Germantown, MD, United States) using the 7500 Real Time PCR (RT-PCR) system. Primers were designed and synthesized by Integrated DNA Technologies (Coralville, CA, United States). All primers used for qPCR were listed in table 1. The mRNA levels were normalized to the expression of RPS17 rRNA and analyzed by $2^{-\Delta\Delta Ct}$ threshold cycle method (31) with the values of WT-PF as 1.

Table 1. Primer Sequences Used for qPCR analysis

Origin.	Name	Forward primer 5'-3'	Reverse primer 5'-3'
Mouse NM_001163689	ATGL	CTTCCTCGGGGTCTACCACA	GCCTCCTTGGACACCTCAATAA
Mouse NM_001039507	HSL	CATCAACCACTGTGAGGGTAAG	AAGGGAGGTGAGATGGTAACT
Mouse NM_001166251	MGL	CTCACTTAGCGCCAGCAATA	AGGCCCTCCGTAAAGATAGA
Mouse NM_026179	CGI-58	TGCCAGTGTACCTAGTCCATA	CAGCTTCCCAACACCTAACA
Mouse NM_010046	DGAT1	GGCCTTACTGGTTGAGTCTATC	GTTGACATCCCGGTAGGAATAA
Mouse NM_026384	DGAT2	GAAGGGCTTCTCTTCTCTTCAC	CTTTCTCCCAACGCCTCATAA
Mouse NM_009693	ApoB100	AGGCTTGTCACCCTTCTTTC	GCCTTGTGAGCACCAGTATTA
Mouse NM_001163457	MTP	TCTGCTTCTTCTCCTCCTACT	GTGGAGTACGTGAGCTTGTATAG
Mouse NM_001293795	TM6SF2	ATCACCTACGACCCTCTCTATG	GCCCATCATGTAGCCATCTT
Mouse NM_001302163	ACSL1	GCTTGTGGATGTGGAAGAAATG	TCTTGCTGGGTCTTTCAAGTAG
Mouse NM_207625	ACSL4	ACTAGGACCGAAGGACACATA	CCAATCCTACAGCCATAGGTAAA
Mouse NM_027976	ACSL5	CCGTGGTTCCTGGCTTATTT	CTCTTTCTCTGTGTAGCTCCTTTC
Mouse NM_008176	CXCL1	GTGTCTAGTTGGTAGGGCATAAT	CAGTCCTTTGAACGTCTCTGT
Mouse NM_008491	LCN2	TCCTCAGGTACAGAGCTACAA	GCTCCTTGGTTCTTCCATACA
Mouse NM_009716	ATF4	CCACTCCAGAGCATTCCTTTAG	CTCCTTTACACATGGAGGGATTAG
Mouse NM_00108130	ATF6	TGGCTTCCTTCACCACATAAA	GTATCCCTGGTTGACCCTTAAC
Mouse NM_007837	CHOP	CAGCGACAGAGCCAGAATAA	CAGGTGTGGTGGTGTATGAA

Mouse NM_007392	α-SMA	CCATCATGCGTCTGGACTT	GGCAGTAGTCACGAAGGAATAG
Mouse NM_007742	COL1A1	GCTTGAAGACCTATGTGGGTATAA	GGTGGAGAAAGGAGCAGAAA
Mouse NM_007743	COL1A2	CCAGAGTGGAACAGCGATTAC	GATGCAGGTTTCACCAGTAGAG
Mouse NM_009370	TGF-β1	GGTGGTATACTGAGACACCTTG	CCCAAGGAAAGGTAGGTGATAG
Mouse NM_009092	RPS17	CAGGAAGAAGAGAGAGAGAGGA	AAGGTTAGAGAGACTGCCAAAG

Quantification of TGs, FFAs, and VLDL-TG

Hepatic TGs and FFAs levels were measured as previously described (27). Briefly, lipids were extracted by 2:1 chloroform: methanol (v/v) mixture, dried, and redissolved in 1:1 5% Triton X-100: methyl alcohol solution (v/v). Hepatic TGs and FFAs levels, as well as plasma TGs and FFAs levels were determined by colorimetric method using TG and FFA quantification kit (BioVision, Milpitas, CA), according to the manufacture's protocols.

Plasma VLDL-TG level was detected by fast protein liquid chromatography (FPLC) assay. In brief, the plasma of three to five $ATGL^{\triangle hep}$ mice *or* $ATGL^{flox/flox}$ WT mice either with or without alcohol feeding were pooled together to become a pooled plasma sample. Then lipoprotein fractions were separated from 100μl of plasma by gel filtration column chromatography. Approximately 70 fractions were collected and the amount of TG and cholesterol in each traction were determined using microtiter plate, enzyme-based assays. Profiles of TG and cholesterol were constructed. Calibration of the column with purified lipoprotein fractions permits quantitation of each lipid in various lipoprotein classes. Then total plasma cholesterol and TG were measured by standard enzymatic assays. HDL cholesterols were measured with the enzymatic method after precipitation of VLDL and LDL using polyethylene glycol reagent (PEG). From these data LDL were calculated using the Friedewald equation, as long as TGs levels are below 400 mg/dL.

Statistical Analysis

Results are expressed as mean ± standard deviation (SD). Data were analyzed using the two-tailed student's *t*-test or one-way ANOVA test, followed by Tukey's test. $P < 0.05$ was considered as statistically significant.

Results

Hepatic ATGL Protein Levels are Increased by Chronic Alcohol Feeding

C57BL/6J mice were subjected to alcohol feeding for 8 weeks as a model of ALD. Histopathologic examination showed that chronic alcohol feeding caused LD accumulation, inflammatory cell infiltration, and hepatocyte degenerative changes as indicated by enlarged size and nuclei disappearance (Fig. 2.2A). As indicators for liver injury, plasma ALT and AST levels were elevated by chronic alcohol feeding (Fig. 2.2B). Hepatic TGs and FFAs levels were both increased by chronic alcohol feeding (Fig. 2.2C). The protein levels of hepatic ATGL were increased after 8 weeks of alcohol feeding. Although the total protein levels of HSL were not affected, p-HSL and MGL protein levels in liver were both increased by alcohol feeding (Fig. 2.2D).

Figure 2.2 Chronic Alcohol Feeding Increases Hepatic ATGL Protein Levels in Association with Lipid Accumulation and Liver Injury

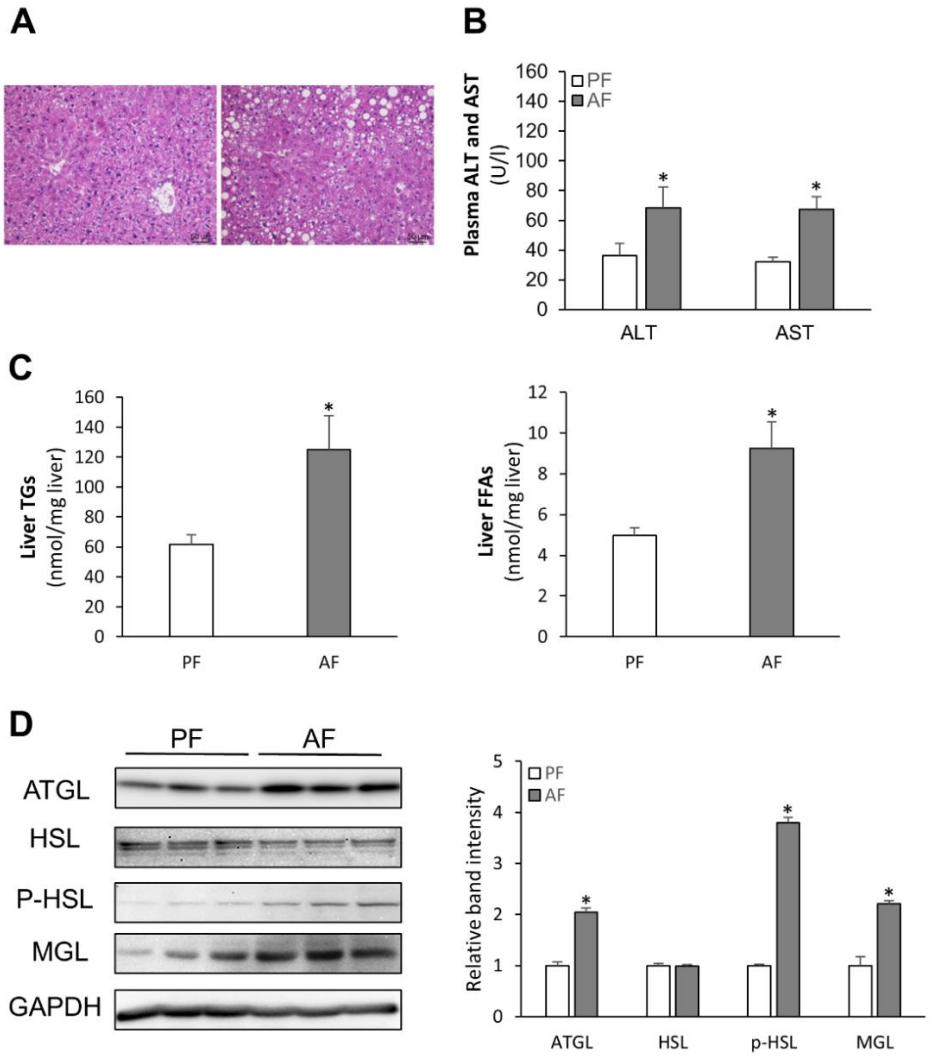

Note. C57BL/6 mice were fed with control (PF) or ethanol (AF) liquid diet for 8 weeks. (A) Histological results (H&E staining) show that hepatocyte-specific ATGL deletion leads to LD accumulation and inflammatory cell infiltration (Scale bars, 50 μm). (B) Plasma ALT levels and AST levels of the mice (n=6/group). (C) Hepatic TGs levels and FFAs levels are both significantly elevated by 8 weeks of alcohol feeding. (D) Western blot and quantification analysis show that chronic alcohol exposure increases ATGL expression in the livers of mice. Data are shown as means ± SD. *$P < .05$.

Hepatocyte-specific ATGL Deletion Dramatically Exacerbated Alcohol-induced Hepatic Steatosis

To investigate the role of ATGL in the pathogenesis of ALD, we then generated hepatocyte-specific ATGL deletion mice ($ATGL^{\triangle hep}$) to investigate how ATGL deletion in hepatocytes may impact alcohol-impaired lipid homeostasis and inflammation in ALD. $ATGL^{\triangle hep}$ mice and floxed control mice were subjected to an 8-week chronic feeding with control (pair-fed, PF) or alcohol (alcohol-fed, AF) liquid diet. We first confirmed the efficiency of ATGL deletion by performing Western blot and qPCR analysis that ATGL was successfully deleted in the livers of $ATGL^{\triangle hep}$ mice (Fig. 2.3A and Fig. 2.3B). Hormone-sensitive lipase (HSL) and monoacylglycerol lipase (MGL) are another two important lipases that catalyze the second and third step of TG hydrolysis, respectively. Although the mRNA levels of HSL were not affected either by alcohol or ATGL deletion, it was significantly decreased when two factors were combined compared to PF control mice (Fig. 2.3C). The mRNA levels of MGL were significantly induced by alcohol feeding but not by ATGL deletion; however, ATGL deletion suppressed alcohol-induced elevation of MGL expression (Fig. 2.3D). Comparative gene identification-58 (CGI-58) is a strong ATGL co-activator during TG hydrolysis. Similar to ATGL, the expression of CGI-58 was significantly induced upon alcohol exposure, ATGL deletion in hepatocytes attenuated alcohol-induced CGI-58 elevation (Fig. 2.3E).

Because ATGL is the rate-limiting enzyme in TG hydrolysis, we hypothesized that ATGL deletion in hepatocytes would increase hepatic TG accumulation, leading to expansion of LDs. Indeed, the liver weight of mice was significantly increased in AF $ATGL^{\triangle hep}$ mice compared to control mice (Fig. 2.4A). The epididymal white adipose tissue (eWAT) mass was reduced by alcohol feeding in AF floxed mice., ATGL deletion in hepatocytes reduced the eWAT mass into a similar level compared with AF floxed mice, and a further reduction was observed in the AF $ATGL^{\triangle hep}$ mice (Fig. 2.4B), indicating a reduced lipid transport from the liver to adipose tissue, and/or an increase in adipose tissue-derived FFAs translocation and deposition into the liver.

Although the liver weights of PF ATGL$^{\triangle hep}$ mice were not significantly increased compared to the PF floxed mice, the liver of PF ATGL$^{\triangle hep}$ mice displayed a discolored change, suggesting significant accumulation of TGs in the liver (Fig. 2.4C). Histological observation by light microscopy demonstrated that ATGL deletion resulted in an increase in hepatic lipid in PF mice as indicated by LD accumulation. Alcohol feeding also induced LD accumulation in the AF floxed mice, however, both the number and the size of LDs were dramatically increased in the livers of AF ATGL$^{\triangle hep}$ mice (Fig. 2.4E). Light microscopy also observed that the size of adipocytes was reduced in the AF floxed mice, ATGL deletion alone reduced the adipocyte size to a similar level as AF floxed mice, and a further reduction was observed in the AF ATGL$^{\triangle hep}$ mice (Fig. 2.4F). We next determined hepatic TGs and FFAs levels. Quantitative biochemical analysis showed that hepatic TG levels were increased in PF ATGL$^{\triangle hep}$ mice compared to the PF floxed mice. Although alcohol feeding increased hepatic TG levels in the floxed mice, a dramatic increase was found in the AF ATGL$^{\triangle hep}$ mice (Fig. 2.4G). Surprisingly, hepatic FFAs levels were also significantly elevated in AF ATGL$^{\triangle hep}$ mice compared to PF ATGL$^{\triangle hep}$ mice (Fig. 2.4H), suggesting FFAs metabolism may be impaired by ATGL deletion in the liver.

Figure 2.3 ATGL is Successfully Deleted in Hepatocytes of ATGL$^{\triangle hep}$ mice

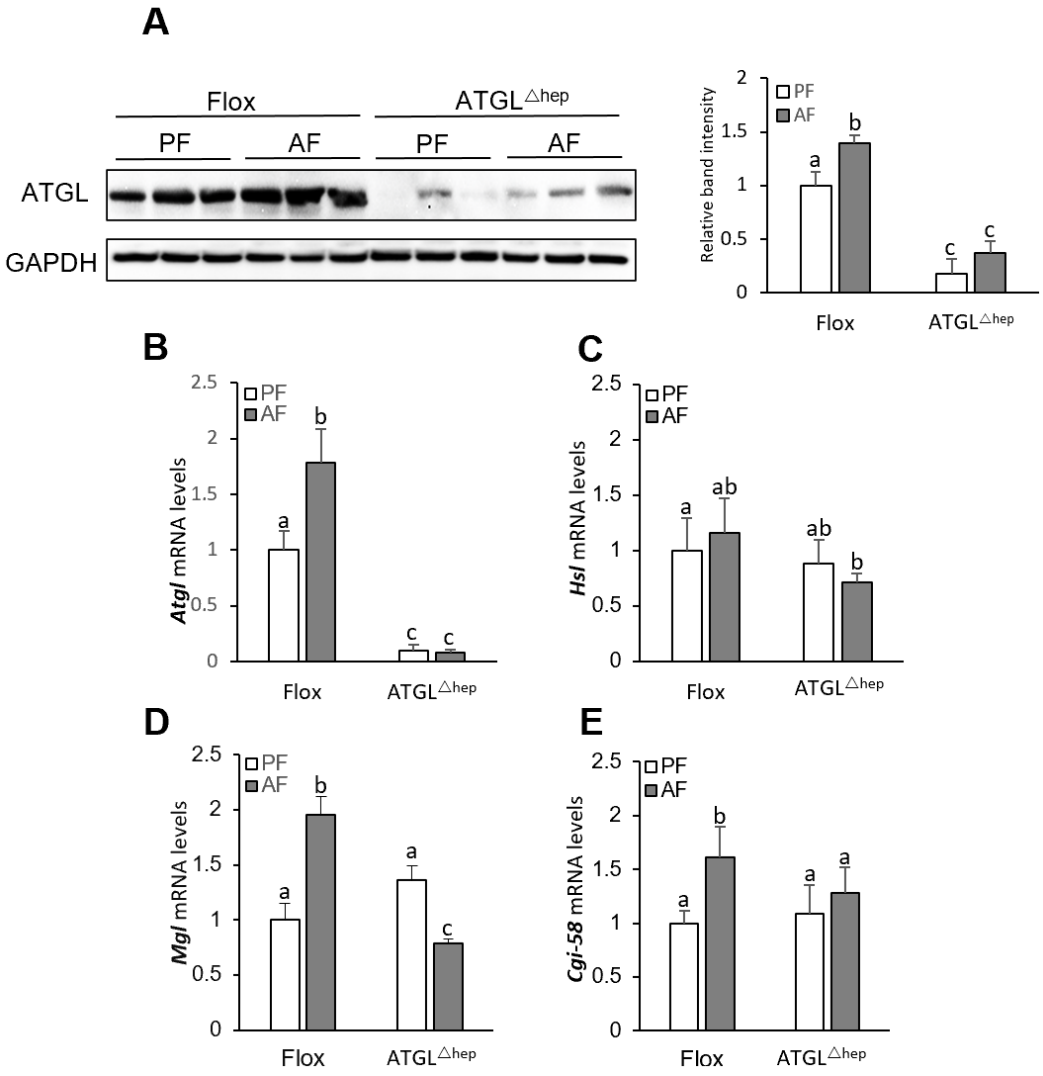

Note. Wild type (flox) and hepatocyte-specific ATGL deletion (ATGL$^{\triangle hep}$) mice were fed with control (PF) or ethanol (AF) liquid diet for 8 weeks. **(**A) Western blot and quantification analysis demonstrate that protein levels of ATGL are dramatically decreased in the livers of ATGL$^{\triangle hep}$ mice compared to their wild type controls. (B) Quantitative polymerase chain reaction (qPCR) result confirms the deletion of ATGL from livers of ATGL$^{\triangle hep}$ mice. (C, D, and E) mRNA levels of enzymes involved in TG catabolism by qPCR (n=4/group). Data are shown as means ± SD, significant differences (P<0.05, two-way ANOVA) are identified with different letters.

Figure 2.4 Hepatocyte-specific Deletion of ATGL Dramatically Exacerbates Alcohol-induced Hepatic Steatosis and Reduction of eWAT Mass

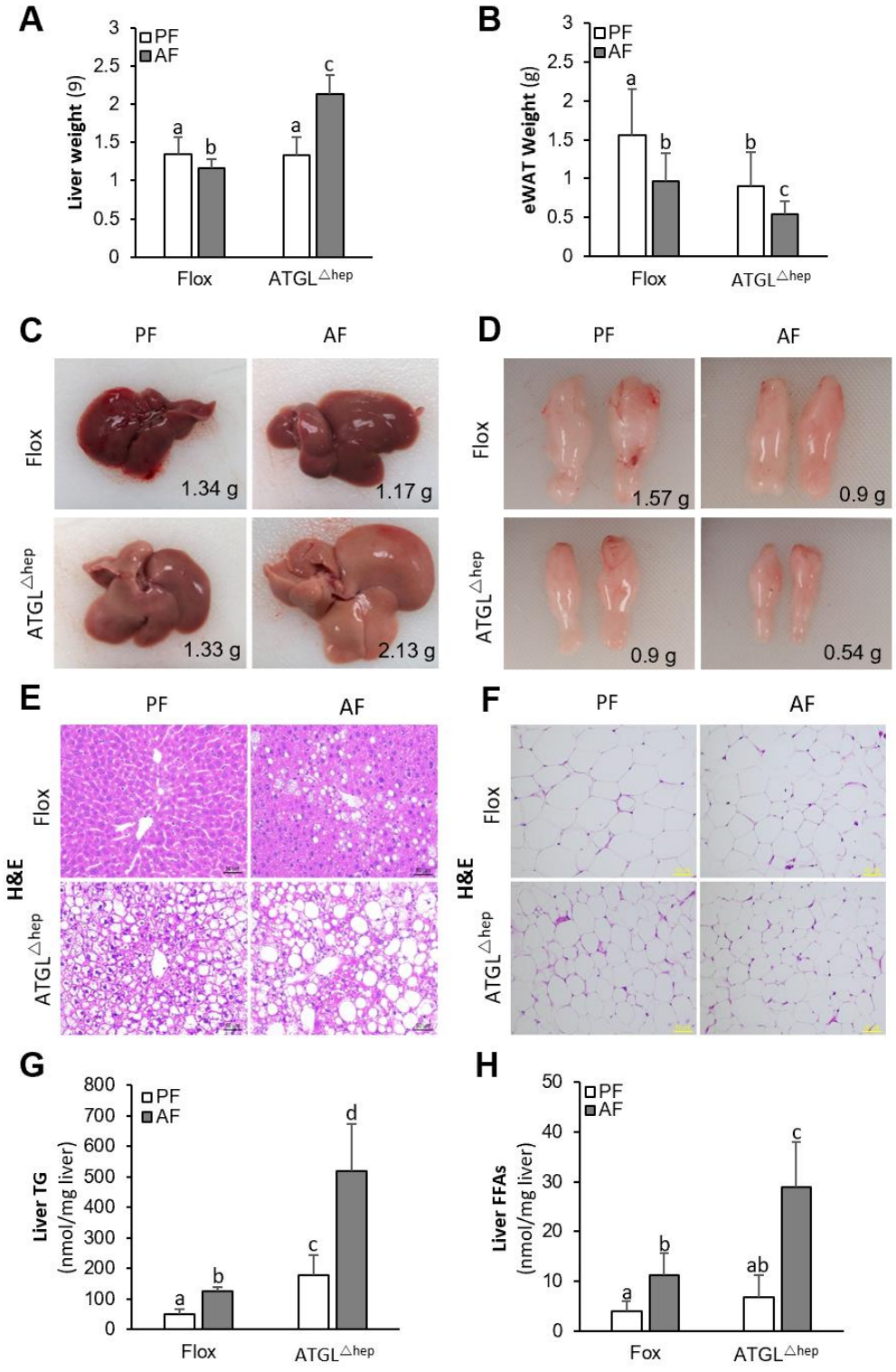

Note. Wild type (flox) and hepatocyte-specific ATGL deletion (ATGL$^{\triangle hep}$) mice were fed with control (PF) or ethanol (AF) liquid diet for 8 weeks. (A and B) Analysis of liver weight and eWAT weight of the mice. (C and D) Liver and eWAT morphology reveals that hepatocyte-specific deletion of ATGL induces severe lipid accumulation in the liver but decreases the lipid storage in eWAT. (E and F) Histological results (H&E staining) of liver and WAT further confirm the observation (Scale bars, 50 μm). (G and H) Analysis of hepatic TGs and FFAs content. Data are shown as mean ± SD from each group (n=6/group). Significant differences (P<0.05, two-way ANOVA) are identified with different letters.

Hepatocyte-specific ATGL Deletion Partially Decreased Fatty Acid Oxidation and TG synthesis in the Liver

To explore the potential mechanisms that mediate hepatic FFAs elevation in AF ATGL$^{\triangle hep}$ mice, we determined hepatic protein levels of enzymes related to fatty acid oxidation, including carnitine palmitoyltransferase 1A (CPT1A), middle-chain acyl-CoA dehydrogenase (MCAD, also known as ACADM), long-chain acyl-CoA dehydrogenase (LCAD, also known as ACADL), Acyl-CoA oxidase 1 (Acox1) and Cytochrome P450 4A1 (CYP4A1). As shown in Fig. 2.5A, while alcohol feeding didn't affect hepatic CPT1A protein levels in AF floxed mice, ATGL deletion significantly suppressed the protein levels of CPT1A regardless of alcohol feeding. Neither alcohol feeding nor ATGL deletion alone significantly impact hepatic ACADM protein levels, however, they were remarkably reduced in AF ATGL$^{\triangle hep}$ mice. Neither alcohol feeding nor ATGL deletion affected hepatic ACOX1 levels, however, the protein levels of ACOX1 were significantly reduced in AF ATGL$^{\triangle hep}$ mice. No significant changes were observed in protein levels of ACADL and CYP4A1 among different groups.

We also examined the gene expression of enzymes involved in hepatic TG synthesis, such as diacylglycerol acyltransferase 1 (DGAT1) and DGAT2. Our results revealed that mRNA levels of both DGAT1 and DGAT2 were significantly increased upon alcohol feeding in floxed mice; ATGL deletion down-regulated DGAT1 mRNA levels in ATGL$^{\triangle hep}$ mice regardless of

alcohol feeding, while DGAT2 mRNA expression was only reduced in AF ATGL$^{\triangle hep}$ mice (Fig. 2.5 B and C).

Figure 2.5 Hepatic Fatty Acid Oxidation and TG Synthesis are Partially Suppressed by Hepatocyte-specific ATGL Deletion

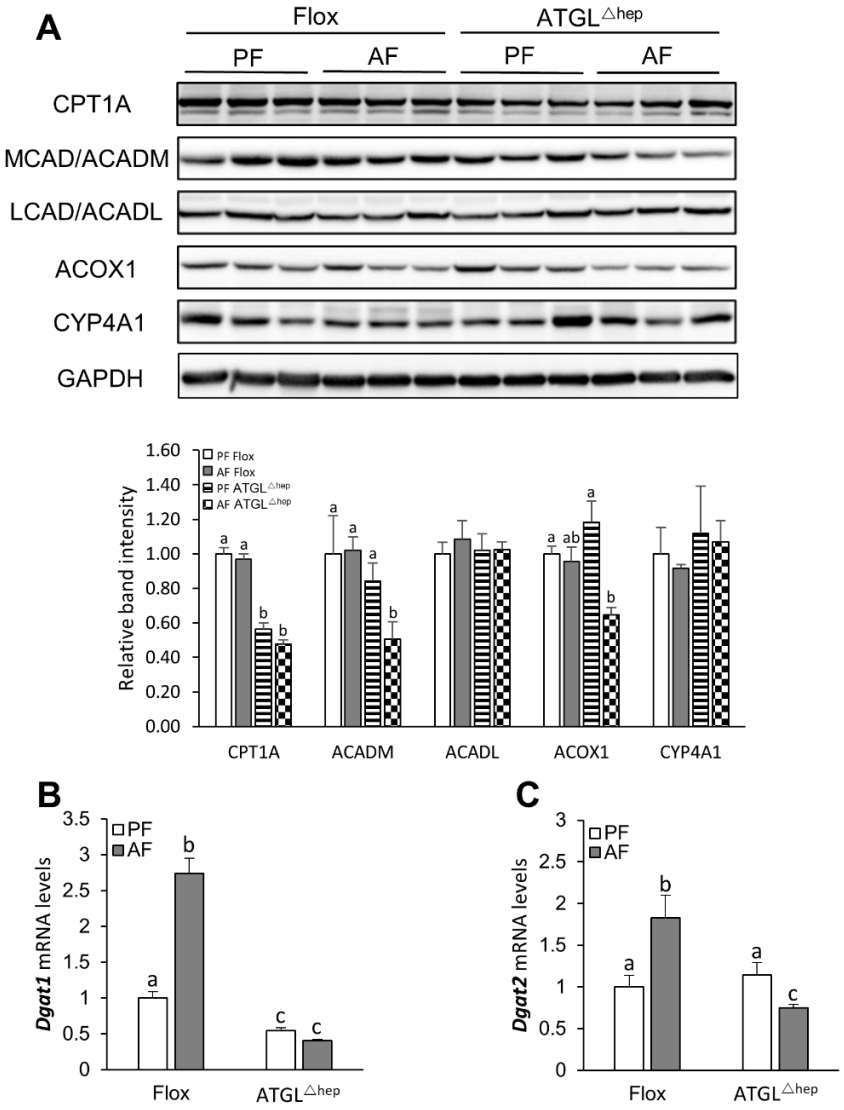

Note. Wild type (flox) and hepatocyte-specific ATGL deletion (ATGL□hep) mice were fed with control (PF) or ethanol (AF) liquid diet for 8 weeks. (A) Western blot and quantification analysis of hepatic protein expressions of enzymes involved in mitochondrial and peroxisomal fatty acid oxidation. (B and C) The mRNA levels of genes involved in TG synthesis were

measured by qPCR. Data are shown as mean ± SD from each group (n=4/group). Significant differences ($P<0.05$, ANOVA) are identified with different letters.

ATGL Deletion in Hepatocytes Significantly Suppressed Hepatic VLDL-TG Secretion Due to Impaired Fatty Acid Activation and VLDL Lipidation

Our results showed that fasting plasma TG and FFA levels were elevated in AF floxed mice, which were attenuated by ATGL deletion (Fig. 2.6A). During the fasting state, liver-derived VLDL particles are the main carriers of TGs in plasma (32). The FPLC analysis revealed that the diminished plasma TG levels in AF ATGL$^{\triangle hep}$ mice were contributed by reduced VLDL-TG particles, suggesting impaired hepatic VLDL secretion in AF ATGL$^{\triangle hep}$ mice (Fig. 2.6B).

To explore the potential mechanisms by which hepatocyte-specific ATGL deletion impairs alcohol-induced VLDL-TG secretion, we examined the protein and mRNA levels of genes involved in VLDL lipidation and secretion, including apolipoprotein B100 (ApoB100), microsomal triglyceride transfer protein (MTP), and transmembrane 6 superfamily member 2 (TM6SF2). Hepatic mRNA levels of ApoB100 were not affected by either alcohol feeding or ATGL deletion (Fig. 2.7A). Hepatic mRNA levels of MTP were not affected in AF floxed mice, while a suppression of this gene was observed in AF ATGL$^{\triangle hep}$ mice (Fig. 2.7B). ATGL deletion down-regulated hepatic TM6SF2 mRNA expression regardless of alcohol feeding (Fig. 2.7C). Interestingly, the protein levels of MTP were not affected by either alcohol feeding or ATGL deletion. Hepatic protein levels of TM6SF2 were lower in AF ATGL$^{\triangle hep}$ mice, compared to other groups. We also measured plasma protein levels of ApoB100 and found that this protein was elevated by alcohol feeding compared to the PF group, while ATGL deletion did not affect plasma ApoB100 protein levels regardless alcohol feeding (Fig. 2.7D).

As aforementioned, hepatic FFAs levels are surprisingly elevated in the livers of AF ATGL$^{\triangle hep}$ mice. Hence, we explored the potential mechanisms that mediate hepatic FFAs accumulation even in the absence of ATGL. The mRNA levels of major hepatic fatty acid activation enzymes, including Long-chain acyl-CoA synthetase 1 (ACSL1), ACSL4, and ACSL5

were measured by qPCR; the protein levels of ACSL1, ACSL4, ACSL5, as well as Liver fatty acid binding protein 1 (FABP1) and fatty acid transport protein 2 (FATP2) were measured by western blot. As shown in Fig. 2.8A, alcohol feeding alone downregulated hepatic ACSL1 and ACSL5 mRNA expression in floxed mice, while ATGL deletion downregulated all three enzymes in PF mice. In addition, under the condition of ATGL deletion, alcohol feeding further reduces hepatic mRNA levels of ACSL1, while no differences were observed in ACSL4 and ACSL5.

As illustrated in Fig. 2.8B, hepatic protein levels of ACSL1 and ACSL5 were not affected by alcohol feeding in floxed mice. ATGL deletion reduced protein levels of both ACSL1 and ACSL5, which were further inhibited in the liver of AF ATGL$^{\triangle hep}$ mice. Neither alcohol nor ATGL deletion affected ACSL4 protein levels, alcohol feeding significantly increased hepatic ACSL4 protein abundance in ATGL$^{\triangle hep}$ mice. Alcohol feeding decreased hepatic FABP1 protein levels, while no further suppression was observed with ATGL deletion. Furthermore, hepatic protein levels of FATP2 were reduced by ATGL deletion regardless alcohol feeding (Fig. 2.8B).

Collectively, these results suggest that hepatocyte-specific ATGL deletion suppresses hepatic VLDL-TG secretion through impairing FAs activation and transport, as well as VLDL bulk lipidation.

Figure 2.6 Hepatocyte-specific Deletion of ATGL Dramatically Suppresses Hepatic VLDL-TG Secretion

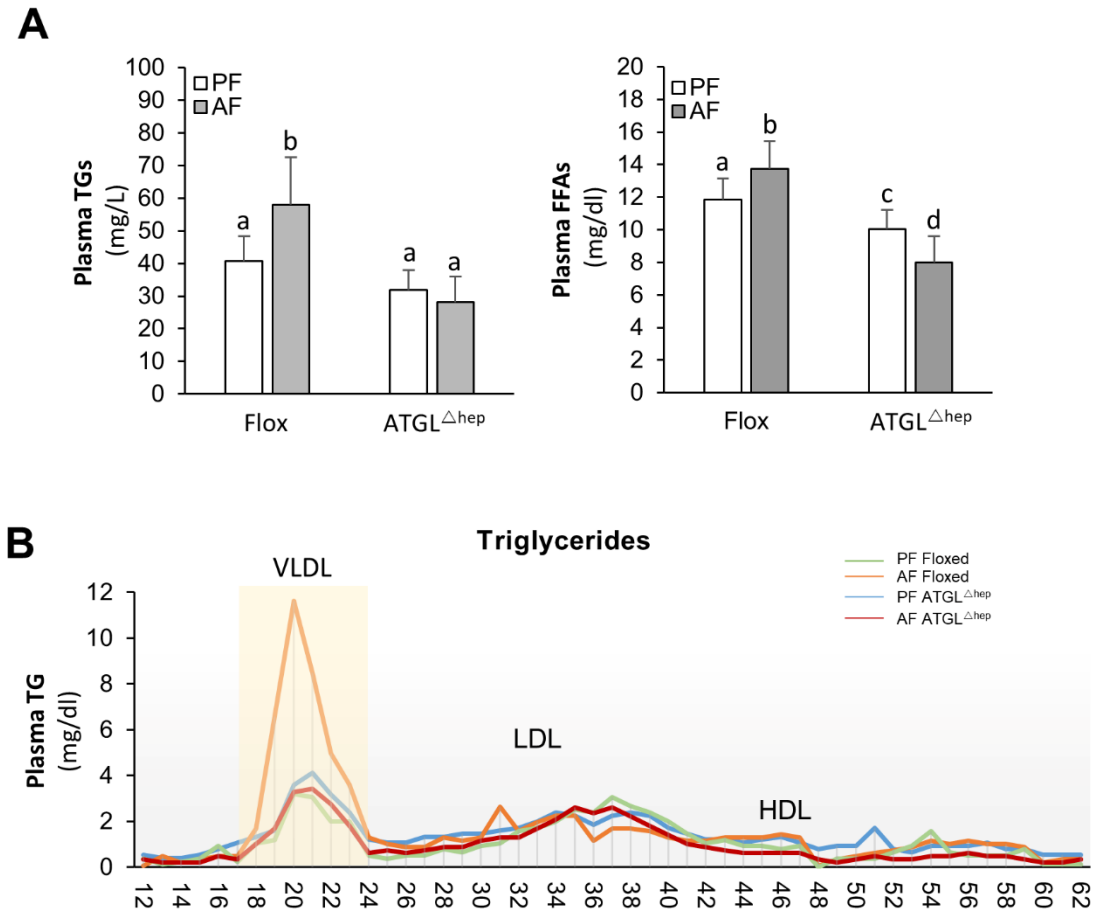

Note. Wild type (flox) and hepatocyte-specific ATGL deletion (ATGL$^{\triangle hep}$) mice were fed with control (PF) or ethanol (AF) liquid diet for 8 weeks. (A) Fasting plasma TG levels and fasting plasma FFAs levels were both significantly reduced in ATGL$^{\triangle hep}$ mice compared to their controls. (B) Fast protein liquid chromatography (FPLC) results show that the reduction of fasting plasma TG levels in ATGL$^{\triangle hep}$ mice is contributed by diminished TG-rich VLDL. Data are shown as mean ± SD from each group (n=6/group). Significant differences (P<0.05, ANOVA) are identified with different letters.

Figure 2.7 Hepatocyte-specific Deletion of ATGL Partially Impairs VLDL-TG Lipidation

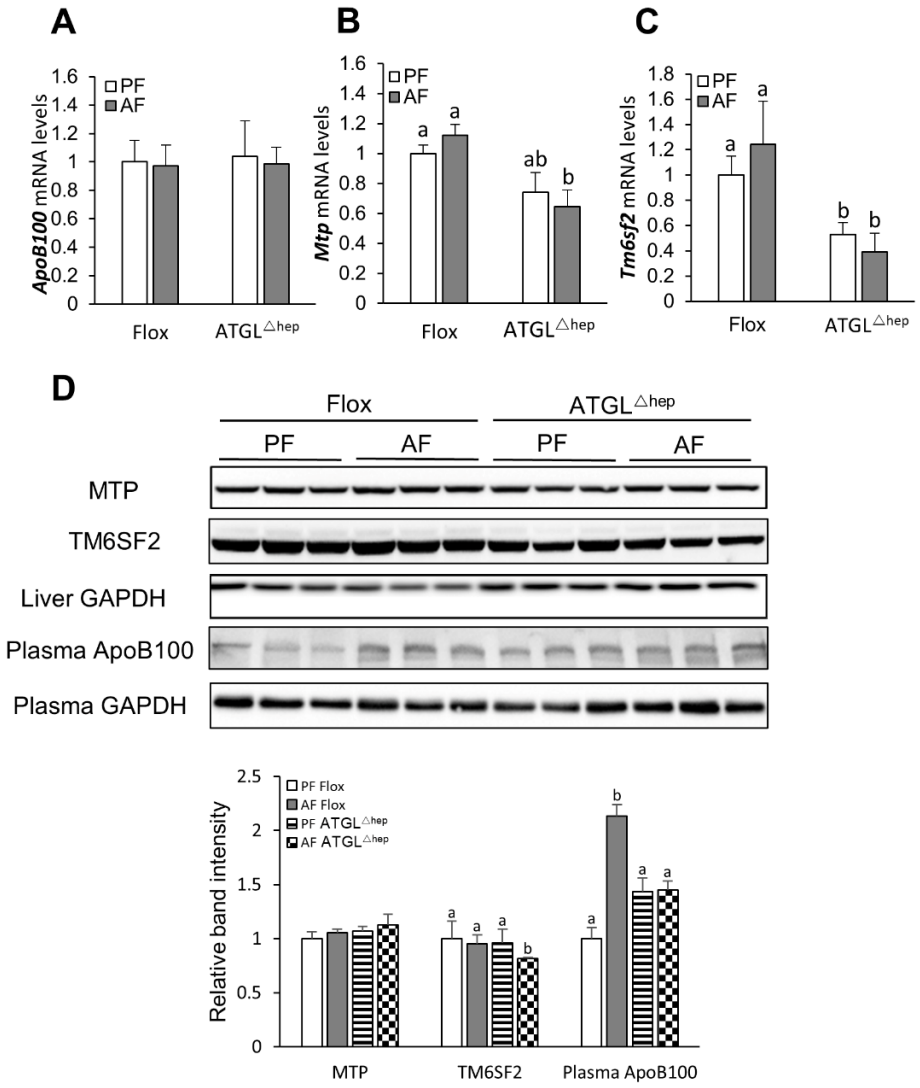

Note. Wild type (flox) and hepatocyte-specific ATGL deletion (ATGL$^{\triangle hep}$) mice were fed with control (PF) or ethanol (AF) liquid diet for 8 weeks. (A, B, and C) The mRNA expression of genes involved in VLDL was measured by qPCR. (D) Western blot and quantification analysis of hepatic protein expressions of enzymes involved in VLDL lipidation. Data are shown as mean ± SD from each group (n=4/group). Significant differences (P<0.05, ANOVA) are identified with different letters.

Figure 2.8 Hepatocyte-specific Deletion of ATGL Significantly Impairs Hepatic Fatty Acid Activation

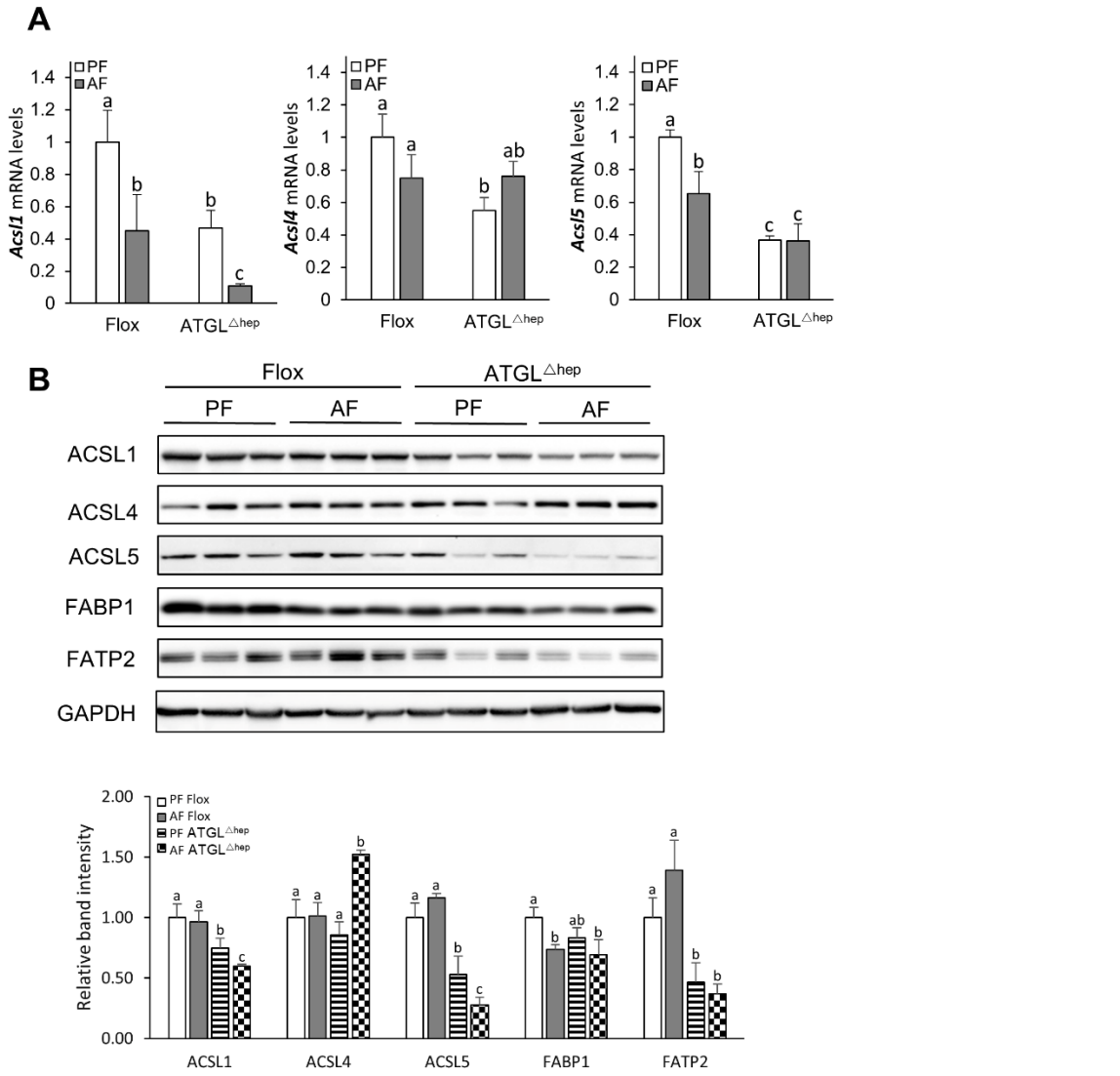

Note. Wild type (flox) and hepatocyte-specific ATGL deletion (ATGL$^{\triangle hep}$) mice were fed with control (PF) or ethanol (AF) liquid diet for 8 weeks. (A) mRNA expression of genes involved in hepatic fatty acid activation was measured by qPCR. (B) Western blot and quantification analysis of hepatic protein expressions of enzymes involved in fatty acid activation and transportation. Data are shown as mean ± SD from each group (n=4/group). Significant differences (P<0.05, ANOVA) are identified with different letters.

Alcohol-induced Liver Injury and Hepatic Inflammation are Aggravated by Hepatocyte-specific ATGL Deletion

Plasma ALT and AST levels have been used as surrogate markers for liver injury (33). We found that alcohol feeding significantly elevated plasma ALT and AST levels in floxed mice, which were further augmented by ATGL deletion (Fig. 2.9A). We then examined the impact of ATGL deletion on liver inflammation by examining the mRNA levels of hepatocyte-derived chemokine C-X-C motif chemokine ligand 1 (CXCLl1) and cytokine lipocalin 2 (LCN2), as well as hepatic tissue distribution of infiltrated neutrophil and resident Kupffer cells by immunofluorescence staining of MPO and F4/80^{+}, respectively. ATGL deletion significantly exacerbated alcohol-induced liver inflammation as indicated by elevated CXCL1 mRNA and LCN2 mRNA levels in AF ATGL$^{\triangle hep}$ mice (Fig. 2.9B and 2.9C). Alcohol-induced hepatic neutrophil infiltration was further exacerbated by ATGL deletion as observed by increased number of myeloperoxidases^{+} (MPO^{+}) cells in the livers of AF ATGL$^{\triangle hep}$ mice (Fig. 2.9D). The results suggest that hepatocyte-specific ATGL deletion exacerbated alcohol-induced liver injury and hepatic inflammation. F4/80 antigen has been widely adopted as a macrophage marker in mice, including liver resident macrophage, Kupffer cell. As shown in Fig. 2.9E, F4/80^{+} macrophages are increased either by alcohol feeding or ATGL deletion; however, the amount of F4/80^{+} macrophages in AF ATGL$^{\triangle hep}$ mice are comparable with floxed mice.

The C/EBP homologous protein (CHOP) plays a critical role in mediating ER-stress induced hepatocyte injury and cell death (34). Activating transcription factors ATF4 and ATF6 have been demonstrated to directly regulate CHOP transcription (35,36). Next, we determined hepatic mRNA expression and protein levels of CHOP, ATF4 and ATF6. As shown in Fig. 2.10A, mRNA levels of both ATF4 and ATF6 were increased by either alcohol feeding or ATGL deletion, while no further impact was observed in the AF ATGL$^{\triangle hep}$ group. Although alcohol feeding did not affect mRNA levels of CHOP in AF control mice, ATGL deletion significantly induced CHOP expression, which was further exacerbated in AF ATGL$^{\triangle hep}$ mice. Moreover,

hepatic protein levels of both ATF4 and ATF6 were increased by alcohol feeding, however, ATGL deletion significantly reduced protein levels of ATF4 regardless alcohol feeding, whereas protein levels of ATF6 were not affected by ATGL deletion. Either alcohol feeding or ATGL deletion is sufficient to significantly increased hepatic protein levels of CHOP, while the highest induction of CHOP was observed in AF ATGL$^{\triangle hep}$ mice (Fig. 2.10B).

Figure 2.9 Hepatocyte-specific Deletion of ATGL Exacerbates Alcohol-induced Liver Inflammation

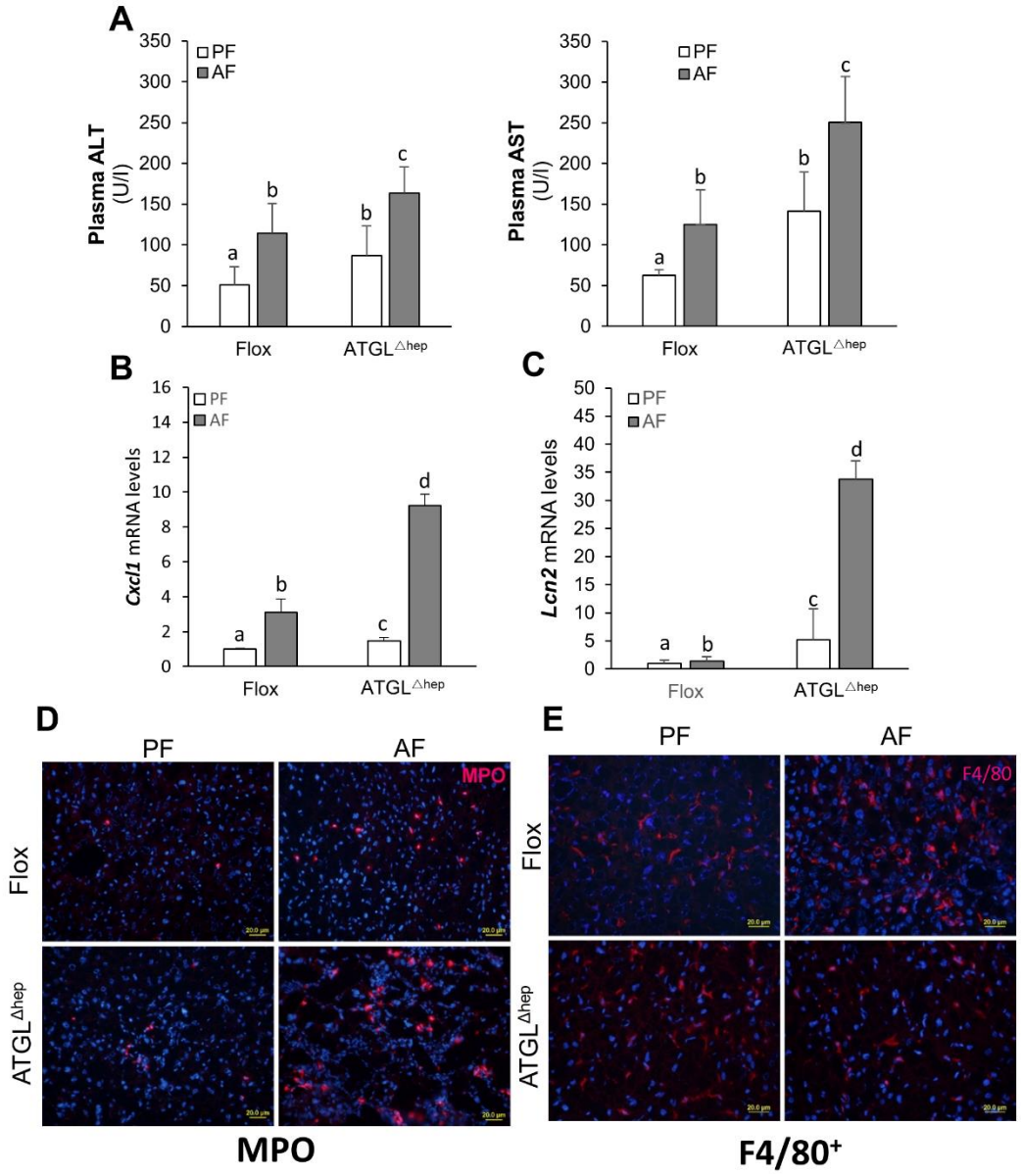

Note. Wild type (flox) and hepatocyte-specific ATGL deletion (ATGL$^{\triangle hep}$) mice were fed with control (PF) or ethanol (AF) liquid diet for 8 weeks. (A) Analysis of plasma ALT and AST levels (n=6/group). (B and C) mRNA expression of Cxcl1 and Lcn2 was measured by q PCR (n=4/group). (D and E) Immunofluorescence staining of hepatic MPO^{+}cells (red) and F4/80^{+} cells (red) (Scale bars, 20 μm). Data are shown as mean ± SD from each group. Significant differences (P<0.05, two-way ANOVA) are identified with different letters.

Figure 2.10 Hepatocyte-specific Deletion of ATGL Exacerbates Alcohol-induced Hepatic ER Stress

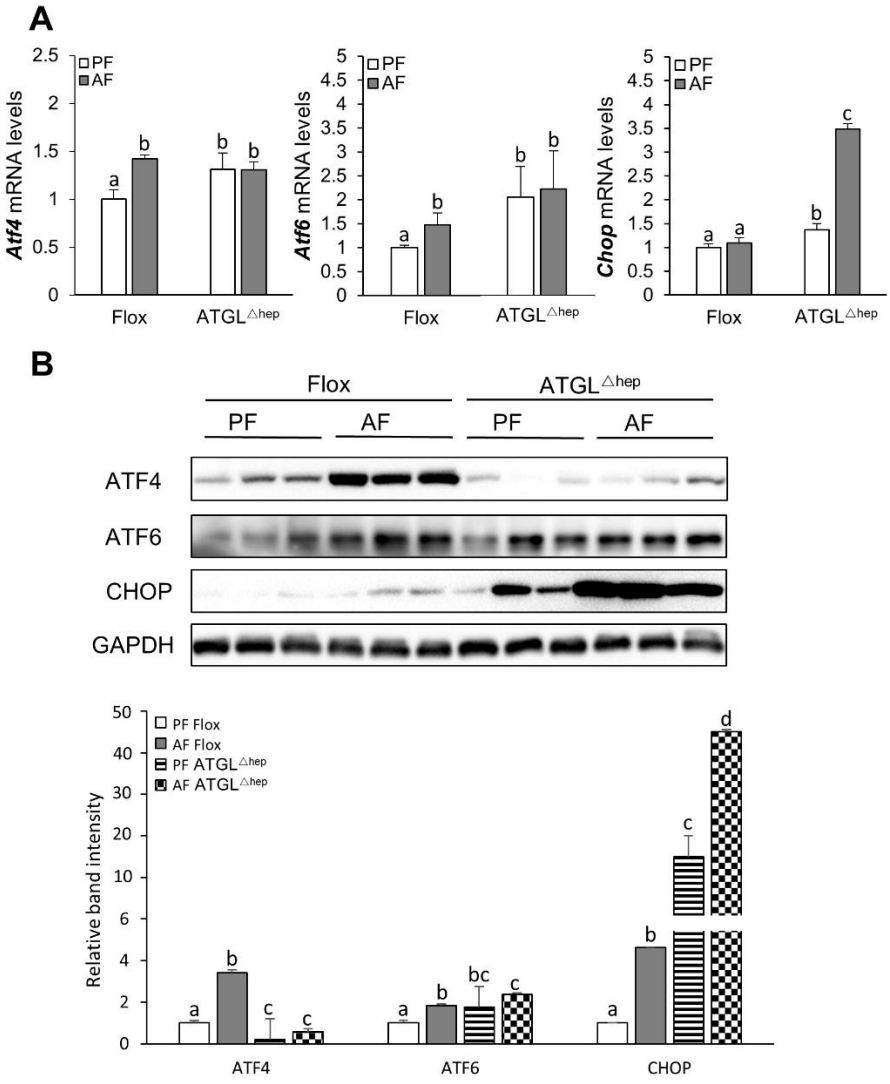

Note. Wild type (flox) and hepatocyte-specific ATGL deletion (ATGL$^{\triangle hep}$) mice were fed with control (PF) or ethanol (AF) liquid diet for 8 weeks. (A) The mRNA levels of genes involved in ER stress was measured by qPCR. (B) Representative western blot images and quantitative analysis of hepatic protein levels of ATF4, CHOP, and ATF6. Data are shown as mean ± SD from each group (n=4/group). Significant differences (P<0.05, two-way ANOVA) are identified with different letters.

Alcohol-induced Hepatic Fibrosis is Exacerbated by ATGL Deletion in Hepatocytes

To evaluate the effect of ATGL deletion in hepatocytes on alcohol-induced hepatic fibrosis, we next examined the expressions of the hallmarks of fibrogenesis, including alpha-smooth muscle action (α-SMA), collagen type I alpha 1 chain (COL1A1), and collagen type I alpha 2 chain (COL1A2). Although alcohol feeding did not significantly affect mRNA levels of α-SMA, COL1A1, and COL1A2, they were all significantly increased by ATGL deletion, which were further exacerbated in AF ATGL $^{\triangle hep}$ mice (Fig. 2.11A-C). The mRNA levels of TGF-β, a master regulator of hepatic fibrosis, were increased by ATGL deletion regardless of alcohol feeding (Fig. 2.11D). In line with that, Sirius Red Staining illustrated that hepatocyte-specific deletion of ATGL markedly exacerbated alcohol-induced fibrosis in the liver (Fig. 2.11E). Taken together, these results suggest that hepatocyte-specific deletion exacerbated alcohol-induced hepatic fibrosis.

Figure 2.11 Hepatocyte-specific Deletion of ATGL Exacerbates Alcohol-induced Hepatic Fibrosis

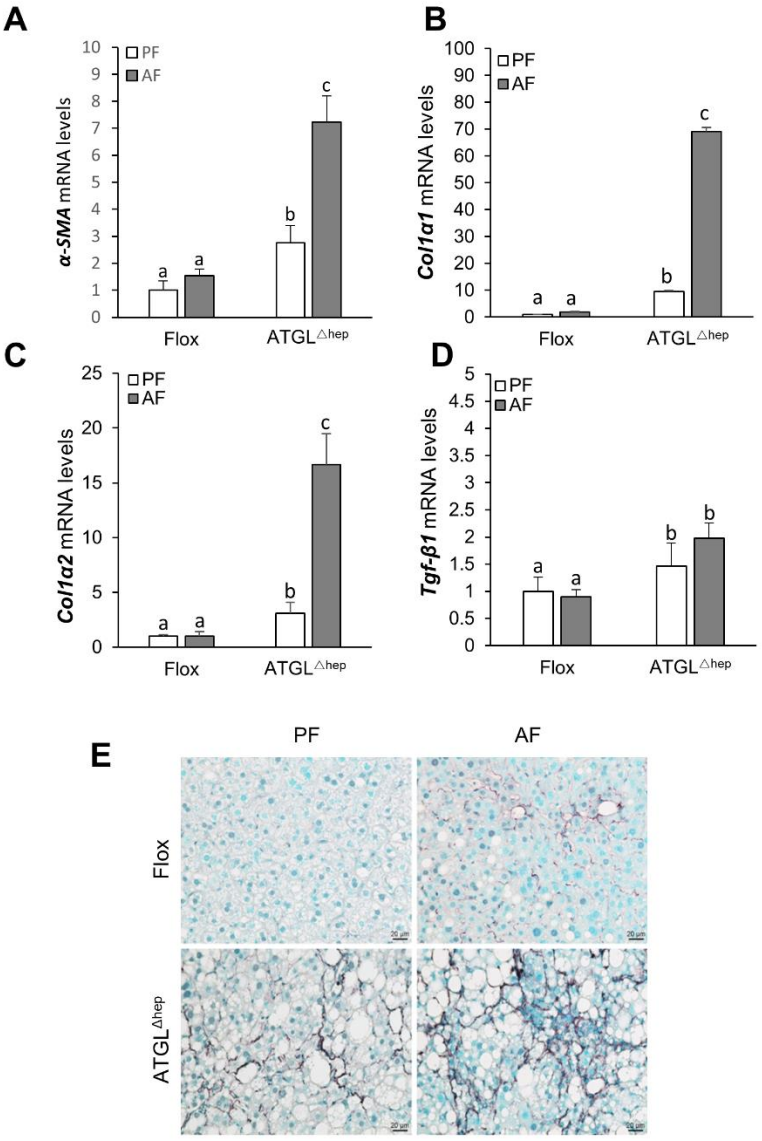

Note. Wild type (flox) and hepatocyte-specific ATGL deletion (ATGL$^{\triangle hep}$) mice were fed with control (PF) or ethanol (AF) liquid diet for 8 weeks. (A-D) The mRNA expression of genes related to fibrosis was measured by qPCR. (E) Representative images of liver tissues stained with Sirius Red (scale bar, 20 μm). Data are shown as mean ± SD from each group (n=4/group). Significant differences (P<0.05, ANOVA) are identified with different letters.

Discussion

In the present study, we generate a mouse model with hepatocyte-specific ATGL deletion to investigate the role of ATGL in alcohol-induced hepatic steatosis, lipotoxicity, inflammation, and fibrogenesis. First, we demonstrate that ATGL deletion in hepatocytes exacerbates alcohol-induced TG/LD accumulation in the liver by impairing VLDL-TG secretion. Next, our data reveals that ATGL might play an important role in reducing VLDL-TG secretion in AF$^{\triangle hep}$ mice. Thirdly, we find that ATGL deletion in hepatocytes exacerbates alcohol-induced liver injury and hepatic inflammation by upregulating CXCL1 and LCN2 expression and subsequent neutrophil infiltration in the liver. We then demonstrate that CHOP-mediated cell death might contribute to the enhanced liver inflammation in AF ATGL$^{\triangle hep}$ mice. Lastly, we observe that hepatocyte-specific deletion of ATGL remarkedly exacerbates alcohol-induced hepatic fibrosis. Taken together, findings in the current study indicate that hepatocyte-specific ATGL deletion exacerbates alcohol-induced hepatic steatosis by impairing VLDL-TG secretion through impaired FFAs activation; and the severe lipotoxicity in AF ATGL$^{\triangle hep}$ mice might be caused by CHOP-associated cell death, as well as CXCL1 and LCN2 upregulation-induced neutrophil infiltration in the liver.

Hepatic steatosis (fatty liver disease) is the most common and the earliest response of the liver to chronic alcohol consumption in the progression of ALD (Donohue, 2007; Torruellas, 2014). Excess lipid accumulation in the liver induces lipotoxicity, leading to organellar dysfunction, abnormal activation of cellular signaling pathways, inflammation, and eventually cell death (Geng et al., 2021). However, the molecular mechanisms by which ‘toxic lipid’ accumulation induces liver injury, hepatic inflammation and fibrosis are still not well established. For years, considerable debate has been sparked over whether it is TG or FFA that incites hepatic lipotoxicity and inflammatory responses. Historically, saturated FFAs are considered as ‘toxic lipid’ that promotes lipotoxicity, causing cell injury and cell death, while TGs are

recognized as inert lipid that is protective against FFA-induced lipotoxicity (Musso et al., 2018; Wang et al., 2006; Wei et al., 2006). Previous studies have shown that ATGL overexpression results in reduced TG content and the size of LD in the livers of experimental mice, while ATGL deletion leads to increased TG content and larger cytoplasmic LDs (Ong et al., 2011; Reid et al., 2008; Turpin et al., 2011; Wu et al., 2011). Initially we find that ATGL is upregulated in the livers of the mice with alcohol feeding. In the mouse model of hepatocyte-specific ATGL deletion, as expected, alcohol-induced TG accumulation was dramatically augmented in the mouse liver, as evidenced by elevated hepatic TG content and amplified cytoplasmatic LDs. Surprisingly, rather than being attenuated, alcohol-induced elevation in liver FFA levels were markedly augmented by ATGL deletion, indicating FFAs utilization in the liver was also impaired. Our data demonstrate that FFAs oxidation in the liver is partially affected by ATGL deletion, suggesting that other factors may contribute to the accumulation of hepatic FFAs.

Along with hepatocellular TG accumulation, we found that alcohol-induced increase in plasma VLDL-TG levels was attenuated in AF ATGL$^{\triangle hep}$ mice, indicating impaired VLDL-TG lipidation and secretion. The biogenesis of VLDL occurs in the lumen of ER where nascent ApoB100 is partially lipidated by TGs to form a lipid-poor primordial VLDL particle, which then fusses with TG-rich particles that already present in the cytosol (Rustaeus et al., 1999; Tiwari & Siddiqi, 2012). Although the process of VLDL assembly and lipidation is not well understood, it has been reported to rely on the activities of MTP and TM6SF2, as well as the availability of TGs (Alves-Bezerra & Cohen, 2017; Mahdessian et al., 2014, p. 2). FFAs are relatively inert molecules, they must first be activated to acyl-CoAs before entering metabolic pathways including TG synthesis (Mashek et al., 2007). We found that ATGL deletion has no impact on either the protein levels of MTP in the liver or that of ApoB100 in the plasma, indicating the synthesis of lipid-poor primordial VLDL was not affected. Although TM6SF2 expression was reduced in ATGL$^{\triangle hep}$ mice, alcohol feeding did not seem to further exacerbate this reduction. ACSL family members catalyze the conversion of long-chain fatty acids into their active acyl-

CoA forms (Mashek et al., 2007). We found that protein levels of ACSL5 were significantly reduced by ATGL deletion, which were further suppressed upon alcohol feeding. ACSL5 is an ER and mitochondrial protein that is predominantly expressed in tissues with high rates of TG synthesis (Bu & Mashek, 2010). *Bu et al.* show that ACSL5 knockdown decreases hepatic TAG secretion proportionately to the decrease in neutral lipid synthesis in primary rat hepatocyte (Bu & Mashek, 2010), while *Bowman et al.* report that mice with global ACSL5 deletion exhibit reduced VLDL-TG secretion, suggesting that ACSL5 plays a critical role in activating and channeling FAs toward TG synthesis and export (Bowman et al., 2016). In line with ACSL5 reduction, ATGL deletion also decreased hepatic protein levels of DGAT1, which is believed to play a critical role in converting FFAs from LDs or exogenous source to TGs for VLDL assembly. Together with elevated FFAs levels in AF ATGL$^{\triangle hep}$ mice, we propose that ATGL deletion-mediated suppression of ACSL5 and subsequently impaired FAs activation and DGAT1-mediated TG synthesis might be responsible for the reduced VLDL-TG secretion in AF ATGL$^{\triangle hep}$ mice. Future studies with hepatocyte-specific ACSL5 modulation are needed to confirm the role of ATGL-ACSL5-DGAT1 pathway in hepatic VLDL-TG secretion.

Chronic ethanol exposure induces various types of cellular stress that promote inflammatory responses via recruiting and activating innate immune cells to the liver (Miyata & Nagy, 2020). Excessive inflammation causes massive hepatocyte cell death; the dying hepatocytes, in turn, further stimulate inflammatory responses for the removal of dead cells by upregulating chemokine/cytokine expression, which consequently worsens liver injury (Brenner et al., 2013). In our mouse model, we observe that ATGL deletion in hepatocytes exacerbates alcohol- elevated plasma ALT and AST levels, suggesting aggravated liver injury. Hepatic expression of CXCL1 and LCN2 are remarkably upregulated in AF ATGL$^{\triangle hep}$ mice, accompanied by increased neutrophil infiltration, indicating enhanced inflammation in the liver. We found that hepatic protein levels of CHOP are induced in ATGL$^{\triangle hep}$ mice, which is further upregulated upon alcohol feeding, suggesting CHOP-associated cell death might be involved in

ATGL deletion-induced liver inflammation. Overall, our results demonstrate that hepatocyte-specific deletion of ATGL aggravated liver injury and hepatic inflammation by, at least partially, inducing CHOP-associated cell death and CXCL1- and LCN2-mediated neutrophil infiltration.

As described above, sustained lipotoxicity and inflammation cause hepatocyte death, which initiates the process of fibrogenesis to fill the space left behind cell death with collagens. Thus, patients with persistent alcohol use disorder will eventually drive expansive perivenular fibrosis, which can rapidly develop into alcohol-related cirrhosis (Chrostek & Panasiuk, 2014; Lackner & Tiniakos, 2019). Virtually all clinical complications of ALD occur in patients with established fibrosis and cirrhosis (Bataller & Gao, 2015), making fibrosis one of the most important prognostic factor in ALD. However, the molecular mechanisms by which hepatic steatosis affects liver fibrosis remain unclear. *Yamaguchi et al.* report that inhibiting TG synthesis attenuates hepatic steatosis but exacerbates liver fibrosis in a MCD-induced NASH mouse model (Yamaguchi et al., 2007). In contrast, *Newberry et al.* show that MTP knock out-induced hepatic TG accumulation, at least in part, promotes the development of fibrosis (Newberry et al., 2017). In our mouse model, we demonstrate that ATGL deletion in hepatocytes exacerbates alcohol-induced fibrosis as evidenced by enhanced collagen accumulation, and the upregulation of hepatic α-SMA, COL1A1, and COL1A2, suggesting that hepatocellular TG accumulation might play critical role in haptic stellate cell activation and subsequently accumulation of extracellular matrix proteins in ALD.

In summary, this study demonstrates a role of ATGL in alcohol-induced hepatic steatosis, lipotoxicity, inflammation, and fibrosis in a hepatocyte-specific ATGL deletion mouse model. First, we demonstrate that ATGL deletion in hepatocytes exacerbates alcohol-induced TG/LD accumulation in the liver via impairing VLDL-TG secretion. Next, our data reveal that protein levels of ACSL5 and DGAT1 are downregulated by ATGL deletion, suggesting that ACSL5-mediated FFAs activation and DGAT1-mediated FFAs conversion to TGs might account for the diminished VLDL-TG secretion in AF ATGL$^{\triangle hep}$ mice. Third, we found that ATGL deletion

in hepatocytes aggravates alcohol-induced liver injury and inflammation as indicated by elevated plasma ALT and AST levels, the upregulation of chemokine CXCL1 mRNA levels and cytokine LCN2 mRNA levels, and subsequent neutrophil infiltration in the liver. We then report that CHOP was dramatically induced in AF ATGL$^{\triangle hep}$ mice, suggesting CHOP-associated cell death might related to the enhanced liver inflammation in AF ATGL$^{\triangle hep}$ mice. Last, we report that alcohol-induced hepatic fibrosis is exacerbated by hepatocyte-specific deletion of ATGL. Taken together, data presented in the current study indicate that hepatocyte-specific deletion of ATGL exacerbates alcohol-induced hepatic steatosis through impairing ACSL5-mediated FFAs activation and their subsequent incorporation into TGs by DGAT1, therefore resulting in suppressed VLDL-TG secretion; hepatic lipotoxicity and inflammation in AF ATGL$^{\triangle hep}$ mice might relate to CHOP-associated cell death, and CXCL1- and LCN2 upregulation-induced neutrophil infiltration in the liver. However, because the levels of liver TGs and FFAs are both significantly elevated in AF ATGL$^{\triangle hep}$ mice, accompanied by enhanced liver injury, we cannot, at this point, rule out either TGs or FFAs for inducing lipotoxicity and cell death, this will become one objective of chapter III where we dissect the role of accumulated TGs and FFAs on inducing cell death.

CHAPTER III: ULTRASTRUCTURAL ALTERATIONS OF THE LIVER INDUCED BY ALCOHOL AND HEPATOCYTE-SPECIFIC ATGL DELETION

Abstract

Biochemical analyses in Chapter II showed that hepatocyte-specific deletion of ATGL exacerbates alcohol-induced lipid accumulation and inflammatory responses in the liver of mice. However, it is unclear how and to what extent such alterations impact on the ultrastructure of the hepatocytes and non-parenchymal cells. Being a highly metabolic active organ in the body, the liver participates in handling large amounts of nutrients, such as amino acids, lipids, carbohydrates, and vitamins, and detoxifying toxicants, including xenobiotics, viruses, and bacterial-derived pathogens. To cope with metabolic demands, the liver is composed of multiple types of cells, each with distinct structure and specialized subcellular components. This study utilized transmission electron microscope (TEM) technique to examine subcellular structural and functional changes in the liver of mice exposed to alcohol with or without hepatocyte-specific ATGL deletion. TEM is a powerful tool for directly examining small physical specimens that are unapproachable by light microscope or other methods. We found that alcohol intoxication caused multiple structural and morphological changes in the hepatocytes, Kupffer cells, hepatic stellate cells, and cholangiocytes, which were exacerbated by hepatic ATGL deficiency. The mostseverely damaged cell type in the liver was the hepatocytes. Examination of the hepatocytes at higher magnification showed that alcohol intoxication resulted in lipid droplets accumulation, ER dilation, mitochondria abnormality, glycogen reduction, nuclei condensation and deformation, and increased autophagy clearance machinery. Hepatocyte-specific ATGL deletion dramatically amplified alcohol-induced lipid droplets accumulation, which may serve as a driving force of the subsequent cellular organelle abnormalities. ATGL deficiency-mediated lipid accumulation was not limited in the hepatocytes. Indeed, excessive lipid droplets were also

found in the sinusoid and cholangiocytes. Collagen deposition, a sign of fibrosis, was detected in the liver of mice deficient in ATGL, which was aggravated after alcohol feeding, suggesting a role of lipotoxicity in the initiation and progression of alcoholic cirrhosis. Taken together, the findings about hepatic ultrastructural changes of mice exposed to alcohol with or without hepatocyte-specific ATGL deletion provides direct visual evidence of lipotoxicity in the pathogenesis of ALD.

Introduction

The liver is the largest gland in the human body. To cope with the demands in handling large amount of nutrients and detoxifying xenobiotics and pathogens, the liver has developed a sophisticated and highly organized structure to support the activities of the organ (Muriel, n.d.). Although great achievements have been made in implementing new biological analyses in the diagnosis and staging of liver diseases, histopathological analysis of liver tissue remains an indispensable and powerful tool in clinical and experimental studies of liver diseases. Transmission electron microscope (TEM) uses a beam of electrons to produce higher resolution images than standard light microscopes. With this unique property, TEM can be used to examine subcellular structures and compartments of a single cell in a wide range of magnification, which is unapproachable by most other techniques (Franken et al., 2020).

The structural and functional unit of the liver is the hepatic lobule, which is composed of parenchymal and vascular elements (Goldblatt & Gunning, 1984). There are three conceptual interpretations of hepatic lobule: 1) the classic hepatic lobule concept based on structural parameters of having an efferent venule at the center and portal tracts at the periphery (Fawcett, 1955); 2) the portal lobule concept based on the bile drainage pathway; 3) the acinus of Rappaport based on the gradient distribution of oxygen (Rappaport, 1973). The liver lobule consists of parenchymal hepatocytes, epithelial cells, cholangiocytes, and non-parenchymal cells, such as Kupffer cells, hepatic stellate cells (HSC), and liver sinusoidal endothelial cells

(LSEC). Hepatocytes are the basic structural component and the most abundant cells in the liver. They account for 60% of the total hepatic cells and 80% of the total liver mass (Sasse et al., 1992). A hepatocyte has a basolateral domain and an apical domain. The basolateral domain contains abundant microvilli and faces the space of Disse, whereas the apical domain borders the bile canaliculus. To fulfill the metabolic functions, the hepatocyte is rich in a complex array of subcellular organelles, the most abundant of which are the mitochondria, endoplasmic reticulum (ER), peroxisomes, and lysosomes (Schulze et al., 2019). Cholangiocytes are epithelial cells of the bile duct (Dianat et al., 2014). They are cuboidal in shape and have elongated nuclei and smaller mitochondria than those of hepatocytes. Sinusoidal cells are the predominant non-parenchymal cells, comprising 35% of the total hepatic cell number, among which 44% are LSECs, 35% for Kupffer cells, 10-25% are HSCs, and 5% are hepatic NK cells (Blouin et al., 1977; Knook & Sleyster, 1980; Weibel et al., 1969). A typical feature of LSECs under TEM is the presence of numerous endocytic vesicles (Eskild et al., 1989). Kupffer cells are residential macrophages in the liver and are anchored to the periportal zone of the liver lobule with irregular shapes. Kupffer cells are featured with cytoplasmic extensions and numerous phagosomes and lysosomes (Bouwens et al., 1986). HSCs are located within the space of Disse and comprise about 1.5% of the hepatic volume. These cells synthesize and secrete a variety of extracellular matrix. HSCs remain in a quiescent and non-proliferative state and can proliferate upon stimulation by Kupffer cells and hepatocytes. The nuclei of HSCs are oval and slightly elongated and identified by the presence of lipid droplets (LDs) containing vitamin A in the cytoplasm (Ito & Nemoto, 1952).

The studies with TEM have been most helpful in visualizing structural and functional changes in the liver during the onset and progression of liver diseases. Hereditary hemochromatosis is an example of the disease characterized by increased accumulation of iron in lysosomal hepatocytes (Jonas et al., 2002). Wilson's disease is a disorder of copper metabolism, and TEM detection of excessive copper deposits in the liver remains a standard

diagnostic method (Johnson & Campbell, 1982). The stages of ALD are diagnosed and characterized by structural changes in the liver (Gao & Bataller, 2011). The earliest and reversible manifestation is alcoholic steatosis, which features the accumulation of lipid droplets in the hepatocytes. Steatohepatitis is a status that fatty liver is accompanied with inflammatory responses. Collagen proliferation and fibrosis in the liver indicate an irreversible stage of ALD, named alcoholic cirrhosis. The liver may eventually advance to hepatocellular carcinoma with malignant transformation of the hepatocytes. Studies investigating the subcellular organelle changes of the liver via TEM have revealed valuable information. In a study examined 100 ALD patients, the most consistent ultrastructural changes in the liver were lipid accumulation and dilation of the ER in the patients compared with control groups (Grases et al., 1987). Of note, collagen deposition was detected earlier and more accurately by TEM compared to light microscope (Grases et al., 1987). In another study, researchers detected changes in multiple subcellular organelles, such as mitochondria, ER, glycogen, and lipid in liver biopsies of patients with ALD, even though these changes did not correlate with disease severity (T. S. Chen et al., 1987). A small cohort study examined 11 patients with ALD and identified myofibroblast proliferation and collagen deposition around the terminal hepatic venule, which is the first lesions for the development of alcoholic cirrhosis (Nakano et al., 1982). Moreover, emerging evidence suggest that dysregulation of autophagy is closely associated with the progression of ALD (Babuta et al., 2019). Autophagy is a lysosomal degradation pathway and represents a major cellular clearance mechanism. Since the discovery of autophagosome in the late 1950s (Rhodin, n.d.), TEM has been one of the main tools used to study the autophagy machinery from autophagosomes to autolysosomes after fusion with lysosomes. It remains unknown that how hepatocyte-specific knockout of ATGL and/or alcohol impact on these cellular degradation machinery components.

In this Chapter, we will implement the unique TEM method to characterize ultrastructural changes in mouse liver after alcohol intoxication. More importantly, we will explore the role of

hepatocyte ATGL in maintaining the structural and functional homeostasis in the liver and determine whether a synergistic effect exists between hepatocyte ATGL and alcohol intoxication.

Materials and Methods

Mice

C57BL/6J wild-type (WT), ATGL floxed mice ($ATGL^{flox/flox}$, stock no. 024218), and albumin-Cre mice (Alb-Cre, stock no. 003574) were purchased from the Jackson Laboratory (Bar Harbor, ME). The breeding strategy for the generation of hepatocyte-specific ATGL knockout mice is previously described in Chapter II, as shown in Fig. 2.1 $ATGL^{flox/flox}$ mice were crossed bred with Alb-Cre mice to generate hepatocyte-specific ATGL knockout ($ATGL^{\triangle hep}$) mice. Mice were handled and all experiments were performed in accordance with the protocol approved by the North Carolina Research Campus Institutional Animal Care and Use Committee.

Chronic Alcohol Feeding and Treatment

Mice were maintained on a 12h light/ 12h dark cycle. Male $ATGL^{\triangle hep}$ mice at 12 weeks old were randomly subjected to either an ethanol-containing Lieber-DeCarli liquid diet (alcohol-fed, AF; n=5) or an isocaloric control (pair-fed, PF; n=5) liquid diet for eight weeks as previously described (23). Littermates of Alb-Cre negative $ATGL^{flox/flox}$ (WT) mice were used as controls. Briefly, ethanol content (%, w/v) in the alcohol diet was gradually increased from 4.00% to 4.14%, 4.28%, and 4.42% every two weeks. The AF mice were fed *ad libitum*, while PF mice were fed with the control diet as the same amount consumed by AF mice in the previous day. All ingredients used in the liquid diets were obtained from *Dyets* (Bethlehem, PA) except for ethanol (Sigma-Aldrich, St Louis, MO). At the end of 8 weeks of feeding, mice were anesthetized with inhalational isoflurane; liver samples were obtained and preserved in 2.5%

glutaraldehyde solution (Electron Microscopy Sciences, Hatfield, PA) for transmission electron microscopy analysis.

Transmission Electron Microscopy

Primary Fixation

Liver samples were cut into 1 cubic millimeter sizes, immerse completely in 2.5% cold glutaraldehyde solution in 0.1 mol/l sodium cacodylate buffer (PH 7.4) with occasional agitation for 2 – 3 hours.

Secondary Fixation

Tissue slices were then rinsed with 0.1 mol/l cacodylate (PH 7.4) for 3 times and 5 – 10 minutes /change, post-fixed with 1% osmium tetroxide (OsO_4) in 0.1 mol/l cacodylate at 4°C for 1 hour and rinsed with 0.1 mol/l cacodylate (PH 7.4) for another 3 times.

Dehydration Series with Solvent

Rinsed tissue slices were dehydrated in ascending series of ethyl alcohol as follows: 50% ethanol for 10 minutes → 75% ethanol for 10 minutes → 100% ethanol for 20 minutes → 100% ethanol for 20 minutes → 100% propylene for 15 minutes → 100% propylene for 15 minutes. All procedures were handled at room temperature.

Resin Infiltration and Embedding

Dehydrated tissues were drained most of the propylene oxide, leaving only a few to avoid drying out. A solution with propylene oxide and embedding medium (Embed 812, Electron Microscopy Sciences) mixture at 2: 1 ratio was used to embed the tissues for 2 hours at room temperature, followed by propylene oxide and embedding medium solution at 1:1 ratio for 2 hours at room temperature, 100% embedding medium overnight, and 100% embedding medium the following morning for another 15 minutes at room temperature. Lastly, the tissues were embedded in pure resin dissolved in 100% embedding medium and let polymerized overnight at 60°C.

Sectioning and Mounting Sections on Specimen Grids

Embedded liver tissue blocks were thick- and ultrathin- sectioned by the Electron Microscopy Laboratory at Atrium Health. Briefly, liver tissue blocks were first thick sectioned, stained with toluidine blue, and studied by a light microscope. Suitable areas were chosen for TEM and sectioned extremely thinly at less than 100 µm. The sections are mounted on specimen grids that fit into the microscope sample holder.

Post Staining and Examination

To increase the contrast of the specimen, the sections were post-stained with lead citrate that binds to cell components and scatters the incident beam electrons. Therefore, the areas of the specimen section which scatter electrons are recorded as darker pixels, whereas background stands out as brighter area. The sections were observed with a JEOL 1400 transmission electron microscope at 120 kV operating voltage (JEOL Ltd., Tokyo, Japan). Ultrastructure of hepatic sinusoid, bile duct, and different types of hepatic cells, including hepatocytes, macrophages, and hepatic stellate cells, was examined.

Results

TEM Analysis of the Ultrastructure of Hepatocytes

Ultrastructure of hepatocytes, particularly the organelles, was observed by TEM. As shown in Fig. 3.1A, normal hepatocytes from PF floxed mice showed euchromatic nuclei and no LD accumulation in the cytoplasm. A small amount of LD was induced in the hepatocytes of AF floxed mice (Fig. 3.1B). Hepatocytes from the liver of PF ATGL$^{\triangle hep}$ mice have irregular sized and shaped nuclei and expanded LDs that distended the hepatocytes (Fig. 3.1C). We further observed that LDs coalesced to form giant LDs in the hepatocytes of AF ATGL$^{\triangle hep}$ mice, resulting in distended hepatocytes, deformed nuclei, and disruption of the normal distribution of organelles (Fig. 3.1D).

Mitochondria remain a focus of ultrastructural studies in hepatic steatosis due to their critical roles in fatty acid oxidation. High-magnification transmission electron micrographs of hepatocytes in PF floxed mice showed the usual number and pattern of mitochondria, normal glycogen storage without LD accumulation in cytoplasm (Fig. 3.2A). Alcohol feeding induced expansion of LDs, reduced the number of mitochondria, let to the presence of swollen mitochondria, and decreased glycogen storage in the cytoplasm of the hepatocytes in AF floxed mice (Fig. 3.2B). We detected large LD accumulation along with a reduced number of mitochondria and decreased cytoplasmic storage of glycogen in the hepatocytes of PF ATGL$^{\triangle hep}$ mice compared to PF floxed mice (Fig. 3.2C). Hepatocytes of AF ATGL$^{\triangle hep}$ mice revealed the process of giant LDs fusing into each other, indicating one of the mechanisms involved in LDs growth and enlargement. Decreased glycogen storage and abnormally shaped nuclei were also observed in the hepatocytes of AF ATGL$^{\triangle hep}$ mice (Fig. 3.2D). Hepatocytes are spatially heterogeneous that react differently to FFAs overload (24). We observed extreme LDs accumulation in one particular hepatocyte from AF ATGL$^{\triangle hep}$ mice where accumulated LDs almost completely occupied the space of cytoplasm, resulting in a disturbed distribution of other organelles (Fig. 3.2E). In addition, an abnormally shaped nucleus with unusual distribution of its chromatin and accumulation of LDs inside the nucleus were also observed in one particular hepatocyte from AF ATGL$^{\triangle hep}$ mice (Fig. 3.2E). Autolysosomes were seen in both AF floxed mice and AF ATGL$^{\triangle hep}$ mice (Fig. 3.2 B, D, and F).

Ultrastructural analysis of the endoplasmic reticulum (ER) is informative due to its critical role in lipid metabolism. Studies have shown that chronic alcohol exposure induces modest ER dilation and fragmentation in hepatocytes of patients with alcohol use disorder and zebrafish (25–27). In our mouse model, hepatocytes from PF floxed mice showed normally distributed rough endoplasmic reticulum (ER) that was closely packed parallel with flattened cisternae (Fig. 3.3A). Indeed, alcohol feeding slightly induced ER dilation in the hepatocyte of AF floxed mice

(Fig. 3.3B). Moreover, we observed apparent ER dilation and fragmentation in hepatocytes of ATGL$^{\triangle hep}$ mice regardless of alcohol feeding (Fig. 3.3 C and D).

Figure 3.1 Low-magnification Transmission Electron Micrographs of Hepatocytes in Mouse Liver

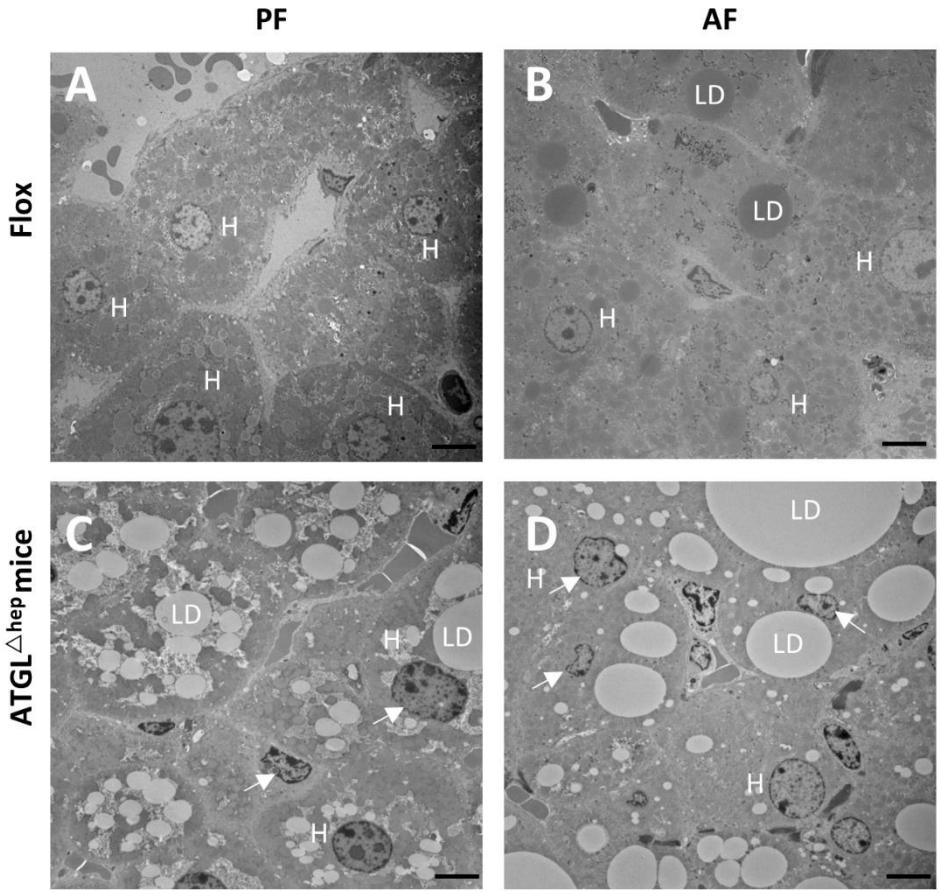

Note. Wild type (flox) and hepatocyte-specific ATGL deletion (ATGL$^{\triangle hep}$) mice were fed with control (PF) or ethanol (AF) liquid diet for 8 weeks. (A-D) Electron micrographs of hepatocytes from PF floxed, AF floxed, PF ATGL$^{\triangle hep}$, and AF ATGL$^{\triangle hep}$ mice, respectively. Note marked LD expansion and abnormal sized and shaped nuclei (white arrows) in the hepatocytes of ATGL$^{\triangle hep}$ mice. Giant LDs, deformed nuclei (white arrows), and disturbed distribution of organelles are observed in distended hepatocytes in AF ATGL$^{\triangle hep}$ mice. H: hepatocyte, LD: lipid droplet, white arrows: deformed nucleus (Scale bars, 6 μm, x 2500).

Figure 3.2 High-magnification Transmission Electron Micrographs of Hepatocytes in Mouse Liver

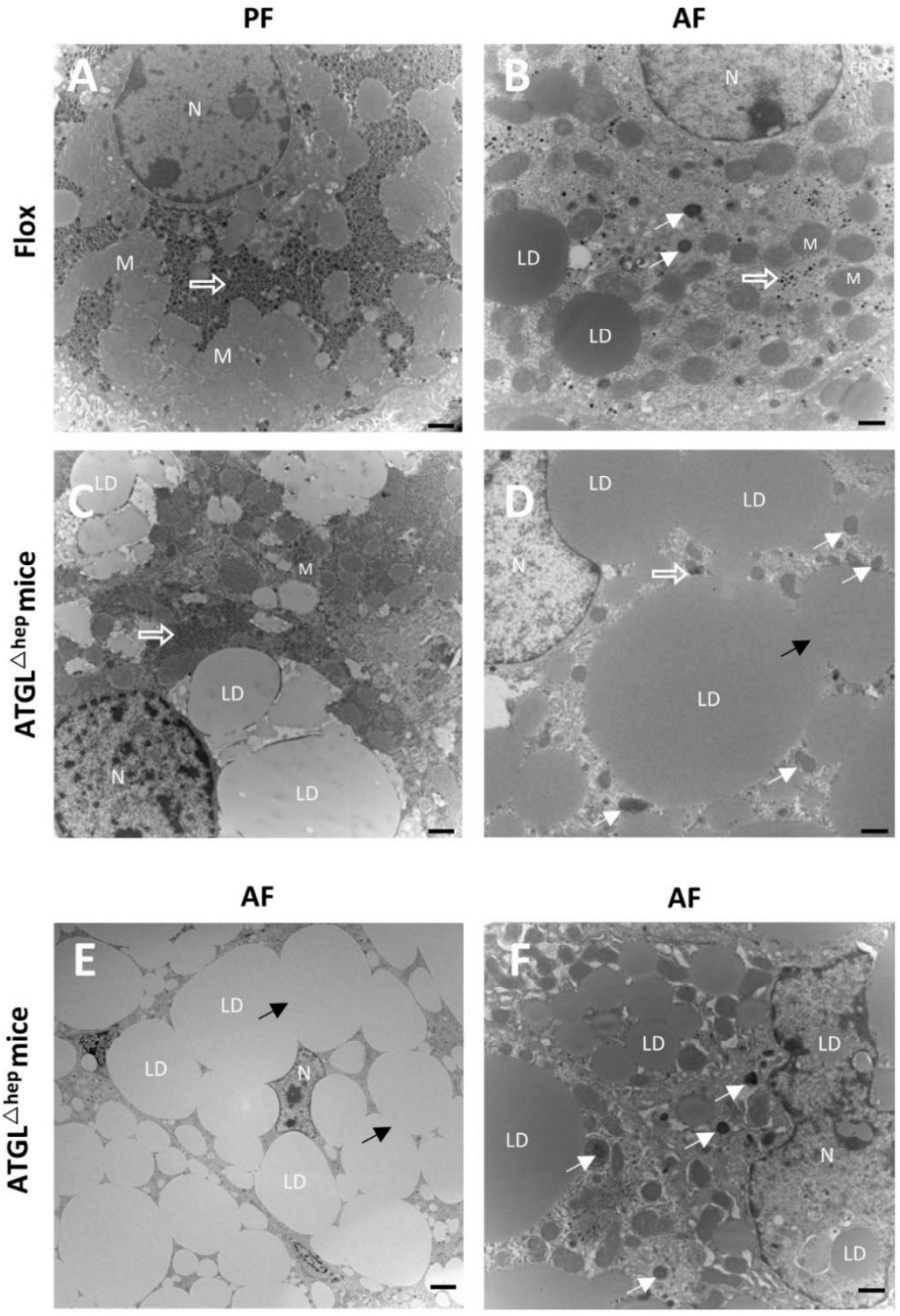

Note. Wild type (flox) and hepatocyte-specific ATGL deletion (ATGL$^{\triangle hep}$) mice were fed with control (PF) or ethanol (AF) liquid diet for 8 weeks. (A-C) Electron micrographs of hepatocytes from PF floxed, AF floxed, and PF ATGL$^{\triangle hep}$ mice, respectively. (D-F) Electron

micrographs of hepatocytes from AF ATGL$^{\triangle hep}$ mice. N: nucleus, M: mitochondria, LD: lipid droplet, white arrows: autolysosomes, hollow arrows: glycogen, black arrows: fusion of lipid droplets (Scale bars, 1 μm, x 10000).

Figure 3.3 Transmission Electron Micrographs of Hepatocytes in Mouse Liver

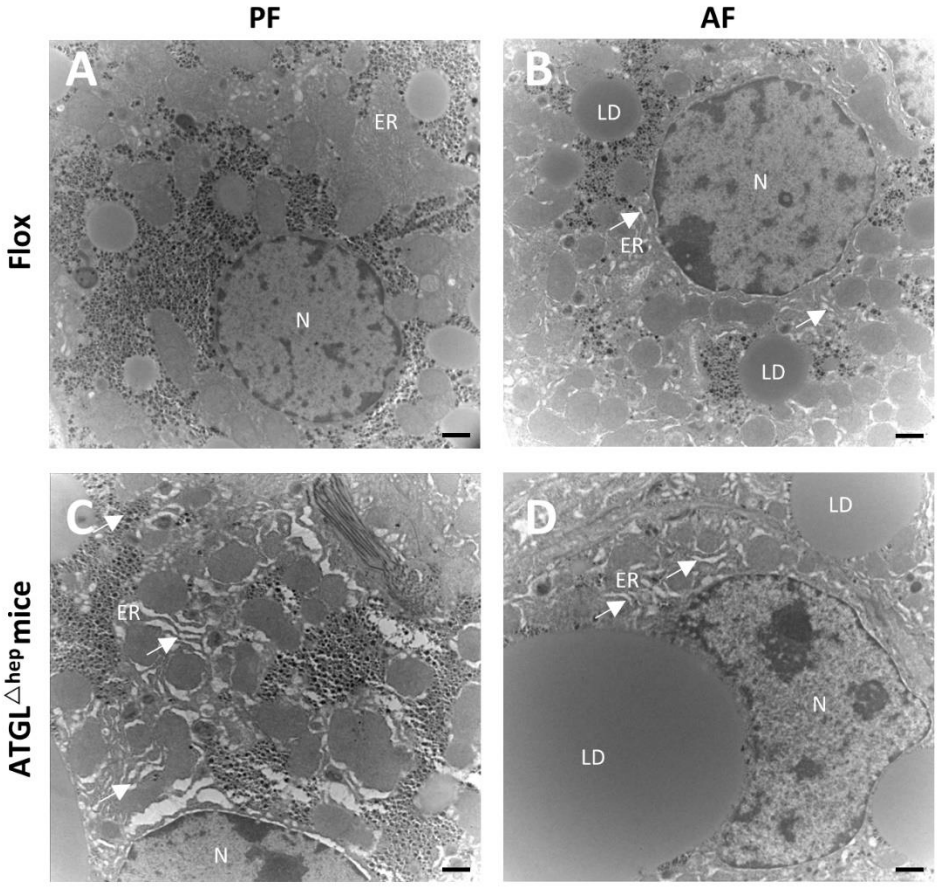

Note. Wild type (flox) and hepatocyte-specific ATGL deletion (ATGL$^{\triangle hep}$) mice were fed with control (PF) or ethanol (AF) liquid diet for 8 weeks. (A-D) Electron micrographs of hepatocytes from PF floxed, AF floxed, PF ATGL$^{\triangle hep}$, and AF ATGL$^{\triangle hep}$ mice, respectively. N: nucleus, LD: lipid droplet, ER: endoplasmic reticulum, white arrows: ER dilation and fragmentation (Scale bars, 1 μm, x 10000).

TEM Analysis of Collagen Deposition in the Liver of Hepatocyte-specific ATGL Deletion Mice

Liver fibrosis is characterized by the accumulation of extracellular matrix components accumulation such as collagen (28). To evaluate how ATGL affects hepatic fibrogenesis, electron micrographs of liver tissues from the mice were obtained. We did not observe collagen deposition in the liver of floxed mice regardless of alcohol feeding (Fig. 3.4 A and B). Hepatocyte-specific ATGL deletion induced collagen deposition in the liver of PF ATGL$^{\triangle hep}$ mice (Fig. 3.4C), while the most collagen deposition was detected in the liver of AF ATGL$^{\triangle hep}$ mice (Fig. 3.4D).

Figure 3.4 Collagen Deposition in the Liver of Mice by Transmission Electron Microscopy

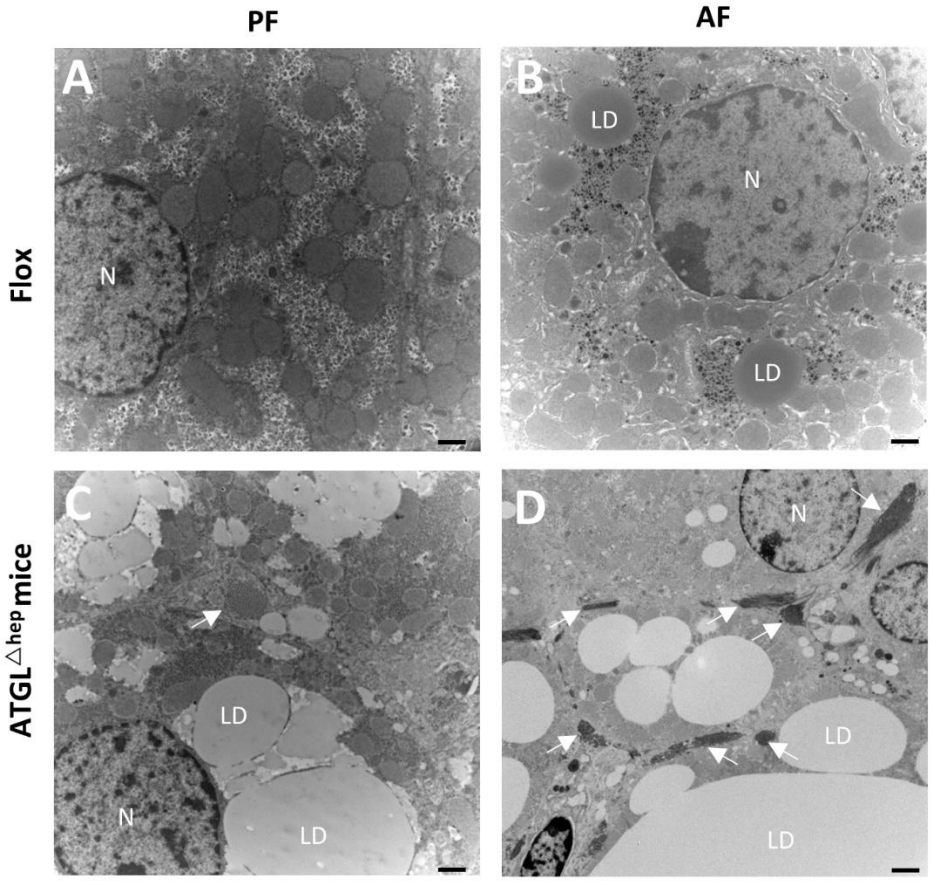

Note. Wild type (flox) and hepatocyte-specific ATGL deletion (ATGL$^{\triangle hep}$) mice were fed with control (PF) or ethanol (AF) liquid diet for 8 weeks. (A-D) Electron micrographs obtained

from liver tissues of PF floxed, AF floxed, PF ATGL$^{\triangle hep}$, and AF ATGL$^{\triangle hep}$ mice, respectively. N: nucleus, LD: lipid droplet, white arrows: collagen deposition (Scale bars, 1 μm, x 10000).

Large Lipid Droplets are Observed in the Sinusoid of the Liver by TEM

The liver filters and clears intestinal and systemic toxins such as endotoxin and ethanol through sinusoidal cells-Kupffer cells, sinusoidal epithelial cells, and hepatic stellate cells-that form the sinusoid wall (29). Electron micrograph of the liver in PF floxed mice showed a normal sinusoid with proper openness and preserved structure of all three types of sinusoidal cells present (Fig. 3.5A). Alcohol feeding or hepatocyte-specific ATGL deletion alone was sufficient to induce small LDs present in the sinusoid of the liver (Fig. 3.5 B and C). We also found an accumulation of large LDs in the sinusoidal lumen of the liver in AF ATGL$^{\triangle hep}$ mice (Fig. 3.5D). Moreover, we observed the process of growing LDs breaking through the space of Disse into the sinusoid, as indicated by white arrows in Fig. 3.5.

Figure 3.5 Large Lipid Droplets are Observed in the Sinusoid of the Liver by Transmission Electron Microscopy

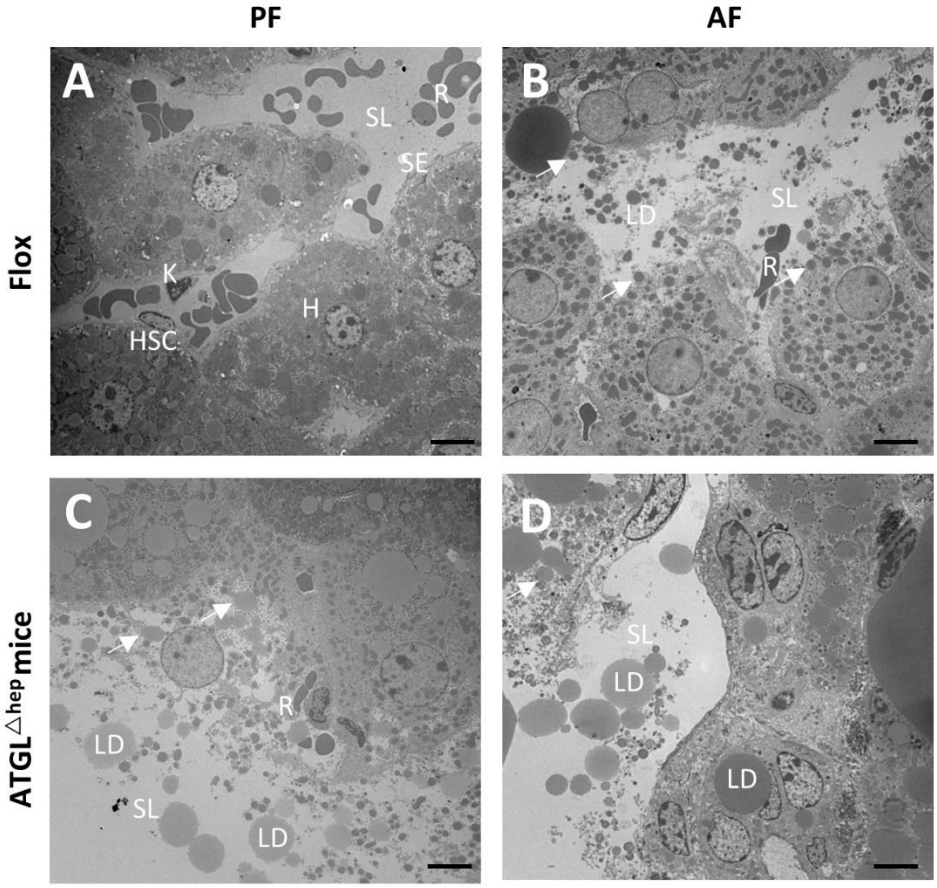

Note. Wild type (flox) and hepatocyte-specific ATGL deletion (ATGL$^{\triangle hep}$) mice were fed with control (PF) or ethanol (AF) liquid diet for 8 weeks. (A-D) Electron micrographs of sinusoid of the liver in PF floxed, AF floxed, PF ATGL$^{\triangle hep}$, and AF ATGL$^{\triangle hep}$ mice, respectively. SL: sinusoidal lumen, R: red blood cells, SE: sinusoidal epithelial cell, K: Kupffer cell, H: hepatocyte, HSC: hepatic stellate cell, LD: lipid droplet, white arrows: LDs breaking space of Disse into sinusoid (Scale bars, 6 μm, x 2500).

TEM Analysis of Kupffer Cell Activation

We next explored how hepatocyte-specific ATGL deletion affects liver-resident macrophages, Kupffer cells, in the mouse liver. Kupffer cells from the liver of both PF floxed

mice and PF ATGL$^{\triangle hep}$ mice showed normal appearance with regular shape, size, and smooth surface (Fig. 3.6 A and C). Kupffer cells from the liver of AF floxed mice showed autolysosome in the cytoplasm and have an irregular shape, extended microvilli and filopodia, and a rough surface (Fig. 3.6B). Activation of Kupffer cell in AF ATGL$^{\triangle hep}$ mice was observed as indicated by the marked increase in size and the accumulation of several autolysosomes in the cytoplasm of Kupffer cell.

Figure 3.6 Transmission Electron Micrographs of Kupffer Cells in Mouse Liver

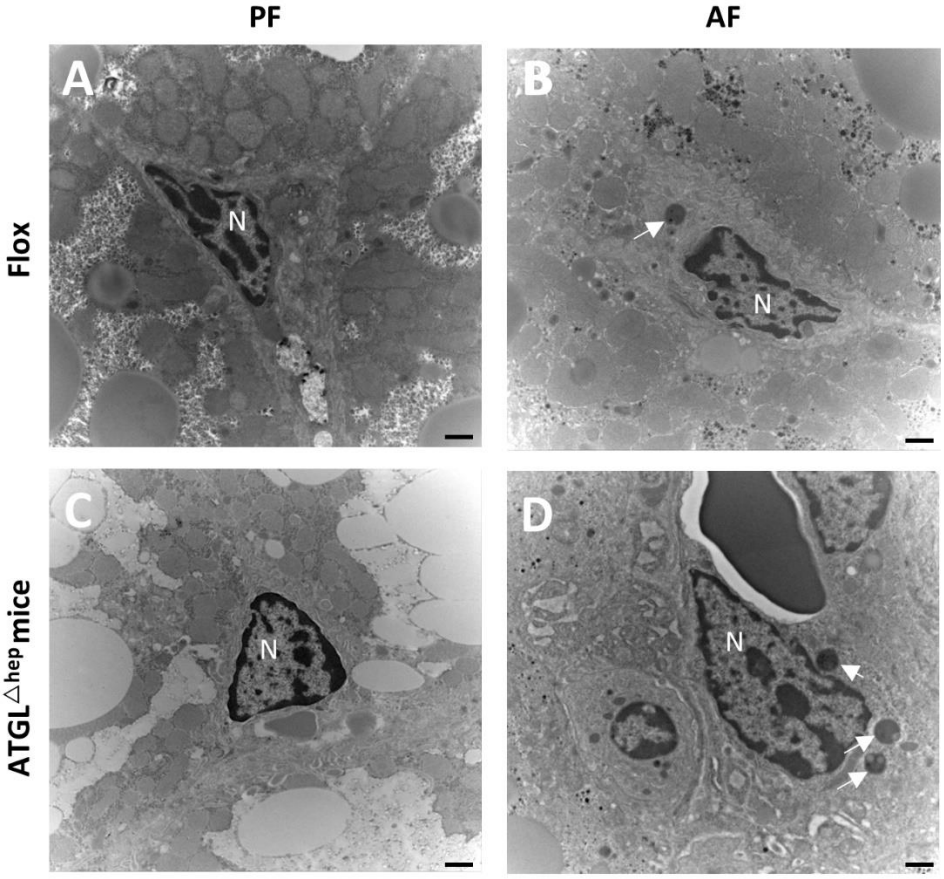

Note. Wild type (flox) and hepatocyte-specific ATGL deletion (ATGL$^{\triangle hep}$) mice were fed with control (PF) or ethanol (AF) liquid diet for 8 weeks. (A-D) Electron micrographs of Kupffer cells in the liver of PF floxed, AF floxed, PF ATGL$^{\triangle hep}$, and AF ATGL$^{\triangle hep}$ mice, respectively. N: nuclei, white arrows: autolysosome (Scale bars, 1 μm, x 10000).

TEM Analysis of the Bile Ducts

The bile duct lumen of PF floxed mice is lined with cholangiocytes with the normal distribution of organelles (Fig. 3.7A). Alcohol feeding did not change the appearance of the cholangiocytes in AF floxed mice (Fig. 3.7B). We observed apparent accumulation of various sizes of LDs in the cholangiocytes in AF ATGL$^{\triangle hep}$ mice (Fig. 3.7C). The higher magnification electron micrograph of the cholangiocytes from AF ATGL$^{\triangle hep}$ mice showed accumulation of giant LDs in the cytoplasm and deformed nuclei. In this particular cholangiocyte, we observed the fusion of small-sized LDs into giant ones (Fig. 3.7D).

Figure 3.7 Transmission Electron Micrographs of Bile Duct Lumen in Mouse Liver

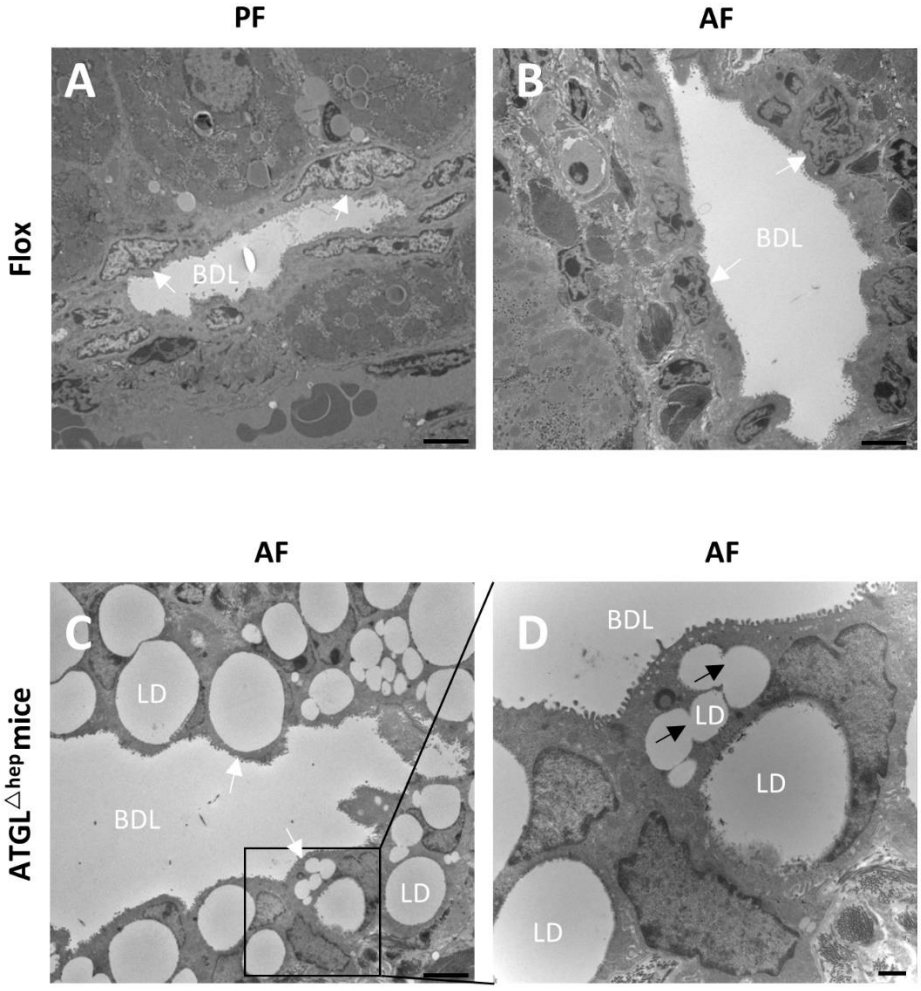

Note. Wild type (flox) and hepatocyte-specific ATGL deletion ($ATGL^{\triangle hep}$) mice were fed with control (PF) or ethanol (AF) liquid diet for 8 weeks. (A-C) Low magnification electron micrographs of bile duct lumen in the liver of PF floxed, AF flox, and AF $ATGL^{\triangle hep}$ mice, respectively. (D) High- magnification electron micrograph of cholangiocytes from the liver of AF $ATGL^{\triangle hep}$ mice. BDL: bile duct lumen, white arrows: cholangiocytes, LD: lipid droplet, black arrows: fusion of lipid droplets (Scale bar A-C, 4 μm, x 4000; Scale bar D, 1 μm, x 10000).

Discussion

In this study, we utilized the transmission electron microscope technique to investigate how alcohol or/and hepatocyte-specific ATGL deletion impact the ultrastructure of the mouse liver. We firstly showed that alcohol intoxication perturbed the normal subcellular structure of hepatocytes in the mice, including the reduced number of mitochondria and glycogen storage, induction of LD accumulation, dilated and fragmented ER, and the presence of autolysosomes in the cytoplasm, which are exacerbated by hepatocyte-specific ATGL deletion. Next, we demonstrated that ATGL deletion alone is sufficient to induce collagen deposition in the liver of the mice, which is aggravated by alcohol intoxication. Third, we observed the presence of LDs in the sinusoid of the liver of mice fed with alcohol; ATGL deletion increases both the number and the size of the LDs released in the sinusoids. Forth, we demonstrate that alcohol intoxication can activate Kupffer cells and induce the formation of autolysosomes in them, which are further exacerbated by ATGL deletion. In addition, we also found severe accumulation of LDs in the cholangiocytes that line up the bile duct lumen. Taken together, by investigating the ultrastructure changes in the liver, we demonstrate that alcohol intoxication and hepatocyte ATGL synergistically impact the subcellular structure and function of the liver. Our findings will shed light on better understanding the pathologic mechanisms and therapeutic strategies of ALD.

As a hepatotoxin, alcohol has been reported to alter the ultrastructure of hepatocytes in the liver of patients with alcohol use disorder and experimental models of ALD (Iseri et al., 1966; Iseri & Gottlieb, 1971). Indeed, our results showed that alcohol feeding induced the formation and accumulation of large LDs, mitochondria enlargement, and ER dilation and fragmentation in the liver of mice fed with alcohol. ATGL deficiency has been shown to alter the ultrastructure of various types of cells, including macrophages, cardiomyocytes, and podocytes (W. Chen et al., 2017; Haemmerle et al., 2011; Lammers et al., 2011). ETM analysis results showed that hepatocyte-specific ATGL deficiency exacerbated alcohol-induced LD accumulation, reduction in numbers of mitochondria, and dilated and fragmented ER in the cytoplasm of hepatocytes. Krähenbühl *et al.* reported that patients with alcoholic cirrhosis have less hepatic glycogen storage per volume of hepatocytes (Krähenbühl et al., 2003). Consistent with that, we found that alcohol feeding decreased glycogen storage in hepatocytes, which was further reduced by ATGL deletion. Autolysosomes are formed in macroautophagy, where autophagosomes fuse with lysosomes to degrade cytosolic materials (Khambu et al., 2017). Ethanol has been reported to induce autophagy (Dolganiuc et al., 2012). Our results demonstrate that alcohol induces autolysosome formation in hepatocytes, which is further augmented by hepatocyte-specific deletion.

Collagen deposition is the initiating event in the fibrogenesis in the liver (Komolkriengkrai et al., 2019). Pellicano *et al.* reported collagen deposition within the hepatic parenchyma in a murine model of nonalcoholic steatohepatitis (NASH). Although alcohol alone did not induce collagen deposition in the liver of the mice, we observed collagen deposition by hepatic-specific ATGL deletion even in the absence of alcohol feeding; moreover, alcohol further exacerbated ATGL deficiency-induced collagen deposition, indicating LD accumulation sensitized the liver to alcohol intoxication.

Liver sinusoids are unique capillaries due to the presence of fenestrae and the lack of a diaphragm and a basal lamina underneath, which render sinusoids high permeability (Braet &

Wisse, 2002). *Wisse* et al. demonstrated that large lipid droplets could escape from parenchymal cells and break into the space of Disse into sinusoids in the human steatotic liver (Wisse et al., 2022). The same phenomenon is observed in our alcohol-induced steatotic liver of the mice. Of note, hepatocyte-specific ATGL deletion induces the release of giant LDs in the sinusoid regardless of alcohol intoxication. The exact mechanisms by which lipid droplets break into the sinusoids are not established; how force generated by LDs fusing into each other and the disruption of cytoplasm might, at least partially, play a role in the process.

Studies have shown that Kupffer cell activation by endotoxins and other soluble mediators plays critical roles in the pathogenesis of ALD (Cubero & Nieto, 2006). Sobaniec-Lotowska *et al.* reported that the number of lysosomes within the cytoplasm were markedly increased in hyperactivated Kupffer cells in patient with Dubin-Johnson syndrome (Sobaniec-Lotowska, 2006). In our samples, TEM analysis showed that alcohol intoxication induced the formation of autolysosomes in the cytoplasm of Kupffer cells; ATGL deletion induced accumulation of autolysosomes and nuclei enlargement in Kupffer cells, indicating that ATGL deletion further exacerbated alcohol-induced Kupffer cell activation in the liver.

Cholangiocytes are the epithelial cells of the bile duct in the liver and are one of the primary targets of many types of disease, such as NASH and ALD (Meadows et al., 2021). The most profound ultrastructural changes of cholangiocytes in hepatic-specific ATGL deletion mice is that the deposition of giant LDs. Another study investigating mice deficient in hepatic CGI-58, a coactivator of ATGL, also detected LDs in the cholangiocytes even in mice fed a chow diet (Yang et al., 2020). This observation along with the current findings provide experimental evidence showing how cholangiocytes react to injured hepatocytes. The pathogenic consequences of abnormal lipid accumulation in cholangiocytes necessitates further investigations.

In summary, the present study with TEM yields much information to our knowledge of cellular structural and functional changes in the liver induced by alcohol intoxication and/or

hepatocyte ATGL deficiency. The use of TEM in exploring the ultrastructure of liver will continue to play an important role in ALD. The concepts and classification of stages of ALD are rooted in morphology. Moreover, looking at a liver biopsy specimen under the microscope is a direct way of visualizing the morphologic changes that affect the liver in ALD. TEM coupled with biological, cytochemical, immunohistochemical, and other analytic techniques will continue to add greatly to our understanding of the liver in health and disease.

CHAPTER IV: ROLE OF TRIGLYCERIDE/LIPID DROPLET ACCUMULATION IN CELL DEATH AND CHEMOKINE/CYTOKINE EXPRESSION IN HEPATOCYTES

Abstract

Emerging evidence suggests that lipotoxicity induces ER stress-mediated hepatocyte cell death, contributing to the pathogenesis of alcohol-related liver disease (ALD). However, findings on the role of hepatic accumulation of triglycerides (TGs) versus free fatty acids (FFAs) in inducing hepatocyte cell death and inflammatory responses are inconsistent. Alcohol-induced gut-derived bacterial products translocation to the liver has been reported to be involved in the pathogenesis of hepatocyte injury and death, however, it remains unclear whether and how bulk TG/lipid droplet (LD) accumulation and endotoxin (lipopolysaccharides, LPS) may synergistically promote inflammatory responses in hepatocytes. In this study, to dissect the role of TG/LD accumulation from FFA accumulation in inducing hepatocyte cell death, we first treated mouse hepatocytes with oleic acid (OA) and ATGL inhibitor, Atglistatin. We found that OA treatment induced the accumulation of cellular TGs but not FFAs, along with reduced hepatocyte cell viability and upregulated CHOP expression. ATGL inhibition further exacerbated OA-induced TG accumulation and CHOP upregulation. We also investigated how ethanol affects intracellular lipid metabolism and cell viability in hepatocytes, our results showed that there were no changes observed either in the cellular content of TG and FFA or cell viability by ethanol treatment. Next, we examined the levels of plasma endotoxin and hepatic bacterial DNAs in hepatocyte-specific ATGL deletion mice and found that alcohol exposure increased plasma endotoxin levels and hepatic bacterial DNAs regardless of ATGL deletion. By treating hepatocytes with oleic acid and LPS, we further demonstrated that TG/LD accumulation and LPS stimulation synergistically reduced hepatocyte cell viability, and upregulated chemokine CXCL1 and cytokine LCN2 expression via IκB-ζ activation. Taken together, this study proposes that alcohol-induced

hepatic steatosis and gut-derived bacterial products translocation to the liver may synergistically promote hepatocyte cell death and hepatic inflammation in the pathogenesis of ALD.

Introduction

Ethanol and its metabolites induce hepatic accumulation of free fatty acids (FFAs) and triglyceride (TG)-enriched lipid droplets (LDs), oxidative stress, hepatocellular cell death, inflammation, and gut-derived bacterial products (i.e. endotoxins/ lipopolysacchride, LPS) translocation to the liver, which are all closely associated with the pathogenesis of ALD (P. Zhang et al., 2021). To date, there is no FDA-approved targeted therapy for ALD. Hence, it is clinically relevant to acquire a deeper understanding of the pathogenic mechanisms of alcoholic hepatic steatosis for discovering novel diagnostic and therapeutic strategies for patients with ALD.

Like other organs, mild inflammation in liver has been shown to be hepatoprotective by repairing damaged tissues and promoting the re-establishment of homeostasis. However, excessive inflammation induces tremendous hepatocyte cell death and exaggerates severity of ALD (Brenner et al., 2013). In response to heavy chronic alcohol exposure, hepatocytes express a large amount of cytokines and chemokines that promote the infiltration of monocytes/macrophages, neutrophils and other immune cells during oxidative stress and cell death (Brenner et al., 2013; Gao et al., 2019; Saiman & Friedman, 2012). Damaged hepatocytes, in turn, further stimulate inflammatory reactions, therefore a highly hepatotoxic feedforward vicious cycle of inflammation and cell death is established in the liver (Brenner et al., 2013). Alcohol-induced hepatocyte injury and death involve multiple factors; acetaldehyde from ethanol metabolism is one of the most known hepatocyte-derived cytotoxic factors. As an early pathological change, the role and mechanisms of how lipid accumulation in hepatocytes contribute to alcohol-induced hepatocyte injury and death have not been well defined. A few studies reported that accumulation of saturated free fatty acids (FFAs) induces apoptotic cell

death in liver and hepatocytes, and TG-enriched LD formation is an initial protective mechanism against FFAs-induced cytotoxicity (Malhi et al., 2006; Wang et al., 2006; Wei et al., 2006). However, contradictory findings have also been reported by several studies in ALD (Nanji et al., 1989, 1997, 2001; Ronis et al., 2004), where saturated fatty acids reduced/prevented alcohol-induced liver injury due to the reduction of steatosis (Ronis et al., 2004). The number and size of hepatic lipid droplets has been considered as gold standard for evaluating the severity of alcohol-related liver disease. Reduction of LDs in number and size have also been found to be associated with improvement of alcohol-induced liver injury. Hence, further research is necessitated to answer the questions: whether and if so, to what extent, the accumulation of intracellular TGs is protective to hepatocytes against cell death upon alcohol exposure. In chapter II, we observed remarked liver injury and inflammation accompanied by a dramatic increase in hepatic TG levels and FFA levels, hence, in this chapter, we sought to dissect the role of TG and FFA in the induction of cell death in hepatocytes.

In addition to intrahepatic factors, increasing evidence suggest that the involvement of extrahepatic factors in the pathogenesis of hepatocyte injury and death. One of the most known extrahepatic factors is gut-derived bacterial products. It has been shown that ethanol promotes gut permeability allowing microbial endotoxins, such as lipopolysaccharides (LPS), to leak into portal circulation and translocate to the liver, where LPS clearance occurs (Miyata & Nagy, 2020). Both resident macrophages (Kupffer cells) and hepatocytes are involved in the clearance of gut-derived LPS through different mechanisms (Mandrekar & Szabo, 2009; Messingham et al., 2002; Szabo & Bala, 2010). In hepatocytes, LPS is recognized by toll like receptor 4 (TLR4), LPS/TLR4 cell signaling pathway plays a critical role in hepatocyte apoptosis, which induces chemokine and cytokine expression (Szabo & Bala, 2010; Q. Zhang et al., 2021). In Chapter II, we demonstrate that hepatocyte-specific deletion of ATGL aggravates alcohol-induced expression of chemokine (CXCL1) and cytokine (LCN2), as well as subsequent neutrophil infiltration. Indeed, CXCL1 and LCN2 have been reported to be involved in ethanol-related liver

injury and inflammation (Asimakopoulou et al., 2014; Chang et al., 2015; Wieser et al., 2016). Chang *et al.* reported that high-fat diet plus acute ethanol consumption synergistically induced liver inflammation as exemplified by hepatic neutrophil infiltration mediated by upregulating CXCL1 expression (Chang et al., 2015). Cai *et al.* revealed that LCN2 overexpression in hepatocytes significantly exacerbated ethanol-induced cellular TG accumulation, while LCN2 ablation alleviated alcoholic steatohepatitis (Cai et al., 2016).

The nuclear factor-kappa B (NF-κB) is an evolutionarily conserved transcription factor, its activation can induce the expression of cytokines and chemokines during LPS stimulation (Yamazaki et al., 2001, 2008). In resting cells, NF-κB is sequestered in cytoplasm by its inhibitors, the IκB family members, including IκB-α, -β, and -ε (Yamazaki et al., 2008). Upon LPS stimulation, IκBs are degraded by the activation of IκB kinase, resulting the release of NF-κB. Liberated NF-κB translocate into the nucleus where it engages in the transcriptional activation of target genes, including CXCL1 and LCN2 (Jang et al., 2012; Listwak et al., 2013; Yamazaki et al., 2008, p.). Different from other cytoplasmic IκB family members, IκB-zeta (IκB-ζ) is an atypical member of IκB family and is mainly localized in nucleus, it was first discovered in murine organs upon LPS stimulation (Kitamura et al., 2000). IκB-ζ (nuclear) is postulated to inhibit NF-κB activity by binding to NF-κB p50 subunit and interfering with p65, and modulate the expression of various NF-κB target genes (Hildebrand et al., 2013, p. 2; Totzke et al., 2006). While the canonical NF-κB pathway directly induces the rapid activation of primary response genes, studies have also demonstrated that IκB-ζ functions not only as an inhibitor of NF-κB, but also an activator for a selective subset of NF-κB target genes (Hildebrand et al., 2013, p. 1; Müller et al., 2018; Yamamoto et al., 2004). Moreover, Brennenstuhl *et al.* demonstrated that IκB-ζ has a direct role in the regulation of CXCL1 expression in a glioma cell line resistant towards NF-κB-dependent cell death (Brennenstuhl et al., 2015).

In our animal model, plasma endotoxin levels and hepatic bacterial DNAs levels were both elevated in AF mice regardless of ATGL deletion in hepatocytes. Given that CXCL1 and

LCN2 are known to be upregulated by lipid-induced lipotoxicity and LPS stimulation, in this chapter, we will investigate the synergistic effect of hepatocellular lipid accumulation and LPS stimulation on the expression of CXCL1 and LCN2 in hepatocytes. Although it is widely reported that NF-κB is tightly involved in CXCL1 and LCN2 upregulation, little is known about whether IκB-ζ has a direct impact on the activation. Hence, it will also be explored in the current chapter.

Materials and Methods

Cell Culture and Treatments

AML12 mouse hepatocyte cells (American Type Culture Collection/ATCC, Manassas, VA) were cultured in Dulbecco's Modified Eagle Medium/Ham's Nutrient Mixture F-12, 1:1 (DMEM/F-12, Thermo Fisher Scientific, Waltham, MA) containing 10% (v/v) fetal bovine serum (Atlanta Biologicals, Lawrenceville, GA), 0.01mg/ml insulin, 0.0055 mg/mL transferrin, 6.7 ng/mL selenium (Insulin-Transferrin Selenium (ITS-G), Thermo Fisher Scientific, Waltham, MA), 40 ng/ml dexamethasone (Sigma-Aldrich, St. Louis, MO), 100 U/mL penicillin, and 100 µg/mL streptomycin (Thermo Fisher Scientific, Waltham, MA) at 37°C in a humidified atmosphere of 5% CO_2. In all experiments, after AML12 cells were seeded overnight and reached 70% confluency, we switched the standard growth medium to serum-starved medium with 2% FBS. When indicated, serum-starved medium was supplemented with various concentrations of oleic acid (OA). Fatty acid-supplemented medium was prepared as previously described (Listenberger et al., 2001). Where indicated, Atglistatin and LPS (Sigma-Aldrich, St. Louis, MO) were treated to AML12 cells at 20 mmol/l and 100 ng/ml, respectively, for 24h.

Cellular Neutral Lipid Staining

AML12 cells were seeded on 8-well chamber slides at a density of 2. 5 x 10^4 cells/cm^2 in 400 µL of standard growth medium per well and reached at 70% confluence overnight. Cells were then washed with phosphate-buffered saline (PBS), the medium was changed to serum-starved medium containing 1% of fatty acid-free bovine serum albumin supplanted with

investigated concentrations of OA, ethanol, with or without Atglistatin for 24h. Cells were washed with PBS and incubated with 2 μmol/l boron-dipyrromethene (BODIPY) 493/503 dye (Thermo Fisher Scientific, Waltham, MA) for 15 minutes at 37°C. Cells were washed with PBS and fixed in 4% formaldehyde (PFA) for 30 minutes at room temperature (RT), we then removed PFA and washed samples 3 x 5 min in PBS and counter stained cells with DAPI (Life Technologies, Carlsbad, CA) for 1 minute. Accumulation of neutral lipids in the cell was visualized by fluorescence microscope.

Quantification of Lipid Content

Cellular lipid content was quantified as total normalized fluorescence intensity (BODIPY intensity). The method was adapted from the protocol of Mallela *et al.* (Mallela et al., 2019). Briefly, AML12 cells were seeded on a 96-well flat-bottomed plate (black polystyrene plates with clear bottom, Sigma-Aldrich, St. Louis, MO) at the density of 0.8 $x10^4$/well in 150 μL of standard growth medium and reached 70% confluency overnight. Cell treatment strategy was described above. On the day of cells fixation, discarded medium by gently inverting the plate and washed the wells with 100 μL of PBS. Fixed the cells by slowing add 100 μL of 4% PFA and incubated at RT for 20 min. Discarded PFA and washed the cells 3 x 5 min in PBS. Incubated the samples with 100 μL of staining solution containing BODIPY and DAPI for 30 mins at RT, then washed the cells 3 x 5 min in PBS. Samples were read by a fluorescence microplate reader; fluorescence intensity were normalized with the values of cells without any treatment defined as 1.

Quantification of Cellular TGs and FFAs

AML12 cells were seeded on 12-well plates at a density of 1 x 10^5 cells/well in 2 mL of standard growth medium per well and reached 70%-80% confluence overnight. Cell treatment strategy was described above. Cellular TGs and FFAs levels were measured as previously described (Guo et al., 2021). Briefly, lipids were extracted by 2:1 chloroform: methanol (v/v) mixture, dried, and redissolved in a 1:1 5% Triton X-100: methyl alcohol solution (v/v). Cellular

TGs and FFAs levels were determined by colorimetric method using TG and FFA quantification kit (BioVision, Milpitas, CA), according to the manufacturer's instructions.

Flow Cytometry

AML12 cells were seeded on 12-well plates at a density of 1 x 10^5 cells/well in 2 mL of standard growth medium per well and reached 70%-80% confluence overnight. Cells were treated with various concentrations of OA and/or Atglistatin for 24h. AML12 cells apoptosis was analyzed with Annexin V and 7-AAD staining. Briefly, cells were collected and washed with ice-cold PBS, resuspended in 200 ul of binding buffer containing 5 µL of Annexin V probe (BioLegend) for 15 mins at RT in the dark, then 5 µL of 7-AAD antibody (BioLegend) was added and incubated for another 5 min. Following incubation, samples were analyzed by FACS flow cytometer (BD Bioscience, San Jose, CA). Data were analyzed with FlowJo software (TreeStar, Ashland, OR).

Cell Viability Tested by CCK-8 Assay

The effects of OA, Atglistatin, and LPS treatment on the cell viability of AML12 cells were tested by CCK-8 assay (Abcam, Cambridge, MA). AML12 cells were seeded in a 96-well flat-bottomed plate at a density of 0.8 x10^4/well in 100 µL of standard growth medium and reached 70% confluency overnight. Cells were then treated with various concentrations of OA, or Atglistatin at 20 mM, or LPS at 100 ng/ml for 24h. After incubation, 10 µL of CCK-8 dye was added to each well, cells were then incubated at 37°C for 2h, the absorbance was determined at 450 nm using microplate reader following the incubation.

Western Blot

Whole protein lysates from AML12 cells were extracted using T-PER tissue extraction reagent (Thermo Scientific) supplemented with protease and phosphatase inhibitors (Sigma-Aldrich, St. Louis, MO). Aliquots containing 30 mg of proteins were subjected to sodium dodecyl sulfate-polyacrylamide gel (8-15%) electrophoresis, transblotted onto polyvinylidene difluoride membranes (Bio-Rad, Hercules, CA), blocked with 5% nonfat dry milk in phosphate-buffered

saline solution containing 1% Tween-20, and then probed overnight with the following antibodies, including anti-ATGL, anti-CHOP (Cell Signaling Technology, Danvers, MA), anti-GAPDH (Abcam, Cambridge, MA), anti-NF-κB, and anti- IκB-ζ (Thermo Fisher Scientific), respectively. Membranes were then washed and incubated with horseradish peroxidase conjugated goat anti-mouse immunoglobulin G or goat anti-rabbit immunoglobulin G (Thermo Fisher Scientific, Rockford, IL). The bound complexes were detected with enhanced chemiluminescence (Thermo Fisher Scientific) and quantified by densitometry analysis.

RNA Isolation and Quantitative Polymerase Chain Reaction

Total RNA was extracted from mouse liver using TRIzol™ reagent (Thermo Fisher Scientific) according to the manufacturer's instruction. Complimentary DNA (cDNA) was generated using TaqMan Reverse Transcription Reagents (Thermo Fisher Scientific). Real-time PCR was performed with SYBR green PCR master mix (Qiagen, Germantown, MD, United States) using the 7500 Real Time PCR (RT-PCR) system. Primers were designed and synthesized by Integrated DNA Technologies (Coralville, CA, United States). All primers used for qPCR were listed in table 1. The mRNA levels were normalized to the expression of RPS17 rRNA and analyzed by $2^{-\Delta\Delta Ct}$ threshold cycle method (Livak & Schmittgen, 2001) with the values of WT-PF as 1.

Endotoxin Levels

Endotoxin levels in mouse blood were determined using an ELISA-based method (EndoLISA Endotoxin Detection Kit; Biovendor, Asheville, NC, United States) as per the manufacturer's instructions. The concentrations of endotoxin were expressed in endotoxin units (EU) per milliliter for plasma.

Statistical Analysis

Results are expressed as mean ± standard deviation (SD). Data were analyzed using the two-tailed student's *t*-test or one-way ANOVA test, followed by Tukey's test. $P < 0.05$ was considered as statistically significant.

Results

OA Induced Intracellular TG Accumulation and LD Expansion in a Dose-dependent Manner, Accompanied by Cell Death in Hepatocytes

Results from in vivo mouse study showed that hepatic TG levels and FFA levels are both dramatically elevated in AF ATGL□hep mice, accompanied by increased liver injury and hepatic inflammation. In this chapter, we sought to dissect the role of accumulated TGs and FFAs on cell death and inflammation. AML12 cells were treated with various concentrations of OA for 24h. Results from BODIPY staining of neutral lipid and neutral lipid quantification by relative fluorescence intensity showed that OA treatment caused cellular LDs formation in a dose-dependent manner (Fig. 4.1A and 1B). Biochemical analysis then demonstrated that, in line with neutral lipid staining results, OA treatment induced intracellular TG accumulation in a dose-dependent manner (Fig. 4.1C). However, intracellular FFA levels had no difference among treatments (Fig. 4.1D). We then investigated the effects of OA treatment on hepatocellular cell death. Flow cytometry results showed that OA treatment induced apoptosis in hepatocytes as exemplified by increased late apoptosis cells in the upper right quadrant (Fig. 4.2A). Our data showed that cell viability was not altered when cells were treated with OA at 200 μM compared with control group, however, OA treatment at 400 and 600 μM reduced cell viability of hepatocytes (Fig. 4.2B). In chapter II, we observed that hepatocyte-specific deletion of ATGL induced CHOP expression in the livers of the mice, which was further aggravated upon alcohol feeding. Hence, we also examined the effects of TG accumulation on CHOP expression in hepatocytes. Immunoblot analysis showed that CHOP was induced by OA treatment in a dose-dependent manner (Fig. 4.2C). These results indicate that it is the accumulation of cellular TGs, rather than FFAs, that account for the induction of ER stress and subsequent apoptosis in hepatocyte which promotes cell death.

Figure 4.1 Oleic Acid (OA) Induces Cellular Lipid Droplet Formation in a Dose-dependent Manner

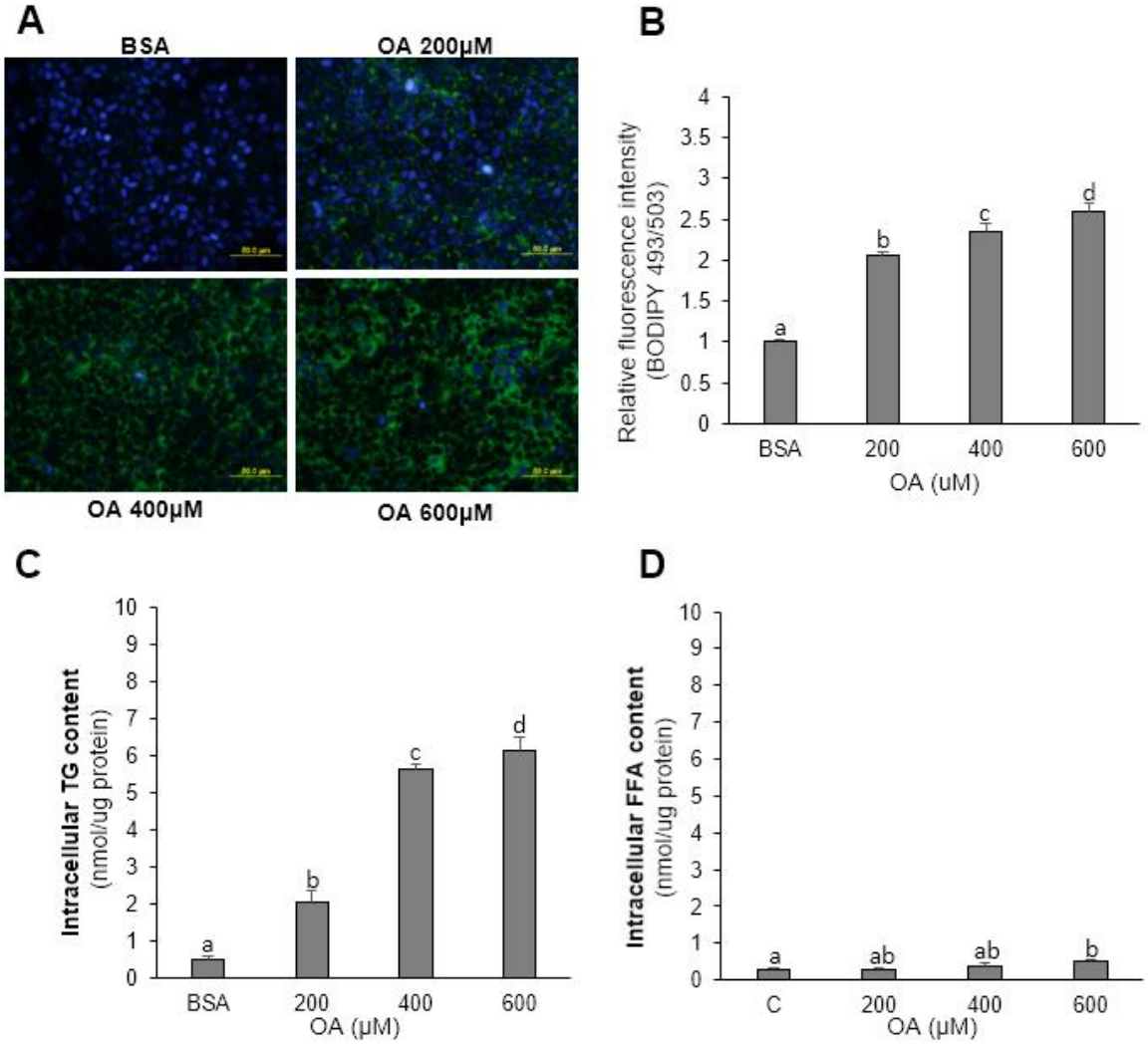

Note. AML12 cells were treated with different concentrations of OA (0, 200, 400, and 600 μM) for 24h. (A) LDs are visualized with BODIPY 493/503 staining (scale bar, 50 μm). (B) Relative fluorescence intensity of AML12 cells after BODIPY 493/503 staining (n=5/group). (C and D) Intracellular TGs and FFAs content are quantified by colorimetric assay kits (n=3/group). Data are shown as mean ± SD from each group. Significant differences (P<0.05, ANOVA) are identified with different letters.

Figure 4.2 OA Induces ATGL Expression and Reduces Cell Viability in a Dose-dependent Manner

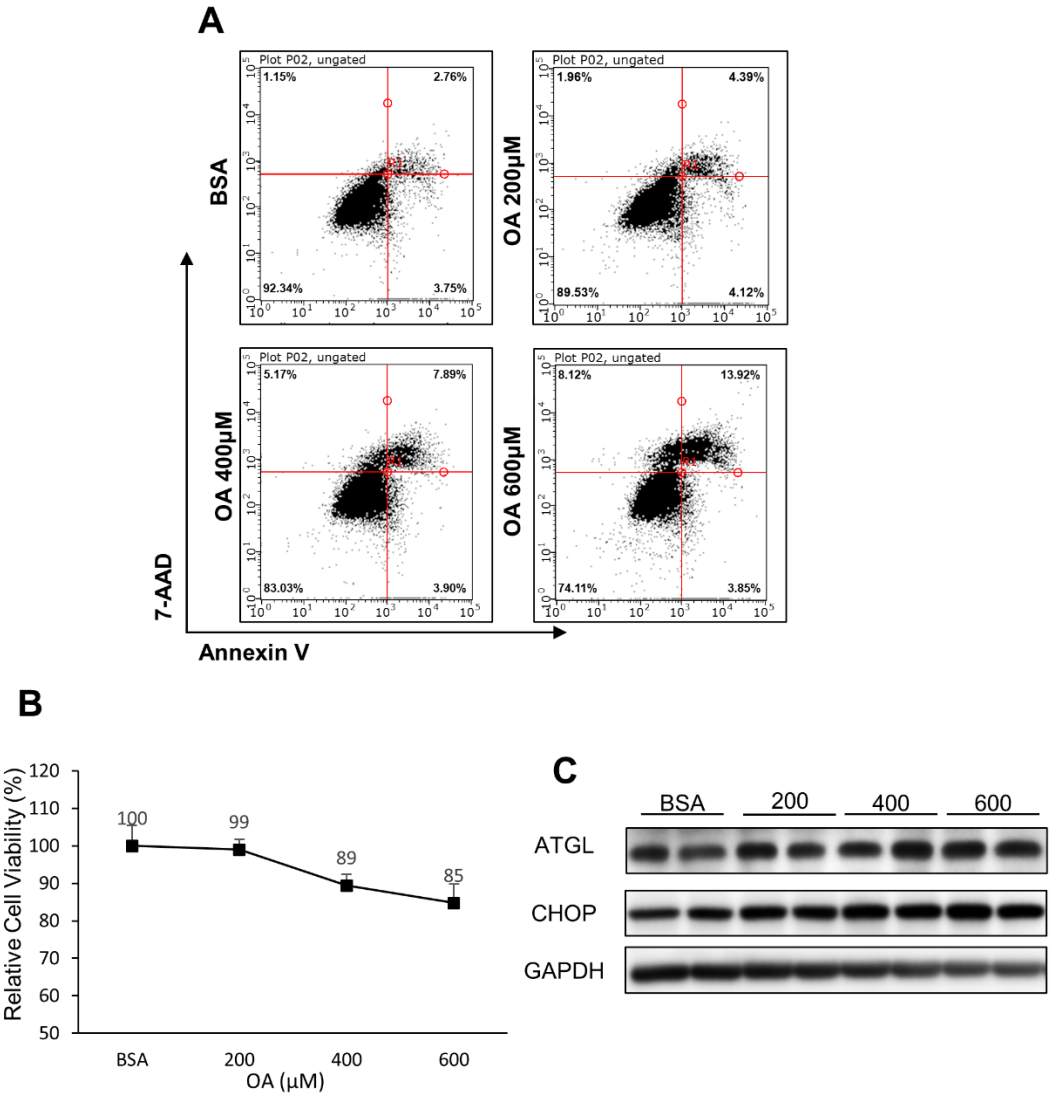

Note. AML12 cells were treated with different concentrations of OA (0, 200, 400, and 600 μM) for 24h. (A) Contour diagram of annexin V^+/7-AAD^+ flow cytometry. The upper left quadrants show the dead cells. The lower left quadrants contain viable cells. The upper right quadrants represent necrotic cells or late apoptotic cells. Lower right quadrants indicate the early apoptotic cells. (B) CCK8 assay showing that OA inhibits AML12 cell viability in a dose-

dependent manner (n=6/group). (C) Representative Western blot images showing that OA induces ATGL and CHOP expression in a dose-dependent manner.

ATGL Inhibition by Atglistatin Further Exacerbated OA-induced Intracellular TG Accumulation and Cell Death in Hepatocytes

Because our results indicated that TG accumulation is responsible for OA-induced hepatocellular cell death, we then treated AML12 cells with ATGL inhibitor, Atglistatin, to further exam whether ATGL inhibition further increase TG accumulation-induced cell death. AML12 cells were treated with OA at 200 μM, Atglistatin at 20 mM, and a combination of OA and Atglistatin for 24 h. Indeed, as shown in Fig. 4.3A, BODIPY staining of neutral lipid showed that Atglistatin alone was sufficient to promote cellular TG accumulation, and OA-induced TG accumulation is further exacerbated by ATGL inhibition in hepatocytes (Fig. 4.3B). Cellular FFA levels were not changed either by OA supplementation or Atglistatin treatment (Fig. 4.3C). We then inspected whether ATGL inhibition affects TG accumulation-induced hepatocellular cell death. Flow cytometry results showed that ATGL inhibition alone did not induce cytotoxicity, however, TG-accumulation induced hepatocyte apoptosis was further augmented with ATGL inhibition (Fig. 4.4A). The same results were observed by cell viability analysis (Fig. 4.4C). Immunoblot results revealed that TG accumulation-induced hepatic CHOP over expression was exacerbated by ATGL inhibition (Fig. 4.4B).

Figure 4.3 ATGL Inhibition by Atglistatin Treatment Exacerbates OA-induced Intracellular TG Accumulation

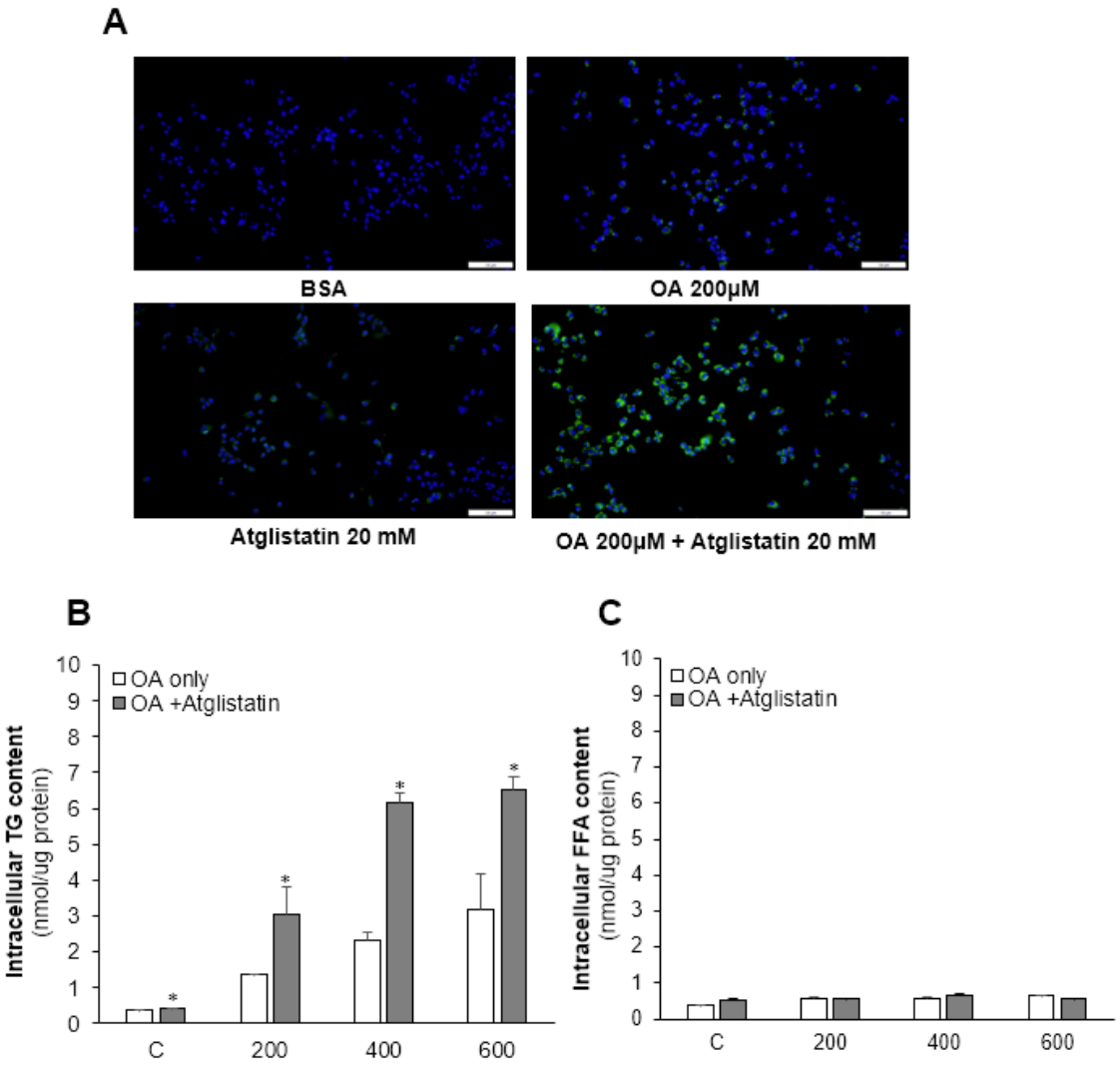

Note. (A) AML12 cells were treated with OA at 200 μM or/and Atglistatin at 20 mM for 24h. LDs were visualized with BODIPY 493/503 staining (scale bar, 100 μm). (B and C) AML12 cells were treated with different concentrations of OA (0, 200, 400, and 600 μM) and with or without Atglistatin (20 mM) for 24h. Intracellular TGs and FFAs content are quantified by colorimetric assay kits, data are presented as means ± SD (n = 3, *$P < 0.05$).

Figure 4.4 Atglistatin Treatment Exacerbated OA-induced CHOP Upregulation but Did Not Significantly Affect Cell Viability

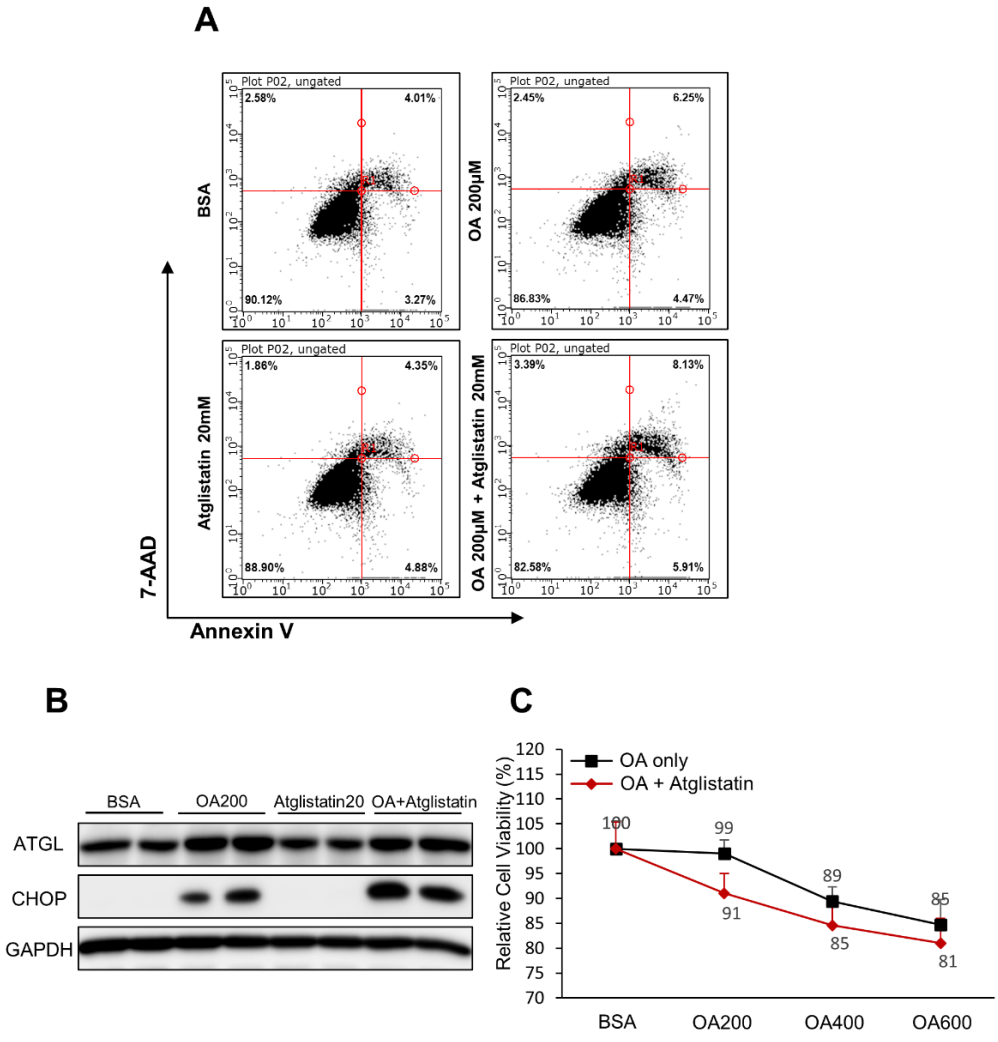

Note. (A and B) AML12 cells were treated with OA 200 μM or/and Atglistatin 20 mM for 24h. (A) Contour diagram of annexin V/7-AAD flow cytometry. The upper left quadrants show the dead cells. The lower left quadrants contain viable cells. The upper right quadrants represent necrotic cells or late apoptotic cells. Lower right quadrants indicate the early apoptotic cells. (C) Representative western blot imagines showing that Atglistatin treatment augmented TG accumulation-induced CHOP upregulation. (C) Cell viability of AML12 cells treated with

different concentrations of OA (0, 200, 400, and 600 μM) and with or without Atglistatin at 20 mM for 24h was determined by CCK8 analysis (n=6/group).

Ethanol Treatment Did Not Influence Intracellular TG Accumulation and Cell Viability

Results from our animal model demonstrated that AF ATGL□hep mice exhibit the worst liver damage and inflammatory response, as evidenced by highest levels of plasma ALT and AST, the most severe neutrophil infiltration, and the most cell death in the livers of AF ATGL□hep mice. We then investigated whether ethanol metabolism plays a direct role in mediating OA-induced TG accumulation and cell death in hepatocytes. AML12 cells were treated with serum-starved medium containing various concentrations of ethanol at 0, 25, 50, and 100 mM for 24h. BODIPY staining of neutral lipid as well as the quantitative neutral lipid analysis consistently demonstrated that ethanol treatment did not directly impact lipid droplet formation in the cells (Fig. 4.5A and 5B). In accordance, biochemical results showed that there is no significant difference in hepatocellular TG content among different treatment groups (Fig. 4.5C). Cell viability also was not affected by ethanal treatment either (Fig. 4.5D).

Next, we investigated whether ethanol treatment influence OA-induced TG accumulation and impaired cell viability. We then treated AML12 cells with 100 mM ethanol, 600 μM OA, or a combination of the two for 24h. Intracellular TG levels were not furthered changed upon ethanol treatment in AML12 cells treated with OA (Fig. 4.6A and 5B), neither was the cell viability (Fig. 4.6C).

Figure 4.5 Ethanol Treatment Does Not Influence Intracellular TG Accumulation and Cell Viability

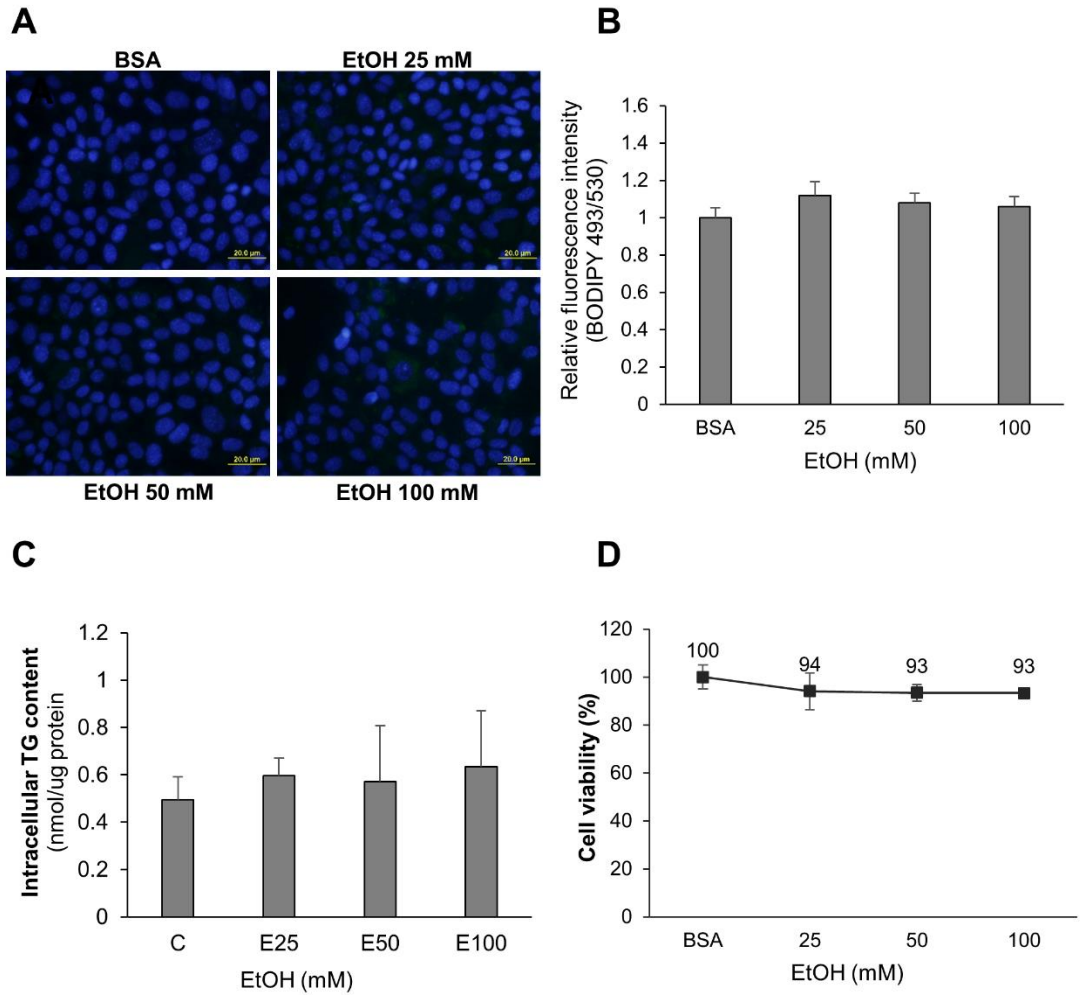

Note. AML12 cells were treated with different concentrations of ethanol (0, 25, 50, and 100 mM) for 24h. (A) LDs were visualized with BODIPY 493/503 staining (scale bar, 20 μm). (B) Relative fluorescence intensity of AML12 cells after BODIPY 493/503 staining (n=5/group). (C) Intracellular TGs were quantified by colorimetric assay kits (n=3/group). (D) Cell viability was determined by CCK8 assay (n=6/group). Data are shown as mean ± SD from each group. Significant differences (*P<0.05*, ANOVA) are identified with different letters.

Figure 4.6 Ethanol Treatment Does Not Affect OA-induced Intracellular TG Accumulation and Cell Death

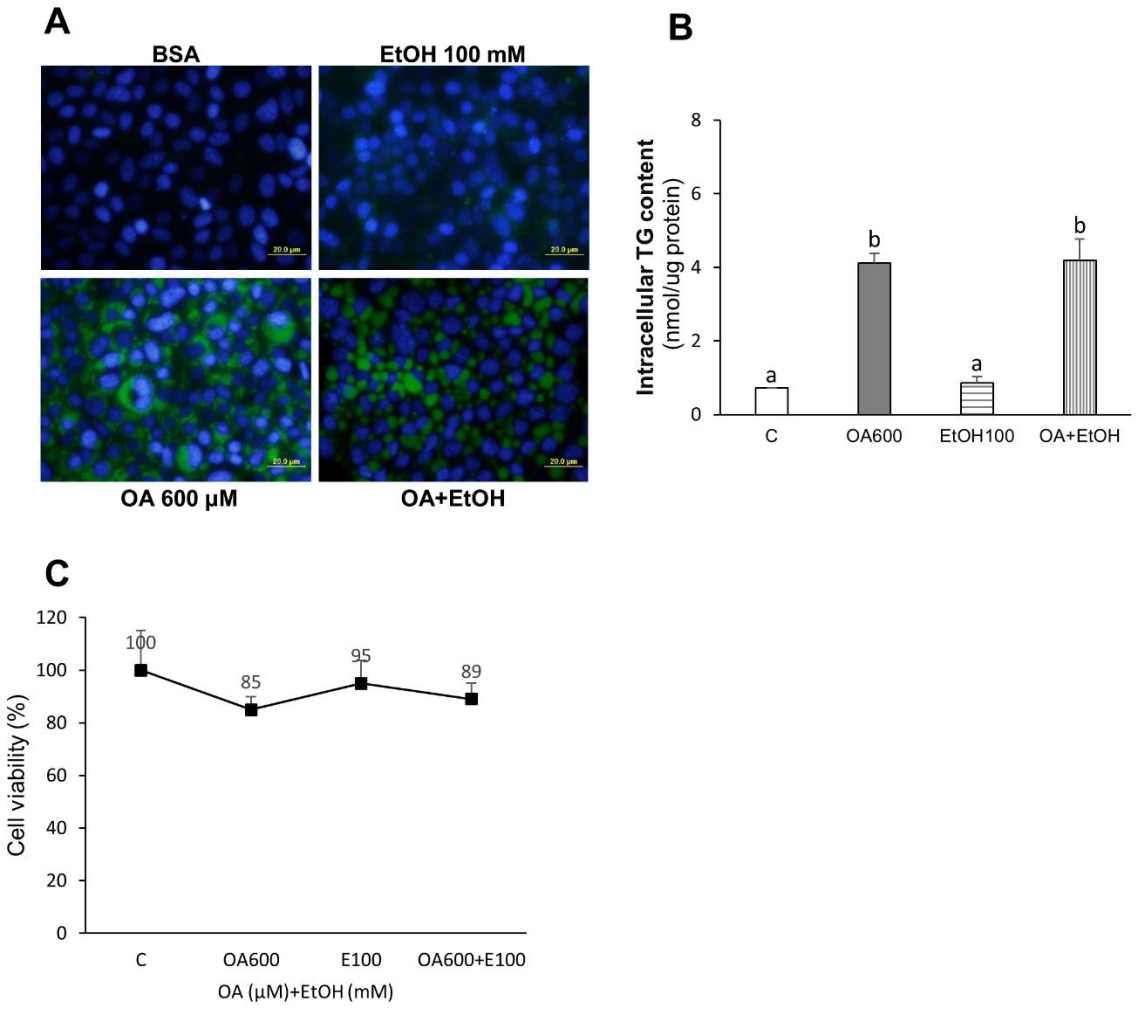

Note. AML12 cells were treated with OA 600 μM with or without ethanol 100 mM for 24h. (A) LDs were visualized with BODIPY 493/503 staining (scale bar, 20 μm). (B) Intracellular TG content was quantified at by colorimetric assay kits. (C) Cell viability was determined by CCK8 assay (n=6/group). Data are shown as mean ± SD from each group. Significant differences (*P<0.05*, ANOVA) are identified with different letters.

Chronic Alcohol Feeding Increased Plasma Endotoxin Levels and Hepatic Bacterial DNAs Levels Regardless of Hepatocyte-specific Deletion of ATGL

Studies have shown that plasma endotoxin levels (LPS) are elevated in patients with ALD compared with healthy subjects, indicating that endotoxin translocation plays a critical part in the pathogenesis of ALD (13,35–37). To examine how hepatocyte-specific deletion of ATGL affect alcohol-induced endotoxin translocation in mice, we measured the plasma levels of endotoxins and hepatic bacterial DNAs. In line with human studies, alcohol feeding significantly elevated plasma endotoxin levels and hepatic bacterial DNAs levels in the AF mice compared to their controls. However, ATGL deletion in hepatocytes did not further exacerbate this elevation, the plasma endotoxin levels and hepatic bacterial DNAs levels in AF ATGL□hep mice were comparable with that in AF control mice (Fig. 4.7A and 7B). These results suggest that hepatocyte-specific deletion of ATGL did not further damage gut permeability and subsequent endotoxin translocation into the liver in ATGL□hep mice. Instead of being the overwhelming factor that promoted liver injury and inflammation in AF ATGL□hep mice, we hypothesize that endotoxin may synergistically combine with intracellular LD/TG accumulation in inducing hepatocellular cell death, therefore contribute to liver injury and inflammation.

Figure 4.7 Hepatocyte-specific Deletion of ATGL Does Not Affect Alcohol-induced Endotoxin Elevation

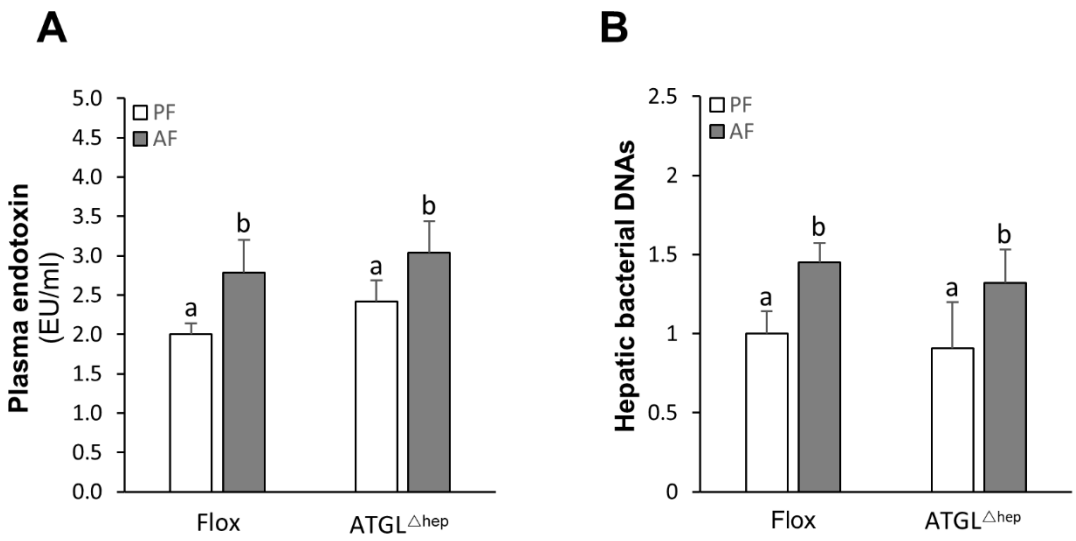

Note. Plasma endotoxin levels (A) and hepatic 16S bacterial rRNAs (B) in wild type (flox) and hepatocyte-specific ATGL deletion (ATGL$^{\triangle hep}$) mice fed with control (PF) or ethanol (AF) liquid diet for 8 weeks. Data are shown as mean ± SD from each group (n=6/group). Significant differences (P<0.05, ANOVA) are identified with different letters.

Intracellular TG Accumulation and LPS Stimulation Synergistically Upregulate Hepatocyte CXCL1 and LCN2 Gene Expression via the Activation of IκB-ζ

Based on our findings that LD/TG accumulation accounts for the OA-induced apoptotic cell death in hepatocytes, as well as LPS levels are elevated both in plasma and livers of mice with alcohol exposure, we hypothesized that TG accumulation and LPS stimulation may synergistically induce hepatocyte injury and subsequently promote CXCL1 and LCN2 expression, which contributes to the pathogenesis of hepatic inflammation. We tested this hypothesis by treating AML12 cells with OA, LPS, or a combination of OA and LPS for 24h. Specifically, cells were primed with OA at 200 μM for 23h prior to the addition of LPS at 100 ng/ml in the medium, cells were then incubated for another 1 h before harvested for mRNA extraction, or whole protein lysates extraction, or subjected to cell viability analysis, as indicated

in (Fig. 4.8A). Cell viability analysis showed that either OA treatment or LPS treatment alone was sufficient to induce cell death in AML12 cells, moreover, cell viability was further decreased when treated with both OA and LPS (Fig. 4.8B). Results from qPCR analysis showed that the mRNA levels of CXCL1 and LCN2 were upregulated by either OA or LPS treatment, with the highest mRNA expression in cells treated with both OA and LPS (Fig. 4.8C and 8D). These results suggest that TG accumulation and LPS stimulation synergistically promote cell death resulting in the upregulation of CXCL1 and LCN2 expression. We then explored the mechanism of the transcriptional regulation of CXCL1 and LCN2, immunoblot results revealed that the protein levels of NF-κB did not vary among treatments, however, the protein levels of IκB-ζ were increased in cells treated with either OA or LPS, with the highest protein abundance in cells treated with both OA and LPS (Fig. 4.8E). Our results demonstrated that OA-induced TG accumulation and LPS synergistically promote hepatocyte injury, which, in turn, further induce hepatocyte overexpression of CXCL1 and LCN1 through activation of IκB-ζ.

Figure 4.8 Intracellular TG Accumulation and LPS Stimulation Synergistically Contribute to the Upregulation of Cxcl1 and Lcn2 mRNA Expression Through IκB-ζ Activation, rather than NF-κB

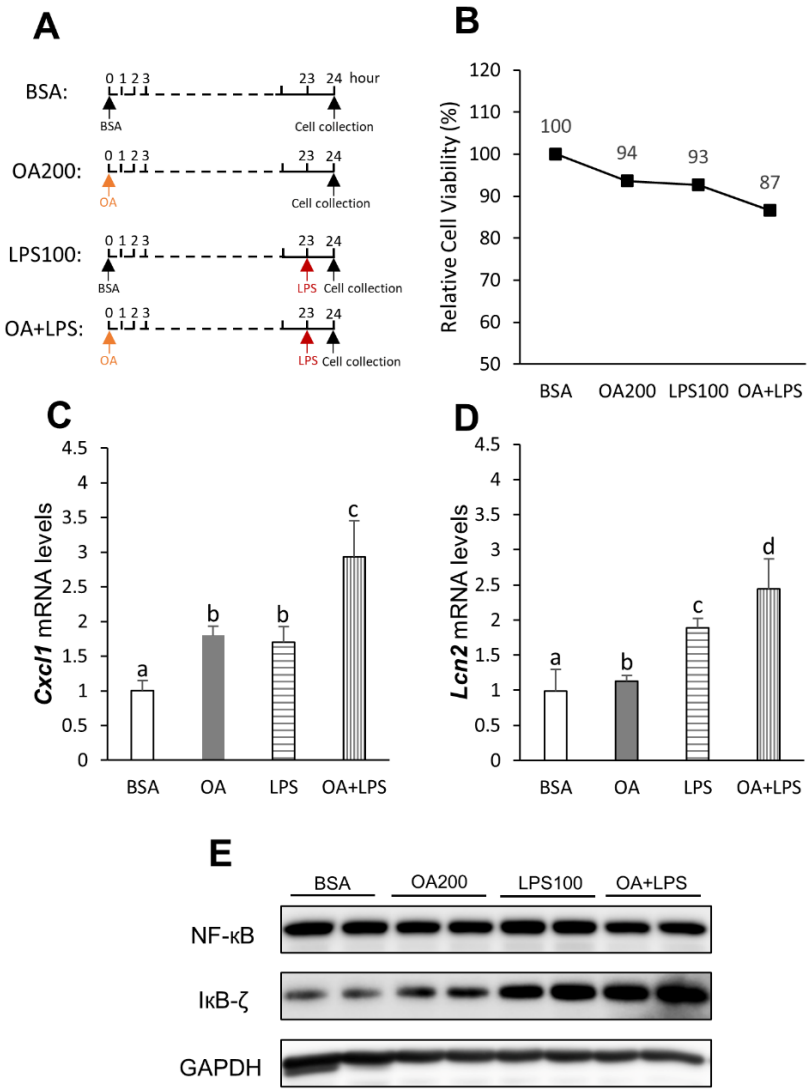

Note. (A) AML12 cells were treated with OA 200 μM and/or LPS 100 ng/ml for 24h (LPS was added in culture media 1h prior to cell collection). (B) Cell viability was determined by CCK8 assay (n=6/group). (C and D) mRNA expression of Cxcl1 and LCN2 in AML12 cells was determined by qPCR (n=4/group). (E) Representative Western blot images of hepatic protein

levels of NF-κB and IκB-ζ in AML12 cells. Data are shown as mean ± SD from each group. Significant differences (P<0.05, ANOVA) are identified with different letters.

Discussion

Based on the findings from present study, we reached the conclusion that excessive accumulation of intracellular TGs/LDs and extracellular LPS stimulation synergistically induce hepatocyte injury and promote the expression of inflammatory chemokine CXCL1 and cytokine LCN2 via IκB-ζ activation. We first dissected the role of intracellular TG accumulation and FFA accumulation in hepatocyte cell death. We found that OA treatment induced intracellular TG accumulation in a dose-dependent manner in hepatocytes but had no significant impact on intracellular FFAs content. Accompanying with elevated intracellular TG content, hepatocellular apoptosis is induced along with decreased cell viability in hepatocytes, indicating cell death. Second, we investigated how ATGL inhibition affect TG/LD accumulation-induced hepatocyte apoptosis. As expected, ATGL inhibition further exacerbated OA-induced intracellular TG accumulation in hepatocytes while had no effects on intracellular FFAs levels. Moreover, ATGL inhibition further aggravated TG/LD accumulation-induced hepatocyte apoptosis. These results confirmed our hypothesis that it is the excessive accumulation of hepatocellular TGs/LDs, rather than FFAs, that accounts for cell death in hepatocytes. Third, we examined whether ethanol has a direct role in elevating intracellular TG content as well as suppressing cell viability in hepatocytes. Our results suggest that ethanol treatment did not influence intracellular TG/LD accumulation in hepatocytes, nor did ethanol affect hepatocellular cell viability. Fourth, given the fact that alcohol-induced endotoxin translocation is closely associated with liver inflammation in patients with ALD (Miyata & Nagy, 2020), we next determined the plasma endotoxin levels and hepatic bacterial DNAs levels in our mouse model. Indeed, alcohol feeding increased the levels of plasma endotoxins and hepatic bacterial DNAs regardless of ATGL deletion in hepatocytes, suggesting that alcohol-induced endotoxin translocation to the liver contributes to the TG/LD

accumulation-induced lipotoxicity and cell death in hepatocytes. Finally, we demonstrated that intracellular TG/LD accumulation and LPS synergistically promote hepatocytes injury and chemokine/cytokine expression via IκB-ζ activation.

Clinical data and animal studies suggest that heavy alcohol consumption can result in severe liver damages, including hepatocyte cell death, a key trigger of the subsequent development of hepatic steatohepatitis, fibrosis, and cirrhosis (Luedde et al., 2014; Nanji & Hiller-Sturmhöfel, 1997). Emerging evidence suggests that hepatic lipotoxicity induces ER stress-mediated hepatocyte cell death, which contribute to the pathogenesis of ALD (Liu & Green, 2019; Nanji, 1998). However, the molecular mechanisms by which hepatic lipotoxicity promote hepatocyte cell death have not been well understood. Some studies postulate that hepatic lipotoxicity is mainly generated by FFAs, especially saturated fatty acids, since supplementation of OA (monounsaturated acid) could rescue palmitic acid (PA, saturated acid)-induced apoptosis by channeling PA to be incorporated into TGs (Listenberger et al., 2003). However, Leamy *et al.* reported OA's protective effect against PA-induced apoptosis dose not require increased incorporation of PA into TGs, as evidenced by knocking down of TG synthesis did not abolish OA's ability to rescue PA-induced lipotoxicity in rate hepatocytes (Leamy et al., 2016). In this study, we firstly investigated whether bulk TG-enriched LD accumulation affect hepatocellular cell death in mouse hepatocytes. we chose OA to treat AML12 cells because OA is easily to be incorporated into TG, therefore we could build this *in vitro* model where TG-enriched LDs are formed in hepatocellular cytoplasm. Our results revealed that cellular TG/LD accumulation, independent of FFAs accumulation, can induce ER stress and CHOP-mediated cell death in hepatocytes.

Increasing evidence indicates ATGL plays a protective role against liver injury and hepatic inflammation in nonalcoholic steatohepatitis (Fuchs et al., 2012; Jha et al., 2014; Johnston et al., 2020; Pearce et al., 2013; Wu et al., 2011). As the rate-limiting enzyme in TG hydrolysis, liver-specific deletion of ATGL leads to the elevation of TG contents and LD

accumulation while overexpression of ATGL attenuates hepatic steatosis (Ong et al., 2011; Reid et al., 2008; Wu et al., 2011). In line with that, our mouse model demonstrates that ATGL deletion in hepatocytes dramatically exacerbated alcohol-induced TG accumulation and LD expansion. We then hypothesized that ATGL inhibition in hepatocytes may exacerbate OA-induced TG/LD accumulation, resulting in bulk accumulation of TGs/LDs in cytoplasm and subsequently worsening apoptotic cell death. Indeed, ATGL inhibition increased the intracellular TG content in a dose-dependent manner but had no effect on cellular FFAs levels. Moreover, ATGL inhibition aggravated TG/LD accumulation-induced ER stress and CHOP-mediated cell death in hepatocytes.

Hepatic steatosis is the most common and earliest clinical manifestation in patients with ALD (Torruellas, 2014). Although many efforts have been made to understand the mechanisms by which alcohol induces hepatocellular cell death, the direct role of ethanol metabolism in that has not been well established. Despite a few studies showed that ethanol treatment at 50 mM was sufficient to induce TG accumulation in hepatocytes (Nagappan et al., 2019; Yin et al., 2012), we did not observe any significant change in intracellular TG content or cell viability in AML12 cells treated with ethanol at up to 100 mM. In our study, serum-reduced medium was used throughout all experiments. Although serum starvation is widely used in cell culture studies to remove known factors and to reduce analytical interference (Rashid & Coombs, 2019), the impact of the condition is not well understood. It is possible that serum starvation-caused “environmental stress” changes AML12 cells cellular activity and is involved in ethanol metabolism and subsequent ethanol-induced lipid dyshomeostasis.

A growing body of evidence indicates that gut-derived endotoxin (LPS) translocation to the liver is closely associated with ALD (Rao, 2009). Endotoxins (LPS) stimulate many types of liver cells, including hepatocytes, releasing chemokines and cytokines that promote hepatic (Affò et al., 2014, p. 2; Hamesch et al., 2015; Li et al., 2004). Indeed, we found that alcohol feeding elevated the levels of plasma endotoxins and bacterial DNAs in the livers of the mice

regardless of ATGL deletion in hepatocytes, suggesting that gut-derived endotoxin translocation in the liver might be partially account for the aggravated liver injury and hepatic inflammation in AF ATGL$^{\triangle hep}$ mice. Given the dramatic TG/LD accumulation observed in the livers of AF ATGL$^{\triangle hep}$ mice, as well as that in AML12 hepatocytes upon OA treatment, we investigated whether TG/LD accumulation and LPS stimulation work synergistically to promote hepatocyte cell death and chemokine/cytokine expression. Our results showed that AML12 cells treated with both OA and LPS exhibit lower cell viability than cells treated with either OA or LPS alone. In agreement with that, CXCL1 and LCN2 expression were significantly increased in AML12 cells treated with both OA and LPS, compared to cells treated with either OA or LPS alone, indicating synergistic effects of OA and LPS on CXCL1 and LCN2 expression. We then explored the potential mechanisms underlying CXCL1 and LCN2 upregulation. NF-κB activation has been shown to induce cytokines and chemokines expression during LPS stimulation (Yamazaki et al., 2001, 2008). In our model, neither OA supplementation nor LPS treatment had significant impact on NF-κB protein levels. Although the classic NF-κB pathway directly induces rapid activation of primary response genes, studies have also demonstrated that IκB-ζ functions not only as an inhibitor of NF-κB, but also an activator for a selective subset of NF-κB target genes (Hildebrand et al., 2013, p. 1; Müller et al., 2018; Yamamoto et al., 2004). Interestingly, we found that the protein expression of IκB-ζ was sufficiently induced by either OA or LPS treatment, with the highest expression in cells treated with both OA and LPS. In agreement with our findings, Brennenstuhl *et al.* demonstrated that IκB-ζ has a direct role in the regulation of CXCL1 expression in a glioma cell line resistant towards NF-κB-dependent cell death (Brennenstuhl et al., 2015). Collectively, our results suggest that intracellular TG/LD accumulation and LPS stimulation synergistically elicit hepatocyte cell injury and CXCL1 and LCN2 expression via the mediation of IκB-ζ activation.

In summary, this study advances the scientific knowledge in the mechanisms underlying lipid lipotoxicity- and LPS-induced cell death and chemokine/cytokine expression in

hepatocytes. Our results reveal that bulk intracellular TG/LD accumulation, independent of FFA accumulation, induces ER stress and CHOP-associated cell death. Our data along with others indicate that ATGL inhibition exacerbated intracellular TG/LD accumulation and subsequent hepatocellular apoptosis and cell death. We verified our hypothesis that intracellular TG/LD accumulation and LPS stimulation synergistically promote cell death and induce chemokine CXCL1 and cytokine LCN2 expression in hepatocytes via the IκB-ζ activation. Taken together, the current study proposes that alcohol-induced gut-derived endotoxin translocation along with hepatic steatosis might synergistically induce hepatocytes cell death and promote hepatic inflammation in the progression of ALD. Our findings will shed light on the development and optimization of novel diagnostic and therapeutic strategies in preventing and treating patients with ALD.

CHAPTER V: EPILOGUE

ALD is a major public health problem worldwide. Despite mortality has been rising alarmingly, there is no FDA-approved targeted therapy for the treatment of ALD ((Moon et al., 2020). Hence, great effort has been made to elucidate the cellular and molecular mechanisms in the pathogenesis of ALD. In this dissertation, we investigated the role of ATGL in alcohol-induced hepatic steatosis, inflammation, fibrosis, and hepatic ultrastructural changes in mouse model of ALD; we also determined the molecular mechanisms by which cellular TG/LD accumulation and LPS stimulation synergistically induce cell death and chemokine/cytokine expression in AML12 mouse hepatocytes.

In chapter II, we demonstrated that alcohol induced hepatic ATGL expression, accumulation of TGs and FFAs, and liver injury. We then generated a mouse model with hepatocyte-specific deletion of ATGL and subjected the mice to chronic alcohol feeding. Hepatocyte-specific ATGL deletion exacerbated alcohol-induced hepatic accumulation of TGs and FFAs but diminished alcohol-induced elevation in VLDL-TG secretion. We then examined enzymes involved in fatty acid oxidation and found that protein levels of CPT1A were reduced by hepatocyte ATGL deficiency regardless of alcohol feeding; hepatic protein levels of ACADM and ACOX1 were suppressed in ATGL deficiency mice with alcohol feeding, indicating partially impaired FFAs oxidation in the liver. We also found that hepatic mRNA levels of TG synthesizing enzyme DGAT1 were decreased by hepatocyte ATGL deletion regardless of alcohol feeding, while the hepatic mRNA levels of DGAT2 were reduced in the mice with ATGL deficiency upon alcohol feeding, suggesting impaired TG synthesis in the liver. Next, we showed that hepatocyte ATGL deficiency reduced hepatic protein levels of enzymes involved in fatty acid activation, including ACSL1, ACSL5, and FATP2; moreover, alcohol feeding further suppressed the reduction of ACSL1 and ACSL5. In addition, we demonstrated that hepatocyte-specific ATGL deletion exacerbated alcohol-induced liver injury by upregulating hepatic mRNA expression of

chemokine CXCL1 and cytokine LCN2 and promoting subsequent neutrophil infiltration in the liver. Furthermore, we observed that both hepatic mRNA levels and protein levels of CHOP were induced by alcohol feeding, which were further augmented by hepatocyte ATGL deletion, indicating that CHOP-related ER stress may be associated with ATGL deficiency-enhanced hepatic inflammation. Last, the mRNA levels of hepatic fibrosis markers, including α-SMA, COL1A1, and COL1A2, were increased by ATGL deletion, which were further augmented by alcohol feeding. Sirius Red Staining results revealed that ATGL deletion amplified alcohol-induced collagen deposition in the liver of the mice. Collectively, data presented in chapter II demonstrated that hepatocyte-specific ATGL deletion exacerbated alcohol-induced hepatic steatosis through impairing VLDL-TG secretion. Furthermore, we hypothesized that impaired ACSL5-mediated FFAs activation and subsequent DGAT1-mediated conversion of FFAs to TGs are associated with diminished VLDL-TG secretion in mice deficient in ATGL. Hepatic ATGL deficiency-enhanced liver inflammation may be related to CHOP-associated cell death and CXCL1/LCN2-mediated neutrophil infiltration in the liver.

In chapter III, we utilized the transmission electron microscope (TEM) technique to examine the ultrastructural and morphological changes in hepatocytes and non-parenchymal cells in the liver of the mice with or without hepatocyte-specific ATGL deletion. Alcohol intoxication resulted in lipid droplet accumulation, mitochondria abnormality, reduction in glycogen storage, ER dilation, nuclei condensation and deformation, and increased autophagy clearance machinery in hepatocytes; these subcellular structural alterations were amplified by hepatocyte ATGL deficiency. We also observed lipid droplet accumulation in sinusoids and cholangiocytes. Autophagy machinery autolysosomes were found in the cytoplasm of Kupffer cells in the liver of the mice with alcohol feeding regardless of ATGL deficiency. In addition, collagen deposition, a sign of fibrosis, was detected in the liver of mice deficient in ATGL, which was amplified by alcohol feeding. Collectively, data presented in chapter III demonstrated that alcohol intoxication and hepatocyte ATGL deficiency synergistically induced ultrastructural and morphological changes in

hepatocytes, Kupffer cells, cholangiocytes, as well as sinusoids, which provides visual evidence of lipotoxicity in the pathogenesis of ALD.

In chapter IV, we examined the mechanisms underlying lipid lipotoxicity- and LPS-induced cell death and chemokine/cytokine expression in hepatocyte. Results revealed that cellular levels of TGs but not FFAs levels were increased by OA treatment in a dose-dependent manner, accompanied by decreased cell viability and increased protein levels of CHOP. ATGL inhibition exacerbated OA-induced accumulation of intracellular TG/LD and protein levels of CHOP, and further reduced hepatocyte cell viability. Ethanol treatment did not affect cellular TGs and FFAs levels and cell viability. Cell viability analysis showed that either OA treatment or LPS treatment alone was sufficient to induce cell death, whereas cell viability was further decreased when treated with both OA and LPS. The mRNA levels of CXCL1 and LCN2 were upregulated by either OA or LPS treatment, with the highest mRNA expression in cells treated with both OA and LPS. Furthermore, the overexpression of CXCL1 and LCN2 by OA and LPS treatment was via IκB-ζ activation. Collectively, data presented in chapter IV demonstrated that TG/LD accumulation, independent of FFA accumulation, induced CHOP-associated cell death, which was exacerbated by ATGL inhibition. In addition, OA-induced intracellular TG/LD accumulation and LPS stimulation synergistically promoted cell death and induced chemokine CXCL1 and cytokine LCN2 expression via IκB-ζ activation.

Taken together, data presented in chapter II, III, and IV significantly contribute to the limited understanding of the role of ATGL in the pathogenesis of ALD. Our observations suggest that hepatocyte-specific ATGL deficiency exacerbates alcohol-induced hepatic steatosis through impairing VLDL-TG secretion. Alcohol intoxication and hepatocyte ATGL deficiency synergistically induce ultrastructural and morphological changes in the liver. In addition, hepatic steatosis and gut-derived endotoxins synergistically induce hepatocyte cell death and promote hepatic inflammation in the progression of ALD.

In chapter II, we observed that hepatic protein levels of ACSL5 were reduced in hepatocyte ATGL deficiency mice, which were further suppressed by alcohol feeding, indicating impaired fatty acid oxidation. Studies have shown that ACSL5 knockdown decreases hepatic TG secretion in vitro (Bu & Mashek, 2010), and global ACSL5 deletion reduces VLDL-TG secretion in vivo (Bowman et al., 2016). We also found that ATGL deletion reduced hepatic protein levels of DGAT1, which is believed to play a critical role in converting FFAs from lipid droplets or exogenous sources to TGs for VLDL assembly in the ER (Irshad, Jan, p. 1). Hence, future studies are necessitated to confirm the role of ATGL-ACSL5-DGAT1 pathway in hepatic VLDL-TG secretion. In addition, hepatocyte-specific ATGL deletion dramatically aggravated alcohol-induced collagen deposition in the liver, as well as upregulated hepatic mRNA levels of fibrosis markers; future research is needed to elucidate the molecular mechanisms by which hepatic stellate cells are activated by massive TG/LD accumulation-induced lipotoxicity.

REFERENCES

Affò, S., Morales-Ibanez, O., Rodrigo-Torres, D., Altamirano, J., Blaya, D., Dapito, D. H., Millán, C., Coll, M., Caviglia, J. M., Arroyo, V., Caballería, J., Schwabe, R. F., Ginès, P., Bataller, R., & Sancho-Bru, P. (2014). CCL20 mediates lipopolysaccharide induced liver injury and is a potential driver of inflammation and fibrosis in alcoholic hepatitis. Gut, 63(11), 1782–1792. https://doi.org/10.1136/gutjnl-2013-306098

Aizarani, N., Saviano, A., Sagar, null, Mailly, L., Durand, S., Herman, J. S., Pessaux, P., Baumert, T. F., & Grün, D. (2019). A human liver cell atlas reveals heterogeneity and epithelial progenitors. Nature, 572(7768), 199–204. https://doi.org/10.1038/s41586-019-1373-2

Alves-Bezerra, M., & Cohen, D. E. (2017). Triglyceride Metabolism in the Liver. Comprehensive Physiology, 8(1), 1–8. https://doi.org/10.1002/cphy.c170012

An, L., Wang, X., & Cederbaum, A. I. (2012). Cytokines in alcoholic liver disease. Archives of Toxicology, 86(9), 1337–1348. https://doi.org/10.1007/s00204-012-0814-6

Arumugam, M. K., Talawar, S., Listenberger, L., Donohue, T. M., Osna, N. A., & Kharbanda, K. K. (2020). Role of Elevated Intracellular S-Adenosylhomocysteine in the Pathogenesis of Alcohol-Related Liver Disease. Cells, 9(6), E1526. https://doi.org/10.3390/cells9061526

Asimakopoulou, A., Borkham-Kamphorst, E., Henning, M., Yagmur, E., Gassler, N., Liedtke, C., Berger, T., Mak, T. W., & Weiskirchen, R. (2014). Lipocalin-2 (LCN2) regulates PLIN5 expression and intracellular lipid droplet formation in the liver. Biochimica Et Biophysica Acta, 1842(10), 1513–1524. https://doi.org/10.1016/j.bbalip.2014.07.017

Babuta, M., Furi, I., Bala, S., Bukong, T. N., Lowe, P., Catalano, D., Calenda, C., Kodys, K., & Szabo, G. (2019). Dysregulated Autophagy and Lysosome Function Are Linked to Exosome Production by Micro-RNA 155 in Alcoholic Liver Disease. Hepatology (Baltimore, Md.), 70(6), 2123–2141. https://doi.org/10.1002/hep.30766

Bartz, R., Zehmer, J. K., Zhu, M., Chen, Y., Serrero, G., Zhao, Y., & Liu, P. (2007). Dynamic Activity of Lipid Droplets: Protein Phosphorylation and GTP-Mediated Protein Translocation. Journal of Proteome Research, 6(8), 3256–3265. https://doi.org/10.1021/pr070158j

Bataller, R., & Gao, B. (2015). Liver Fibrosis in Alcoholic Liver Disease. Seminars in Liver Disease, 35(02), 146–156. https://doi.org/10.1055/s-0035-1550054

Blouin, A., Bolender, R. P., & Weibel, E. R. (1977). Distribution of organelles and membranes between hepatocytes and nonhepatocytes in the rat liver parenchyma. A stereological study. The Journal of Cell Biology, 72(2), 441–455. https://doi.org/10.1083/jcb.72.2.441

Borg, M. L., Andrews, Z. B., Duh, E. J., Zechner, R., Meikle, P. J., & Watt, M. J. (2011). Pigment Epithelium–Derived Factor Regulates Lipid Metabolism via Adipose Triglyceride Lipase. Diabetes, 60(5), 1458–1466. https://doi.org/10.2337/db10-0845

Borkham-Kamphorst, E., van de Leur, E., Zimmermann, H. W., Karlmark, K. R., Tihaa, L., Haas, U., Tacke, F., Berger, T., Mak, T. W., & Weiskirchen, R. (2013). Protective effects of lipocalin-2 (LCN2) in acute liver injury suggest a novel function in liver homeostasis. Biochimica Et Biophysica Acta, 1832(5), 660–673. https://doi.org/10.1016/j.bbadis.2013.01.014

Bouwens, L., Baekeland, M., De Zanger, R., & Wisse, E. (1986). Quantitation, tissue distribution and proliferation kinetics of Kupffer cells in normal rat liver. Hepatology (Baltimore, Md.), 6(4), 718–722. https://doi.org/10.1002/hep.1840060430

Bowman, T. A., O'Keeffe, K. R., D'Aquila, T., Yan, Q. W., Griffin, J. D., Killion, E. A., Salter, D. M., Mashek, D. G., Buhman, K. K., & Greenberg, A. S. (2016). Acyl CoA synthetase 5 (ACSL5) ablation in mice increases energy expenditure and insulin sensitivity and delays fat absorption. Molecular Metabolism, 5(3), 210–220. https://doi.org/10.1016/j.molmet.2016.01.001

Braet, F., & Wisse, E. (2002). Structural and functional aspects of liver sinusoidal endothelial cell fenestrae: A review. Comparative Hepatology, 1(1), 1. https://doi.org/10.1186/1476-5926-1-1

Brasaemle, D. L. (2007). Thematic review series: Adipocyte biology. The perilipin family of structural lipid droplet proteins: stabilization of lipid droplets and control of lipolysis. Journal of Lipid Research, 48(12), 2547–2559. https://doi.org/10.1194/jlr.R700014-JLR200

Brennenstuhl, H., Armento, A., Braczysnki, A. K., Mittelbronn, M., & Naumann, U. (2015). IκBζ, an atypical member of the inhibitor of nuclear factor kappa B family, is induced by γ-

irradiation in glioma cells, regulating cytokine secretion and associated with poor prognosis. International Journal of Oncology, 47(5), 1971–1980. https://doi.org/10.3892/ijo.2015.3159

Brenner, C., Galluzzi, L., Kepp, O., & Kroemer, G. (2013). Decoding cell death signals in liver inflammation. Journal of Hepatology, 59(3), 583–594. https://doi.org/10.1016/j.jhep.2013.03.033

Bu, S. Y., & Mashek, D. G. (2010). Hepatic long-chain acyl-CoA synthetase 5 mediates fatty acid channeling between anabolic and catabolic pathways. Journal of Lipid Research, 51(11), 3270–3280. https://doi.org/10.1194/jlr.M009407

Cai, Y., Jogasuria, A., Yin, H., Xu, M.-J., Hu, X., Wang, J., Kim, C., Wu, J., Lee, K., Gao, B., & You, M. (2016). The Detrimental Role Played by Lipocalin-2 in Alcoholic Fatty Liver in Mice. The American Journal of Pathology, 186(9), 2417–2428. https://doi.org/10.1016/j.ajpath.2016.05.006

Cerk, I. K., Wechselberger, L., & Oberer, M. (2018). Adipose Triglyceride Lipase Regulation: An Overview. Current Protein & Peptide Science, 19(2), 221–233. https://doi.org/10.2174/1389203718666170918160110

Chakrabarti, P., Kim, J. Y., Singh, M., Shin, Y.-K., Kim, J., Kumbrink, J., Wu, Y., Lee, M.-J., Kirsch, K. H., Fried, S. K., & Kandror, K. V. (2013). Insulin inhibits lipolysis in adipocytes via the evolutionarily conserved mTORC1-Egr1-ATGL-mediated pathway. Molecular and Cellular Biology, 33(18), 3659–3666. https://doi.org/10.1128/MCB.01584-12

Chakravarthy, M. V., Lodhi, I. J., Yin, L., Malapaka, R. R. V., Xu, H. E., Turk, J., & Semenkovich, C. F. (2009). Identification of a physiologically relevant endogenous ligand for PPARalpha in liver. Cell, 138(3), 476–488. https://doi.org/10.1016/j.cell.2009.05.036

Chang, B., Xu, M.-J., Zhou, Z., Cai, Y., Li, M., Wang, W., Feng, D., Bertola, A., Wang, H., Kunos, G., & Gao, B. (2015). Short- or long-term high-fat diet feeding plus acute ethanol binge synergistically induce acute liver injury in mice: An important role for CXCL1. Hepatology (Baltimore, Md.), 62(4), 1070–1085. https://doi.org/10.1002/hep.27921

Chen, C., Deng, M., Sun, Q., Loughran, P., Billiar, T. R., & Scott, M. J. (2014). Lipopolysaccharide Stimulates p62-Dependent Autophagy-Like Aggregate Clearance in

Hepatocytes. BioMed Research International, 2014, 1–13. https://doi.org/10.1155/2014/267350

Chen, T. S., Murphy, D. P., Marquet, G., Chedid, A., Mendenhall, C. L., & Rabin, L. (1987). Morphometric study of hepatic ultrastructure in alcoholic hepatitis. Veterans Administration Cooperative Study Group on Alcoholic Hepatitis. Histology and Histopathology, 2(4), 429–432.

Chen, W., Jiang, Y., Han, J., Hu, J., He, T., Yan, T., Huang, N., Zhang, Q., Mei, H., Liao, Y., Huang, Y., & Chen, B. (2017). Atgl deficiency induces podocyte apoptosis and leads to glomerular filtration barrier damage. The FEBS Journal, 284(7), 1070–1081. https://doi.org/10.1111/febs.14038

Cholankeril, G., & Ahmed, A. (2018). Alcoholic Liver Disease Replaces Hepatitis C Virus Infection as the Leading Indication for Liver Transplantation in the United States. Clinical Gastroenterology and Hepatology: The Official Clinical Practice Journal of the American Gastroenterological Association, 16(8), 1356–1358. https://doi.org/10.1016/j.cgh.2017.11.045

Chrostek, L., & Panasiuk, A. (2014). Liver fibrosis markers in alcoholic liver disease. World Journal of Gastroenterology, 20(25), 8018–8023. https://doi.org/10.3748/wjg.v20.i25.8018

Cnop, M., Hannaert, J. C., Hoorens, A., Eizirik, D. L., & Pipeleers, D. G. (2001). Inverse relationship between cytotoxicity of free fatty acids in pancreatic islet cells and cellular triglyceride accumulation. Diabetes, 50(8), 1771–1777. https://doi.org/10.2337/diabetes.50.8.1771

Cornaciu, I., Boeszoermenyi, A., Lindermuth, H., Nagy, H. M., Cerk, I. K., Ebner, C., Salzburger, B., Gruber, A., Schweiger, M., Zechner, R., Lass, A., Zimmermann, R., & Oberer, M. (2011). The minimal domain of adipose triglyceride lipase (ATGL) ranges until leucine 254 and can be activated and inhibited by CGI-58 and G0S2, respectively. PloS One, 6(10), e26349. https://doi.org/10.1371/journal.pone.0026349

Crabb, D. W., Im, G. Y., Szabo, G., Mellinger, J. L., & Lucey, M. R. (2020). Diagnosis and Treatment of Alcohol-Associated Liver Diseases: 2019 Practice Guidance From the American Association for the Study of Liver Diseases. Hepatology (Baltimore, Md.), 71(1), 306–333. https://doi.org/10.1002/hep.30866

Cubero, F. J., & Nieto, N. (2006). Kupffer cells and alcoholic liver disease. Revista Espanola De Enfermedades Digestivas: Organo Oficial De La Sociedad Espanola De Patologia Digestiva, 98(6), 460–472. https://doi.org/10.4321/s1130-01082006000600007

Dahlquist, K. J. V., Voth, L. C., Fee, A. J., & Stoeckman, A. K. (2020). An Autocrine Role for CXCL1 in Progression of Hepatocellular Carcinoma. Anticancer Research, 40(11), 6075–6081. https://doi.org/10.21873/anticanres.14628

Dang, K., Hirode, G., Singal, A. K., Sundaram, V., & Wong, R. J. (2020). Alcoholic Liver Disease Epidemiology in the United States: A Retrospective Analysis of 3 US Databases. The American Journal of Gastroenterology, 115(1), 96–104. https://doi.org/10.14309/ajg.0000000000000380

de Vries, J. E., Vork, M. M., Roemen, T. H., de Jong, Y. F., Cleutjens, J. P., van der Vusse, G. J., & van Bilsen, M. (1997). Saturated but not mono-unsaturated fatty acids induce apoptotic cell death in neonatal rat ventricular myocytes. Journal of Lipid Research, 38(7), 1384–1394.

Dianat, N., Dubois-Pot-Schneider, H., Steichen, C., Desterke, C., Leclerc, P., Raveux, A., Combettes, L., Weber, A., Corlu, A., & Dubart-Kupperschmitt, A. (2014). Generation of functional cholangiocyte-like cells from human pluripotent stem cells and HepaRG cells. Hepatology (Baltimore, Md.), 60(2), 700–714. https://doi.org/10.1002/hep.27165

Dolganiuc, A., Thomes, P. G., Ding, W.-X., Lemasters, J. J., & Donohue, T. M. (2012). Autophagy in alcohol-induced liver diseases. Alcoholism, Clinical and Experimental Research, 36(8), 1301–1308. https://doi.org/10.1111/j.1530-0277.2012.01742.x

Dominguez, M., Miquel, R., Colmenero, J., Moreno, M., García-Pagán, J.-C., Bosch, J., Arroyo, V., Ginès, P., Caballería, J., & Bataller, R. (2009). Hepatic expression of CXC chemokines predicts portal hypertension and survival in patients with alcoholic hepatitis. Gastroenterology, 136(5), 1639–1650. https://doi.org/10.1053/j.gastro.2009.01.056

Donohue, T. M. (2007). Alcohol-induced steatosis in liver cells. World Journal of Gastroenterology, 13(37), 4974–4978. https://doi.org/10.3748/wjg.v13.i37.4974

Duncan, R. E., Wang, Y., Ahmadian, M., Lu, J., Sarkadi-Nagy, E., & Sul, H. S. (2010). Characterization of desnutrin functional domains: Critical residues for triacylglycerol

hydrolysis in cultured cells. Journal of Lipid Research, 51(2), 309–317. https://doi.org/10.1194/jlr.M000729

Eichmann, T. O., Grumet, L., Taschler, U., Hartler, J., Heier, C., Woblistin, A., Pajed, L., Kollroser, M., Rechberger, G., Thallinger, G. G., Zechner, R., Haemmerle, G., Zimmermann, R., & Lass, A. (2015). ATGL and CGI-58 are lipid droplet proteins of the hepatic stellate cell line HSC-T6. Journal of Lipid Research, 56(10), 1972–1984. https://doi.org/10.1194/jlr.M062372

Eskild, W., Kindberg, G. M., Smedsrod, B., Blomhoff, R., Norum, K. R., & Berg, T. (1989). Intracellular transport of formaldehyde-treated serum albumin in liver endothelial cells after uptake via scavenger receptors. The Biochemical Journal, 258(2), 511–520. https://doi.org/10.1042/bj2580511

Fawcett, D. W. (1955). Observations on the cytology and electron microscopy of hepatic cells. Journal of the National Cancer Institute, 15(5, Suppl.), 1475–1503.

Fischer, J., Lefèvre, C., Morava, E., Mussini, J.-M., Laforêt, P., Negre-Salvayre, A., Lathrop, M., & Salvayre, R. (2007). The gene encoding adipose triglyceride lipase (PNPLA2) is mutated in neutral lipid storage disease with myopathy. Nature Genetics, 39(1), 28–30. https://doi.org/10.1038/ng1951

Franken, L. E., Grünewald, K., Boekema, E. J., & Stuart, M. C. A. (2020). A Technical Introduction to Transmission Electron Microscopy for Soft-Matter: Imaging, Possibilities, Choices, and Technical Developments. Small, 16(14), 1906198. https://doi.org/10.1002/smll.201906198

Fuchs, C. D., Claudel, T., Kumari, P., Haemmerle, G., Pollheimer, M. J., Stojakovic, T., Scharnagl, H., Halilbasic, E., Gumhold, J., Silbert, D., Koefeler, H., & Trauner, M. (2012). Absence of adipose triglyceride lipase protects from hepatic endoplasmic reticulum stress in mice. Hepatology (Baltimore, Md.), 56(1), 270–280. https://doi.org/10.1002/hep.25601

Fuchs, C. D., Radun, R., Dixon, E. D., Mlitz, V., Timelthaler, G., Halilbasic, E., Herac, M., Jonker, J. W., Ronda, O. A. H. O., Tardelli, M., Haemmerle, G., Zimmermann, R., Scharnagl, H., Stojakovic, T., Verkade, H. J., & Trauner, M. (2022). Hepatocyte-specific deletion of adipose triglyceride lipase (adipose triglyceride lipase/patatin-like phospholipase

domain containing 2) ameliorates dietary induced steatohepatitis in mice. Hepatology, 75(1), 125–139. https://doi.org/10.1002/hep.32112

Fusakio, M. E., Willy, J. A., Wang, Y., Mirek, E. T., Al Baghdadi, R. J. T., Adams, C. M., Anthony, T. G., & Wek, R. C. (2016). Transcription factor ATF4 directs basal and stress-induced gene expression in the unfolded protein response and cholesterol metabolism in the liver. Molecular Biology of the Cell, 27(9), 1536–1551. https://doi.org/10.1091/mbc.E16-01-0039

Gao, B., Ahmad, M. F., Nagy, L. E., & Tsukamoto, H. (2019). Inflammatory pathways in alcoholic steatohepatitis. Journal of Hepatology, 70(2), 249–259. https://doi.org/10.1016/j.jhep.2018.10.023

Gao, B., & Bataller, R. (2011). Alcoholic Liver Disease: Pathogenesis and New Therapeutic Targets. Gastroenterology, 141(5), 1572–1585. https://doi.org/10.1053/j.gastro.2011.09.002

Geng, Y., Faber, K. N., de Meijer, V. E., Blokzijl, H., & Moshage, H. (2021). How does hepatic lipid accumulation lead to lipotoxicity in non-alcoholic fatty liver disease? Hepatology International, 15(1), 21–35. https://doi.org/10.1007/s12072-020-10121-2

Ghosh, M., Niyogi, S., Bhattacharyya, M., Adak, M., Nayak, D. K., Chakrabarti, S., & Chakrabarti, P. (2016). Ubiquitin Ligase COP1 Controls Hepatic Fat Metabolism by Targeting ATGL for Degradation. Diabetes, 65(12), 3561–3572. https://doi.org/10.2337/db16-0506

Gimm, T., Wiese, M., Teschemacher, B., Deggerich, A., Schödel, J., Knaup, K. X., Hackenbeck, T., Hellerbrand, C., Amann, K., Wiesener, M. S., Höning, S., Eckardt, K.-U., & Warnecke, C. (2010). Hypoxia-inducible protein 2 is a novel lipid droplet protein and a specific target gene of hypoxia-inducible factor-1. FASEB Journal: Official Publication of the Federation of American Societies for Experimental Biology, 24(11), 4443–4458. https://doi.org/10.1096/fj.10-159806

Gluchowski, N. L., Becuwe, M., Walther, T. C., & Farese, R. V. (2017). Lipid droplets and liver disease: From basic biology to clinical implications. Nature Reviews. Gastroenterology & Hepatology, 14(6), 343–355. https://doi.org/10.1038/nrgastro.2017.32

Goldblatt, P. J., & Gunning, W. T. (1984). Ultrastructure of the liver and biliary tract in health and disease. Annals of Clinical and Laboratory Science, 14(2), 159–167.

Grahn, T. H. M., Kaur, R., Yin, J., Schweiger, M., Sharma, V. M., Lee, M.-J., Ido, Y., Smas, C. M., Zechner, R., Lass, A., & Puri, V. (2014). Fat-specific Protein 27 (FSP27) Interacts with Adipose Triglyceride Lipase (ATGL) to Regulate Lipolysis and Insulin Sensitivity in Human Adipocytes. Journal of Biological Chemistry, 289(17), 12029–12039. https://doi.org/10.1074/jbc.M113.539890

Grases, P. J., Millard, P. R., & McGee, J. O. (1987). The ultrastructure of alcoholic liver disease: A review and analysis of 100 biopsies. Histology and Histopathology, 2(1), 19–29.

Griswold, M. G., Fullman, N., Hawley, C., Arian, N., Zimsen, S. R. M., Tymeson, H. D., Venkateswaran, V., Tapp, A. D., Forouzanfar, M. H., Salama, J. S., Abate, K. H., Abate, D., Abay, S. M., Abbafati, C., Abdulkader, R. S., Abebe, Z., Aboyans, V., Abrar, M. M., Acharya, P., … Gakidou, E. (2018). Alcohol use and burden for 195 countries and territories, 1990–2016: A systematic analysis for the Global Burden of Disease Study 2016. The Lancet, 392(10152), 1015–1035. https://doi.org/10.1016/S0140-6736(18)31310-2

Guo, W., Zhong, W., Hao, L., Dong, H., Sun, X., Yue, R., Li, T., & Zhou, Z. (2021). Fatty Acids Inhibit LAMP2-Mediated Autophagy Flux via Activating ER Stress Pathway in Alcohol-Related Liver Disease. Cellular and Molecular Gastroenterology and Hepatology, 12(5), 1599–1615. https://doi.org/10.1016/j.jcmgh.2021.07.002

Haemmerle, G., Lass, A., Zimmermann, R., Gorkiewicz, G., Meyer, C., Rozman, J., Heldmaier, G., Maier, R., Theussl, C., Eder, S., Kratky, D., Wagner, E. F., Klingenspor, M., Hoefler, G., & Zechner, R. (2006). Defective lipolysis and altered energy metabolism in mice lacking adipose triglyceride lipase. Science (New York, N.Y.), 312(5774), 734–737. https://doi.org/10.1126/science.1123965

Haemmerle, G., Moustafa, T., Woelkart, G., Büttner, S., Schmidt, A., van de Weijer, T., Hesselink, M., Jaeger, D., Kienesberger, P. C., Zierler, K., Schreiber, R., Eichmann, T., Kolb, D., Kotzbeck, P., Schweiger, M., Kumari, M., Eder, S., Schoiswohl, G., Wongsiriroj, N., … Zechner, R. (2011). ATGL-mediated fat catabolism regulates cardiac mitochondrial function via PPAR-α and PGC-1. Nature Medicine, 17(9), 1076–1085. https://doi.org/10.1038/nm.2439

Hamesch, K., Borkham-Kamphorst, E., Strnad, P., & Weiskirchen, R. (2015). Lipopolysaccharide-induced inflammatory liver injury in mice. Laboratory Animals, 49(1_suppl), 37–46. https://doi.org/10.1177/0023677215570087

Hanck, C., Rossol, S., Böcker, U., Tokus, M., & Singer, M. V. (1998). Presence of plasma endotoxin is correlated with tumour necrosis factor receptor levels and disease activity in alcoholic cirrhosis. Alcohol and Alcoholism (Oxford, Oxfordshire), 33(6), 606–608. https://doi.org/10.1093/alcalc/33.6.606

Hildebrand, D. G., Alexander, E., Hörber, S., Lehle, S., Obermayer, K., Münck, N.-A., Rothfuss, O., Frick, J.-S., Morimatsu, M., Schmitz, I., Roth, J., Ehrchen, J. M., Essmann, F., & Schulze-Osthoff, K. (2013). IκBζ is a transcriptional key regulator of CCL2/MCP-1. Journal of Immunology (Baltimore, Md.: 1950), 190(9), 4812–4820. https://doi.org/10.4049/jimmunol.1300089

Howarth, D. L., Vacaru, A. M., Tsedensodnom, O., Mormone, E., Nieto, N., Costantini, L. M., Snapp, E. L., & Sadler, K. C. (2012). Alcohol disrupts endoplasmic reticulum function and protein secretion in hepatocytes. Alcoholism, Clinical and Experimental Research, 36(1), 14–23. https://doi.org/10.1111/j.1530-0277.2011.01602.x

Irshad, Z. (Jan). Hepatic VLDL secretion: DGAT1 determins particle size nut not particle number, which can be supported entirely bu DGAT2. Journal of Lipid Research, 60(1), 111–120.

Iseri, O. A., & Gottlieb, L. S. (1971). Alcoholic hyalin and megamitochondria as separate and distinct entities in liver disease associated with alcoholism. Gastroenterology, 60(6), 1027–1035.

Iseri, O. A., Lieber, C. S., & Gottlieb, L. S. (1966). The ultrastructure of fatty liver induced by prolonged ethanol ingestion. The American Journal of Pathology, 48(4), 535–555.

Ito, T., & Nemoto, M. (1952). [Kupfer's cells and fat storing cells in the capillary wall of human liver]. Okajimas Folia Anatomica Japonica, 24(4), 243–258. https://doi.org/10.2535/ofaj1936.24.4_243

Jang, Y., Lee, J. H., Wang, Y., & Sweeney, G. (2012). Emerging clinical and experimental evidence for the role of lipocalin-2 in metabolic syndrome. Clinical and Experimental

Pharmacology & Physiology, 39(2), 194–199. https://doi.org/10.1111/j.1440-1681.2011.05557.x

Jenkins, C. M., Mancuso, D. J., Yan, W., Sims, H. F., Gibson, B., & Gross, R. W. (2004). Identification, cloning, expression, and purification of three novel human calcium-independent phospholipase A2 family members possessing triacylglycerol lipase and acylglycerol transacylase activities. The Journal of Biological Chemistry, 279(47), 48968–48975. https://doi.org/10.1074/jbc.M407841200

Jha, P., Claudel, T., Baghdasaryan, A., Mueller, M., Halilbasic, E., Das, S. K., Lass, A., Zimmermann, R., Zechner, R., Hoefler, G., & Trauner, M. (2014). Role of adipose triglyceride lipase (PNPLA2) in protection from hepatic inflammation in mouse models of steatohepatitis and endotoxemia. Hepatology (Baltimore, Md.), 59(3), 858–869. https://doi.org/10.1002/hep.26732

Ji, C., Mehrian-Shai, R., Chan, C., Hsu, Y.-H., & Kaplowitz, N. (2005). Role of CHOP in hepatic apoptosis in the murine model of intragastric ethanol feeding. Alcoholism, Clinical and Experimental Research, 29(8), 1496–1503. https://doi.org/10.1097/01.alc.0000174691.03751.11

Johnson, R. E., & Campbell, R. J. (1982). Wilson's disease. Electron microscopic, x-ray energy spectroscopic, and atomic absorption spectroscopic studies of corneal copper deposition and distribution. Laboratory Investigation; a Journal of Technical Methods and Pathology, 46(6), 564–569.

Johnston, M. P., Patel, J., & Byrne, C. D. (2020). Causes of Mortality in Non-Alcoholic Fatty Liver Disease (NAFLD) and Alcohol Related Fatty Liver Disease (AFLD). Current Pharmaceutical Design, 26(10), 1079–1092. https://doi.org/10.2174/1381612826666200128094231

Jokelainen, K., Reinke, L. A., & Nanji, A. A. (2001). Nf-kappab activation is associated with free radical generation and endotoxemia and precedes pathological liver injury in experimental alcoholic liver disease. Cytokine, 16(1), 36–39. https://doi.org/10.1006/cyto.2001.0930

Jonas, L., Fulda, G., Kyank, U., Steiner, M., Sarich, W., & Nizze, H. (2002). Hereditary hemochromatosis of a young girl: Detection of early iron deposition in liver cell lysosomes

using transmission electron microscopy and electron energy loss spectroscopy. Ultrastructural Pathology, 26(1), 23–26. https://doi.org/10.1080/01913120252934297

Kang, L., Chen, X., Sebastian, B. M., Pratt, B. T., Bederman, I. R., Alexander, J. C., Previs, S. F., & Nagy, L. E. (2007). Chronic ethanol and triglyceride turnover in white adipose tissue in rats: Inhibition of the anti-lipolytic action of insulin after chronic ethanol contributes to increased triglyceride degradation. The Journal of Biological Chemistry, 282(39), 28465–28473. https://doi.org/10.1074/jbc.M705503200

Kato, M., Higuchi, N., & Enjoji, M. (2008). Reduced hepatic expression of adipose tissue triglyceride lipase and CGI-58 may contribute to the development of non-alcoholic fatty liver disease in patients with insulin resistance. Scandinavian Journal of Gastroenterology, 43(8), 1018–1019. https://doi.org/10.1080/00365520802008140

Kaushik, S., & Cuervo, A. M. (2015). Degradation of lipid droplet-associated proteins by chaperone-mediated autophagy facilitates lipolysis. Nature Cell Biology, 17(6), 759–770. https://doi.org/10.1038/ncb3166

Kawaratani, H., Tsujimoto, T., Douhara, A., Takaya, H., Moriya, K., Namisaki, T., Noguchi, R., Yoshiji, H., Fujimoto, M., & Fukui, H. (2013). The Effect of Inflammatory Cytokines in Alcoholic Liver Disease. Mediators of Inflammation, 2013, 1–10. https://doi.org/10.1155/2013/495156

Khambu, B., Wang, L., Zhang, H., & Yin, X.-M. (2017). The Activation and Function of Autophagy in Alcoholic Liver Disease. Current Molecular Pharmacology, 10(3), 165–171. https://doi.org/10.2174/1874467208666150817112654

Kharbanda, K. K., McVicker, D. L., Zetterman, R. K., & Donohue, T. M. (1995). Ethanol consumption reduces the proteolytic capacity and protease activities of hepatic lysosomes. Biochimica Et Biophysica Acta, 1245(3), 421–429. https://doi.org/10.1016/0304-4165(95)00121-2

Kharbanda, K. K., McVicker, D. L., Zetterman, R. K., & Donohue, T. M. (1996). Ethanol consumption alters trafficking of lysosomal enzymes and affects the processing of procathepsin L in rat liver. Biochimica Et Biophysica Acta, 1291(1), 45–52. https://doi.org/10.1016/0304-4165(96)00043-8

Kitamura, H., Kanehira, K., Okita, K., Morimatsu, M., & Saito, M. (2000). MAIL, a novel nuclear IκB protein that potentiates LPS-induced IL-6 production. FEBS Letters, 485(1), 53–56. https://doi.org/10.1016/S0014-5793(00)02185-2

Knook, D. L., & Sleyster, E. C. (1980). Isolated parenchymal, Kupffer and endothelial rat liver cells characterized by their lysosomal enzyme content. Biochemical and Biophysical Research Communications, 96(1), 250–257. https://doi.org/10.1016/0006-291x(80)91207-3

Kobayashi, K., Inoguchi, T., Maeda, Y., Nakashima, N., Kuwano, A., Eto, E., Ueno, N., Sasaki, S., Sawada, F., Fujii, M., Matoba, Y., Sumiyoshi, S., Kawate, H., & Takayanagi, R. (2008). The lack of the C-terminal domain of adipose triglyceride lipase causes neutral lipid storage disease through impaired interactions with lipid droplets. The Journal of Clinical Endocrinology and Metabolism, 93(7), 2877–2884. https://doi.org/10.1210/jc.2007-2247

Komolkriengkrai, M., Nopparat, J., Vongvatcharanon, U., Anupunpisit, V., & Khimmaktong, W. (2019). Effect of glabridin on collagen deposition in liver and amelioration of hepatocyte destruction in diabetes rats. Experimental and Therapeutic Medicine. https://doi.org/10.3892/etm.2019.7664

Krähenbühl, L., Lang, C., Lüdes, S., Seiler, C., Schäfer, M., Zimmermann, A., & Krähenbühl, S. (2003). Reduced hepatic glycogen stores in patients with liver cirrhosis. Liver International: Official Journal of the International Association for the Study of the Liver, 23(2), 101–109. https://doi.org/10.1034/j.1600-0676.2003.00805.x

Kralisch, S., Klein, J., Lossner, U., Bluher, M., Paschke, R., Stumvoll, M., & Fasshauer, M. (2005). Isoproterenol, TNFα, and insulin downregulate adipose triglyceride lipase in 3T3-L1 adipocytes. Molecular and Cellular Endocrinology, 240(1–2), 43–49. https://doi.org/10.1016/j.mce.2005.06.002

Lackner, C., & Tiniakos, D. (2019). Fibrosis and alcohol-related liver disease. Journal of Hepatology, 70(2), 294–304. https://doi.org/10.1016/j.jhep.2018.12.003

Lake, A. C., Sun, Y., Li, J.-L., Johnson, J. W., Li, D., Revett, T., Shih, H. H., Liu, W., Paulsen, J. E., & Gimeno, R. E. (2005). Expression, regulation, and triglyceride hydrolase activity of Adiponutrin family members. Journal of Lipid Research, 46(11), 2477–2487. https://doi.org/10.1194/jlr.M500290-JLR200

Lammers, B., Chandak, P. G., Aflaki, E., Van Puijvelde, G. H. M., Radovic, B., Hildebrand, R. B., Meurs, I., Out, R., Kuiper, J., Van Berkel, T. J. C., Kolb, D., Haemmerle, G., Zechner, R., Levak-Frank, S., Van Eck, M., & Kratky, D. (2011). Macrophage Adipose Triglyceride Lipase Deficiency Attenuates Atherosclerotic Lesion Development in Low-Density Lipoprotein Receptor Knockout Mice. Arteriosclerosis, Thrombosis, and Vascular Biology, 31(1), 67–73. https://doi.org/10.1161/ATVBAHA.110.215814

Lane, B. P., & Lieber, C. S. (1966). Ultrastructural alterations in human hepatocytes following ingestion of ethanol with adequate diets. The American Journal of Pathology, 49(4), 593–603.

Lass, A., Zimmermann, R., Haemmerle, G., Riederer, M., Schoiswohl, G., Schweiger, M., Kienesberger, P., Strauss, J. G., Gorkiewicz, G., & Zechner, R. (2006). Adipose triglyceride lipase-mediated lipolysis of cellular fat stores is activated by CGI-58 and defective in Chanarin-Dorfman Syndrome. Cell Metabolism, 3(5), 309–319. https://doi.org/10.1016/j.cmet.2006.03.005

Leamy, A. K., Hasenour, C. M., Egnatchik, R. A., Trenary, I. A., Yao, C.-H., Patti, G. J., Shiota, M., & Young, J. D. (2016). Knockdown of triglyceride synthesis does not enhance palmitate lipotoxicity or prevent oleate-mediated rescue in rat hepatocytes. Biochimica Et Biophysica Acta, 1861(9 Pt A), 1005–1014. https://doi.org/10.1016/j.bbalip.2016.05.013

Li, T., Guo, W., & Zhou, Z. (2021). Adipose Triglyceride Lipase in Hepatic Physiology and Pathophysiology. Biomolecules, 12(1), 57. https://doi.org/10.3390/biom12010057

Li, X., Klintman, D., Liu, Q., Sato, T., Jeppsson, B., & Thorlacius, H. (2004). Critical role of CXC chemokines in endotoxemic liver injury in mice. Journal of Leukocyte Biology, 75(3), 443–452. https://doi.org/10.1189/jlb.0603297

Listenberger, L. L., Han, X., Lewis, S. E., Cases, S., Farese, R. V., Ory, D. S., & Schaffer, J. E. (2003). Triglyceride accumulation protects against fatty acid-induced lipotoxicity. Proceedings of the National Academy of Sciences, 100(6), 3077–3082. https://doi.org/10.1073/pnas.0630588100

Listenberger, L. L., Ory, D. S., & Schaffer, J. E. (2001). Palmitate-induced apoptosis can occur through a ceramide-independent pathway. The Journal of Biological Chemistry, 276(18), 14890–14895. https://doi.org/10.1074/jbc.M010286200

Listwak, S. J., Rathore, P., & Herkenham, M. (2013). Minimal NF-κB activity in neurons. Neuroscience, 250, 282–299. https://doi.org/10.1016/j.neuroscience.2013.07.013

Liu, X., & Green, R. M. (2019). Endoplasmic reticulum stress and liver diseases. Liver Research, 3(1), 55–64. https://doi.org/10.1016/j.livres.2019.01.002

Livak, K. J., & Schmittgen, T. D. (2001). Analysis of relative gene expression data using real-time quantitative PCR and the 2(-Delta Delta C(T)) Method. Methods (San Diego, Calif.), 25(4), 402–408. https://doi.org/10.1006/meth.2001.1262

Lu, X., Yang, X., & Liu, J. (2010). Differential control of ATGL-mediated lipid droplet degradation by CGI-58 and G0S2. Cell Cycle (Georgetown, Tex.), 9(14), 2719–2725. https://doi.org/10.4161/cc.9.14.12181

Luedde, T., Kaplowitz, N., & Schwabe, R. F. (2014). Cell Death and Cell Death Responses in Liver Disease: Mechanisms and Clinical Relevance. Gastroenterology, 147(4), 765-783.e4. https://doi.org/10.1053/j.gastro.2014.07.018

Maedler, K., Spinas, G. A., Dyntar, D., Moritz, W., Kaiser, N., & Donath, M. Y. (2001). Distinct effects of saturated and monounsaturated fatty acids on beta-cell turnover and function. Diabetes, 50(1), 69–76. https://doi.org/10.2337/diabetes.50.1.69

Mahdessian, H., Taxiarchis, A., Popov, S., Silveira, A., Franco-Cereceda, A., Hamsten, A., Eriksson, P., & van't Hooft, F. (2014). TM6SF2 is a regulator of liver fat metabolism influencing triglyceride secretion and hepatic lipid droplet content. Proceedings of the National Academy of Sciences of the United States of America, 111(24), 8913–8918. https://doi.org/10.1073/pnas.1323785111

Malhi, H., Bronk, S. F., Werneburg, N. W., & Gores, G. J. (2006). Free fatty acids induce JNK-dependent hepatocyte lipoapoptosis. The Journal of Biological Chemistry, 281(17), 12093–12101. https://doi.org/10.1074/jbc.M510660200

Malhi, H., & Gores, G. J. (2008). Molecular mechanisms of lipotoxicity in nonalcoholic fatty liver disease. Seminars in Liver Disease, 28(4), 360–369. https://doi.org/10.1055/s-0028-1091980

Mallela, S. K., Patel, D. M., Ducasa, G. M., Merscher, S., Fornoni, A., & Al-Ali, H. (2019). Detection and Quantification of Lipid Droplets in Differentiated Human Podocytes. In S. K. Bhattacharya (Ed.), Metabolomics (Vol. 1996, pp. 199–206). Springer New York. https://doi.org/10.1007/978-1-4939-9488-5_17

Mandrekar, P., & Szabo, G. (2009). Signalling pathways in alcohol-induced liver inflammation. Journal of Hepatology, 50(6), 1258–1266. https://doi.org/10.1016/j.jhep.2009.03.007

Mashek, D. G. (2021). Hepatic lipid droplets: A balancing act between energy storage and metabolic dysfunction in NAFLD. Molecular Metabolism, 50, 101115. https://doi.org/10.1016/j.molmet.2020.101115

Mashek, D. G., Li, L. O., & Coleman, R. A. (2007). Long-chain acyl-CoA synthetases and fatty acid channeling. Future Lipidology, 2(4), 465–476. https://doi.org/10.2217/17460875.2.4.465

Mathurin, P., Deng, Q. G., Keshavarzian, A., Choudhary, S., Holmes, E. W., & Tsukamoto, H. (2000). Exacerbation of alcoholic liver injury by enteral endotoxin in rats. Hepatology (Baltimore, Md.), 32(5), 1008–1017. https://doi.org/10.1053/jhep.2000.19621

Mavrelis, P. G., Ammon, H. V., Gleysteen, J. J., Komorowski, R. A., & Charaf, U. K. (1983). Hepatic free fatty acids in alcoholic liver disease and morbid obesity. Hepatology (Baltimore, Md.), 3(2), 226–231. https://doi.org/10.1002/hep.1840030215

Mayer, N., Schweiger, M., Romauch, M., Grabner, G. F., Eichmann, T. O., Fuchs, E., Ivkovic, J., Heier, C., Mrak, I., Lass, A., Höfler, G., Fledelius, C., Zechner, R., Zimmermann, R., & Breinbauer, R. (2013). Development of small-molecule inhibitors targeting adipose triglyceride lipase. Nature Chemical Biology, 9(12), 785–787. https://doi.org/10.1038/nchembio.1359

McClain, C., Barve, S., Deaciuc, I., Kugelmas, M., & Hill, D. (1999). Cytokines in Alcoholic Liver Disease. Seminars in Liver Disease, 19(02), 205–219. https://doi.org/10.1055/s-2007-1007110

Meadows, V., Baiocchi, L., Kundu, D., Sato, K., Fuentes, Y., Wu, C., Chakraborty, S., Glaser, S., Alpini, G., Kennedy, L., & Francis, H. (2021). Biliary Epithelial Senescence in Liver

Disease: There Will Be SASP. Frontiers in Molecular Biosciences, 8, 803098. https://doi.org/10.3389/fmolb.2021.803098

Mellinger, J. L., Shedden, K., Winder, G. S., Tapper, E., Adams, M., Fontana, R. J., Volk, M. L., Blow, F. C., & Lok, A. S. F. (2018). The high burden of alcoholic cirrhosis in privately insured persons in the United States. Hepatology (Baltimore, Md.), 68(3), 872–882. https://doi.org/10.1002/hep.29887

Mello, T., Ceni, E., Surrenti, C., & Galli, A. (2008). Alcohol induced hepatic fibrosis: Role of acetaldehyde. Molecular Aspects of Medicine, 29(1–2), 17–21. https://doi.org/10.1016/j.mam.2007.10.001

Mello, T., Nakatsuka, A., Fears, S., Davis, W., Tsukamoto, H., Bosron, W. F., & Sanghani, S. P. (2008). Expression of carboxylesterase and lipase genes in rat liver cell-types. Biochemical and Biophysical Research Communications, 374(3), 460–464. https://doi.org/10.1016/j.bbrc.2008.07.024

Messingham, K. A. N., Faunce, D. E., & Kovacs, E. J. (2002). Alcohol, injury, and cellular immunity. Alcohol (Fayetteville, N.Y.), 28(3), 137–149. https://doi.org/10.1016/s0741-8329(02)00278-1

Missaglia, S., Coleman, R. A., Mordente, A., & Tavian, D. (2019). Neutral Lipid Storage Diseases as Cellular Model to Study Lipid Droplet Function. Cells, 8(2). https://doi.org/10.3390/cells8020187

Mittendorfer, B., Yoshino, M., Patterson, B. W., & Klein, S. (2016). VLDL Triglyceride Kinetics in Lean, Overweight, and Obese Men and Women. The Journal of Clinical Endocrinology & Metabolism, 101(11), 4151–4160. https://doi.org/10.1210/jc.2016-1500

Miyata, T., & Nagy, L. E. (2020). Programmed cell death in alcohol-associated liver disease. Clinical and Molecular Hepatology, 26(4), 618–625. https://doi.org/10.3350/cmh.2020.0142

Moon, A. M., Yang, J. Y., Barritt, A. S., Bataller, R., & Peery, A. F. (2020). Rising Mortality From Alcohol-Associated Liver Disease in the United States in the 21st Century. The American Journal of Gastroenterology, 115(1), 79–87. https://doi.org/10.14309/ajg.0000000000000442

Müller, A., Hennig, A., Lorscheid, S., Grondona, P., Schulze-Osthoff, K., Hailfinger, S., & Kramer, D. (2018). IκBζ is a key transcriptional regulator of IL-36–driven psoriasis-related gene expression in keratinocytes. Proceedings of the National Academy of Sciences, 115(40), 10088–10093. https://doi.org/10.1073/pnas.1801377115

Muriel, P. (Ed.). (n.d.). Structure and ultrastructure of the normal and diseased liver. In Liver Pathophysiology (1st ed., Vol. 1–2, pp. 23–44).

Musso, G., Cassader, M., Paschetta, E., & Gambino, R. (2018). Bioactive Lipid Species and Metabolic Pathways in Progression and Resolution of Nonalcoholic Steatohepatitis. Gastroenterology, 155(2), 282-302.e8. https://doi.org/10.1053/j.gastro.2018.06.031

Nafady, A., Ahmed, O., & Ghafeer, H. (2017). Scanning and transmission electron microscopy of the cells forming the hepatic sinusoidal wall of rat in acetaminophen and Escherichia coli endotoxin-induced hepatotoxicity. Journal of Microscopy and Ultrastructure, 5(1), 21. https://doi.org/10.1016/j.jmau.2016.04.003

Nagappan, A., Kim, J.-H., Jung, D. Y., & Jung, M. H. (2019). Cryptotanshinone from the Salvia miltiorrhiza Bunge Attenuates Ethanol-Induced Liver Injury by Activation of AMPK/SIRT1 and Nrf2 Signaling Pathways. International Journal of Molecular Sciences, 21(1), 265. https://doi.org/10.3390/ijms21010265

Nakano, M., Worner, T. M., & Lieber, C. S. (1982). Perivenular fibrosis in alcoholic liver injury: Ultrastructure and histologic progression. Gastroenterology, 83(4), 777–785.

Nanji, A. A. (1998). Apoptosis and alcoholic liver disease. Seminars in Liver Disease, 18(2), 187–190. https://doi.org/10.1055/s-2007-1007154

Nanji, A. A., & Hiller-Sturmhöfel, S. (1997). Apoptosis and necrosis: Two types of cell death in alcoholic liver disease. Alcohol Health and Research World, 21(4), 325–330.

Nanji, A. A., Jokelainen, K., Fotouhinia, M., Rahemtulla, A., Thomas, P., Tipoe, G. L., Su, G. L., & Dannenberg, A. J. (2001). Increased severity of alcoholic liver injury in female rats: Role of oxidative stress, endotoxin, and chemokines. American Journal of Physiology. Gastrointestinal and Liver Physiology, 281(6), G1348-1356. https://doi.org/10.1152/ajpgi.2001.281.6.G1348

Nanji, A. A., Jokelainen, K., Tipoe, G. L., Rahemtulla, A., & Dannenberg, A. J. (2001). Dietary saturated fatty acids reverse inflammatory and fibrotic changes in rat liver despite continued ethanol administration. The Journal of Pharmacology and Experimental Therapeutics, 299(2), 638–644.

Nanji, A. A., Mendenhall, C. L., & French, S. W. (1989). Beef fat prevents alcoholic liver disease in the rat. Alcoholism, Clinical and Experimental Research, 13(1), 15–19. https://doi.org/10.1111/j.1530-0277.1989.tb00276.x

Nanji, A. A., Zakim, D., Rahemtulla, A., Daly, T., Miao, L., Zhao, S., Khwaja, S., Tahan, S. R., & Dannenberg, A. J. (1997). Dietary saturated fatty acids down-regulate cyclooxygenase-2 and tumor necrosis factor alfa and reverse fibrosis in alcohol-induced liver disease in the rat. Hepatology (Baltimore, Md.), 26(6), 1538–1545. https://doi.org/10.1002/hep.510260622

Nelson, S., & Kolls, J. K. (2002). Alcohol, host defence and society. Nature Reviews. Immunology, 2(3), 205–209. https://doi.org/10.1038/nri744

Newberry, E. P., Xie, Y., Kennedy, S. M., Graham, M. J., Crooke, R. M., Jiang, H., Chen, A., Ory, D. S., & Davidson, N. O. (2017). Prevention of hepatic fibrosis with liver microsomal triglyceride transfer protein deletion in liver fatty acid binding protein null mice. Hepatology (Baltimore, Md.), 65(3), 836–852. https://doi.org/10.1002/hep.28941

Nguyen, T. B., & Olzmann, J. A. (2017). Lipid droplets and lipotoxicity during autophagy. Autophagy, 13(11), 2002–2003. https://doi.org/10.1080/15548627.2017.1359451

Niyogi, S., Ghosh, M., Adak, M., & Chakrabarti, P. (2019). PEDF promotes nuclear degradation of ATGL through COP1. Biochemical and Biophysical Research Communications, 512(4), 806–811. https://doi.org/10.1016/j.bbrc.2019.03.111

Olzmann, J. A., & Carvalho, P. (2019). Dynamics and functions of lipid droplets. Nature Reviews Molecular Cell Biology, 20(3), 137–155. https://doi.org/10.1038/s41580-018-0085-z

Ong, K. T., Mashek, M. T., Bu, S. Y., Greenberg, A. S., & Mashek, D. G. (2011). Adipose triglyceride lipase is a major hepatic lipase that regulates triacylglycerol turnover and fatty acid signaling and partitioning. Hepatology (Baltimore, Md.), 53(1), 116–126. https://doi.org/10.1002/hep.24006

Osna, N. A., Donohue, T. M., & Kharbanda, K. K. (2017). Alcoholic Liver Disease: Pathogenesis and Current Management. Alcohol Research: Current Reviews, 38(2), 147–161.

Parlesak, A., Schäfer, C., Schütz, T., Bode, J. C., & Bode, C. (2000). Increased intestinal permeability to macromolecules and endotoxemia in patients with chronic alcohol abuse in different stages of alcohol-induced liver disease. Journal of Hepatology, 32(5), 742–747. https://doi.org/10.1016/s0168-8278(00)80242-1

Pawlak, M., Lefebvre, P., & Staels, B. (2015). Molecular mechanism of PPARα action and its impact on lipid metabolism, inflammation and fibrosis in non-alcoholic fatty liver disease. Journal of Hepatology, 62(3), 720–733. https://doi.org/10.1016/j.jhep.2014.10.039

Pearce, S. G., Thosani, N. C., & Pan, J.-J. (2013). Noninvasive biomarkers for the diagnosis of steatohepatitis and advanced fibrosis in NAFLD. Biomarker Research, 1(1), 7. https://doi.org/10.1186/2050-7771-1-7

Pegoraro, V., Missaglia, S., Marozzo, R., Tavian, D., & Angelini, C. (2020). MiRNAs as biomarkers of phenotype in neutral lipid storage disease with myopathy. Muscle & Nerve, 61(2), 253–257. https://doi.org/10.1002/mus.26761

Porta, E. A., Koch, O. R., & Hartroft, W. S. (1970). Recent advances in molecular pathology: A review of the effects of alcohol on the liver. Experimental and Molecular Pathology, 12(1), 104–132. https://doi.org/10.1016/0014-4800(70)90078-x

Poulsen, K. L., Fan, X. D., Kibler, C. D., Huang, E., Wu, X., McMullen, M. R., Leng, L., Bucala, R., Ventura-Cots, M., Argemi, J., Bataller, R., & Nagy, L. E. (2021). Role of MIF in coordinated expression of hepatic chemokines in patients with alcohol-associated hepatitis. JCI Insight. https://doi.org/10.1172/jci.insight.141420

Rada, P., González-Rodríguez, Á., García-Monzón, C., & Valverde, Á. M. (2020). Understanding lipotoxicity in NAFLD pathogenesis: Is CD36 a key driver? Cell Death & Disease, 11(9), 802. https://doi.org/10.1038/s41419-020-03003-w

Rao, R. (2009). Endotoxemia and gut barrier dysfunction in alcoholic liver disease. Hepatology (Baltimore, Md.), 50(2), 638–644. https://doi.org/10.1002/hep.23009

Rappaport, A. M. (1973). The microcirculatory hepatic unit. Microvascular Research, 6(2), 212–228. https://doi.org/10.1016/0026-2862(73)90021-6

Rashid, M., & Coombs, K. M. (2019). Serum-reduced media impacts on cell viability and protein expression in human lung epithelial cells. Journal of Cellular Physiology, 234(6), 7718–7724. https://doi.org/10.1002/jcp.27890

Reid, B. N., Ables, G. P., Otlivanchik, O. A., Schoiswohl, G., Zechner, R., Blaner, W. S., Goldberg, I. J., Schwabe, R. F., Chua, S. C., & Huang, L.-S. (2008). Hepatic overexpression of hormone-sensitive lipase and adipose triglyceride lipase promotes fatty acid oxidation, stimulates direct release of free fatty acids, and ameliorates steatosis. The Journal of Biological Chemistry, 283(19), 13087–13099. https://doi.org/10.1074/jbc.M800533200

Rhodin, J. (n.d.). Correlation of ultrastructural organization: And function in normal and experimentally changed proximal convoluted tubule cells of the mouse kidney: An electron microscopic study. [PhD diss.].

Rocco, A. (2014). Alcoholic disease: Liver and beyond. World Journal of Gastroenterology, 20(40), 14652. https://doi.org/10.3748/wjg.v20.i40.14652

Ronis, M. J. J., Korourian, S., Zipperman, M., Hakkak, R., & Badger, T. M. (2004). Dietary saturated fat reduces alcoholic hepatotoxicity in rats by altering fatty acid metabolism and membrane composition. The Journal of Nutrition, 134(4), 904–912. https://doi.org/10.1093/jn/134.4.904

Rustaeus, S., Lindberg, K., Stillemark, P., Claesson, C., Asp, L., Larsson, T., Borén, J., & Olofsson, S. O. (1999). Assembly of very low density lipoprotein: A two-step process of apolipoprotein B core lipidation. The Journal of Nutrition, 129(2S Suppl), 463S-466S. https://doi.org/10.1093/jn/129.2.463S

Saiman, Y., & Friedman, S. L. (2012). The Role of Chemokines in Acute Liver Injury. Frontiers in Physiology, 3. https://doi.org/10.3389/fphys.2012.00213

Sasse, D., Spornitz, U. M., & Maly, I. P. (1992). Liver architecture. Enzyme, 46(1–3), 8–32. https://doi.org/10.1159/000468776

Sawant, K. V., Poluri, K. M., Dutta, A. K., Sepuru, K. M., Troshkina, A., Garofalo, R. P., & Rajarathnam, K. (2016). Chemokine CXCL1 mediated neutrophil recruitment: Role of glycosaminoglycan interactions. Scientific Reports, 6(1), 33123. https://doi.org/10.1038/srep33123

Schäfer, C., Parlesak, A., Schütt, C., Bode, J. C., & Bode, C. (2002). Concentrations of lipopolysaccharide-binding protein, bactericidal/permeability-increasing protein, soluble CD14 and plasma lipids in relation to endotoxaemia in patients with alcoholic liver disease. Alcohol and Alcoholism (Oxford, Oxfordshire), 37(1), 81–86. https://doi.org/10.1093/alcalc/37.1.81

Schulze, R. J., & Ding, W.-X. (2019). Lipid droplet dynamics in alcoholic fatty liver disease. Liver Research, 3(3–4), 185–190. https://doi.org/10.1016/j.livres.2019.09.002

Schulze, R. J., Schott, M. B., Casey, C. A., Tuma, P. L., & McNiven, M. A. (2019). The cell biology of the hepatocyte: A membrane trafficking machine. The Journal of Cell Biology, 218(7), 2096–2112. https://doi.org/10.1083/jcb.201903090

Schumacher, C., Clark-Lewis, I., Baggiolini, M., & Moser, B. (1992). High- and low-affinity binding of GRO alpha and neutrophil-activating peptide 2 to interleukin 8 receptors on human neutrophils. Proceedings of the National Academy of Sciences of the United States of America, 89(21), 10542–10546. https://doi.org/10.1073/pnas.89.21.10542

Schweiger, M., Paar, M., Eder, C., Brandis, J., Moser, E., Gorkiewicz, G., Grond, S., Radner, F. P. W., Cerk, I., Cornaciu, I., Oberer, M., Kersten, S., Zechner, R., Zimmermann, R., & Lass, A. (2012). G0/G1 switch gene-2 regulates human adipocyte lipolysis by affecting activity and localization of adipose triglyceride lipase. Journal of Lipid Research, 53(11), 2307–2317. https://doi.org/10.1194/jlr.M027409

Schweiger, M., Romauch, M., Schreiber, R., Grabner, G. F., Hütter, S., Kotzbeck, P., Benedikt, P., Eichmann, T. O., Yamada, S., Knittelfelder, O., Diwoky, C., Doler, C., Mayer, N., De Cecco, W., Breinbauer, R., Zimmermann, R., & Zechner, R. (2017). Pharmacological inhibition of adipose triglyceride lipase corrects high-fat diet-induced insulin resistance and hepatosteatosis in mice. Nature Communications, 8, 14859. https://doi.org/10.1038/ncomms14859

Schweiger, M., Schoiswohl, G., Lass, A., Radner, F. P. W., Haemmerle, G., Malli, R., Graier, W., Cornaciu, I., Oberer, M., Salvayre, R., Fischer, J., Zechner, R., & Zimmermann, R. (2008). The C-terminal region of human adipose triglyceride lipase affects enzyme activity and lipid droplet binding. The Journal of Biological Chemistry, 283(25), 17211–17220. https://doi.org/10.1074/jbc.M710566200

Schweiger, M., & Zechner, R. (2015). Breaking the Barrier—Chaperone-Mediated Autophagy of Perilipins Regulates the Lipolytic Degradation of Fat. Cell Metabolism, 22(1), 60–61. https://doi.org/10.1016/j.cmet.2015.06.017

Sobaniec-Lotowska, M. E. (2006). Ultrastructure of Kupffer cells and hepatocytes in the Dubin-Johnson syndrome: A case report. World Journal of Gastroenterology, 12(6), 987. https://doi.org/10.3748/wjg.v12.i6.987

Steiner, J., & Lang, C. (2017). Alcohol, Adipose Tissue and Lipid Dysregulation. Biomolecules, 7(4), 16. https://doi.org/10.3390/biom7010016

Stickel, F., Datz, C., Hampe, J., & Bataller, R. (2017). Pathophysiology and Management of Alcoholic Liver Disease: Update 2016. Gut and Liver, 11(2), 173–188. https://doi.org/10.5009/gnl16477

Sun, Q., Zhong, W., Zhang, W., & Zhou, Z. (2016). Defect of mitochondrial respiratory chain is a mechanism of ROS overproduction in a rat model of alcoholic liver disease: Role of zinc deficiency. American Journal of Physiology. Gastrointestinal and Liver Physiology, 310(3), G205-214. https://doi.org/10.1152/ajpgi.00270.2015

Szabo, G., & Bala, S. (2010). Alcoholic liver disease and the gut-liver axis. World Journal of Gastroenterology, 16(11), 1321–1329. https://doi.org/10.3748/wjg.v16.i11.1321

Tavian, D., Missaglia, S., Redaelli, C., Pennisi, E. M., Invernici, G., Wessalowski, R., Maiwald, R., Arca, M., & Coleman, R. A. (2012). Contribution of novel ATGL missense mutations to the clinical phenotype of NLSD-M: A strikingly low amount of lipase activity may preserve cardiac function. Human Molecular Genetics, 21(24), 5318–5328. https://doi.org/10.1093/hmg/dds388

Thompson, K. J., McKillop, I. H., & Schrum, L. W. (2011). Targeting collagen expression in alcoholic liver disease. World Journal of Gastroenterology, 17(20), 2473–2481. https://doi.org/10.3748/wjg.v17.i20.2473

Tiwari, S., & Siddiqi, S. A. (2012). Intracellular trafficking and secretion of VLDL. Arteriosclerosis, Thrombosis, and Vascular Biology, 32(5), 1079–1086. https://doi.org/10.1161/ATVBAHA.111.241471

Torruellas, C. (2014). Diagnosis of alcoholic liver disease. World Journal of Gastroenterology, 20(33), 11684. https://doi.org/10.3748/wjg.v20.i33.11684

Totzke, G., Essmann, F., Pohlmann, S., Lindenblatt, C., Jänicke, R. U., & Schulze-Osthoff, K. (2006). A novel member of the IkappaB family, human IkappaB-zeta, inhibits transactivation of p65 and its DNA binding. The Journal of Biological Chemistry, 281(18), 12645–12654. https://doi.org/10.1074/jbc.M511956200

Tsukamoto, H., Machida, K., Dynnyk, A., & Mkrtchyan, H. (2009). “Second hit” models of alcoholic liver disease. Seminars in Liver Disease, 29(2), 178–187. https://doi.org/10.1055/s-0029-1214373

Turpin, S. M., Hoy, A. J., Brown, R. D., Rudaz, C. G., Honeyman, J., Matzaris, M., & Watt, M. J. (2011). Adipose triacylglycerol lipase is a major regulator of hepatic lipid metabolism but not insulin sensitivity in mice. Diabetologia, 54(1), 146–156. https://doi.org/10.1007/s00125-010-1895-5

Villena, J. A., Roy, S., Sarkadi-Nagy, E., Kim, K.-H., & Sul, H. S. (2004). Desnutrin, an adipocyte gene encoding a novel patatin domain-containing protein, is induced by fasting and glucocorticoids: Ectopic expression of desnutrin increases triglyceride hydrolysis. The Journal of Biological Chemistry, 279(45), 47066–47075. https://doi.org/10.1074/jbc.M403855200

Wang, D., Wei, Y., & Pagliassotti, M. J. (2006). Saturated fatty acids promote endoplasmic reticulum stress and liver injury in rats with hepatic steatosis. Endocrinology, 147(2), 943–951. https://doi.org/10.1210/en.2005-0570

Wei, X., Shi, X., Zhong, W., Zhao, Y., Tang, Y., Sun, W., Yin, X., Bogdanov, B., Kim, S., McClain, C., Zhou, Z., & Zhang, X. (2013). Chronic Alcohol Exposure Disturbs Lipid

Homeostasis at the Adipose Tissue-Liver Axis in Mice: Analysis of Triacylglycerols Using High-Resolution Mass Spectrometry in Combination with In Vivo Metabolite Deuterium Labeling. PLoS ONE, 8(2), e55382. https://doi.org/10.1371/journal.pone.0055382

Wei, Y., Wang, D., Topczewski, F., & Pagliassotti, M. J. (2006). Saturated fatty acids induce endoplasmic reticulum stress and apoptosis independently of ceramide in liver cells. American Journal of Physiology. Endocrinology and Metabolism, 291(2), E275-281. https://doi.org/10.1152/ajpendo.00644.2005

Weibel, E. R., Stäubli, W., Gnägi, H. R., & Hess, F. A. (1969). Correlated morphometric and biochemical studies on the liver cell. I. Morphometric model, stereologic methods, and normal morphometric data for rat liver. The Journal of Cell Biology, 42(1), 68–91. https://doi.org/10.1083/jcb.42.1.68

Wieser, V., Tymoszuk, P., Adolph, T. E., Grander, C., Grabherr, F., Enrich, B., Pfister, A., Lichtmanegger, L., Gerner, R., Drach, M., Moser, P., Zoller, H., Weiss, G., Moschen, A. R., Theurl, I., & Tilg, H. (2016). Lipocalin 2 drives neutrophilic inflammation in alcoholic liver disease. Journal of Hepatology, 64(4), 872–880. https://doi.org/10.1016/j.jhep.2015.11.037

Wilfling, F., Thiam, A. R., Olarte, M.-J., Wang, J., Beck, R., Gould, T. J., Allgeyer, E. S., Pincet, F., Bewersdorf, J., Farese, R. V., & Walther, T. C. (2014). Arf1/COPI machinery acts directly on lipid droplets and enables their connection to the ER for protein targeting. ELife, 3, e01607. https://doi.org/10.7554/eLife.01607

Wisse, E., Braet, F., Shami, G. J., Zapotoczny, B., Vreuls, C., Verhaegh, P., Frederik, P., Peters, P. J., Olde Damink, S., & Koek, G. (2022). Fat causes necrosis and inflammation in parenchymal cells in human steatotic liver. Histochemistry and Cell Biology, 157(1), 27–38. https://doi.org/10.1007/s00418-021-02030-8

Wu, J. W., Wang, S. P., Alvarez, F., Casavant, S., Gauthier, N., Abed, L., Soni, K. G., Yang, G., & Mitchell, G. A. (2011). Deficiency of liver adipose triglyceride lipase in mice causes progressive hepatic steatosis. Hepatology (Baltimore, Md.), 54(1), 122–132. https://doi.org/10.1002/hep.24338

Xu, M.-J., Feng, D., Wu, H., Wang, H., Chan, Y., Kolls, J., Borregaard, N., Porse, B., Berger, T., Mak, T. W., Cowland, J. B., Kong, X., & Gao, B. (2015). Liver is the major source of elevated serum lipocalin-2 levels after bacterial infection or partial hepatectomy: A critical

role for IL-6/STAT3. Hepatology (Baltimore, Md.), 61(2), 692–702. https://doi.org/10.1002/hep.27447

Yamaguchi, K., Yang, L., McCall, S., Huang, J., Yu, X. X., Pandey, S. K., Bhanot, S., Monia, B. P., Li, Y.-X., & Diehl, A. M. (2007). Inhibiting triglyceride synthesis improves hepatic steatosis but exacerbates liver damage and fibrosis in obese mice with nonalcoholic steatohepatitis. Hepatology, 45(6), 1366–1374. https://doi.org/10.1002/hep.21655

Yamamoto, M., Yamazaki, S., Uematsu, S., Sato, S., Hemmi, H., Hoshino, K., Kaisho, T., Kuwata, H., Takeuchi, O., Takeshige, K., Saitoh, T., Yamaoka, S., Yamamoto, N., Yamamoto, S., Muta, T., Takeda, K., & Akira, S. (2004). Regulation of Toll/IL-1-receptor-mediated gene expression by the inducible nuclear protein IkappaBzeta. Nature, 430(6996), 218–222. https://doi.org/10.1038/nature02738

Yamazaki, S., Matsuo, S., Muta, T., Yamamoto, M., Akira, S., & Takeshige, K. (2008). Gene-specific Requirement of a Nuclear Protein, IκB-ζ, for Promoter Association of Inflammatory Transcription Regulators. Journal of Biological Chemistry, 283(47), 32404–32411. https://doi.org/10.1074/jbc.M802148200

Yamazaki, S., Muta, T., & Takeshige, K. (2001). A novel IkappaB protein, IkappaB-zeta, induced by proinflammatory stimuli, negatively regulates nuclear factor-kappaB in the nuclei. The Journal of Biological Chemistry, 276(29), 27657–27662. https://doi.org/10.1074/jbc.M103426200

Yang, H., Niemeijer, M., van de Water, B., & Beltman, J. B. (2020). ATF6 Is a Critical Determinant of CHOP Dynamics during the Unfolded Protein Response. IScience, 23(2), 100860. https://doi.org/10.1016/j.isci.2020.100860

Yang, P., Wang, Y., Tang, W., Sun, W., Ma, Y., Lin, S., Jing, J., Jiang, L., Shi, H., Song, Z., & Yu, L. (2020). Western diet induces severe nonalcoholic steatohepatitis, ductular reaction, and hepatic fibrosis in liver CGI-58 knockout mice. Scientific Reports, 10(1), 4701. https://doi.org/10.1038/s41598-020-61473-6

Yavuz, A., Ünverengil, G., Yıldırım, A. N. T., Maraşlı, H. Ş., & Tuncer, İ. (2020). Late-Onset Lipid Storage Myopathy with Fatal Hepatosteatosis. European Journal of Case Reports in Internal Medicine, 7(12), 001980. https://doi.org/10.12890/2020_001980

Yin, H., Hu, M., Zhang, R., Shen, Z., Flatow, L., & You, M. (2012). MicroRNA-217 Promotes Ethanol-induced Fat Accumulation in Hepatocytes by Down-regulating SIRT1. Journal of Biological Chemistry, 287(13), 9817–9826. https://doi.org/10.1074/jbc.M111.333534

Zhang, P., Wang, W., Mao, M., Gao, R., Shi, W., Li, D., Calderone, R., Sui, B., Tian, X., & Meng, X. (2021). Similarities and Differences: A Comparative Review of the Molecular Mechanisms and Effectors of NAFLD and AFLD. Frontiers in Physiology, 12, 710285. https://doi.org/10.3389/fphys.2021.710285

Zhang, Q., Ma, C., Duan, Y., Heinrich, B., Rosato, U., Diggs, L. P., Ma, L., Roy, S., Fu, Q., Brown, Z. J., Wabitsch, S., Thovarai, V., Fu, J., Feng, D., Ruf, B., Cui, L. L., Subramanyam, V., Frank, K. M., Wang, S., … Greten, T. F. (2021). Gut Microbiome Directs Hepatocytes to Recruit MDSCs and Promote Cholangiocarcinoma. Cancer Discovery, 11(5), 1248–1267. https://doi.org/10.1158/2159-8290.CD-20-0304

Zhong, W., Wei, X., Hao, L., Lin, T., Yue, R., Sun, X., Guo, W., Dong, H., Li, T., Ahmadi, A. R., Sun, Z., Zhang, Q., Zhao, J., & Zhou, Z. (2020). Paneth Cell Dysfunction Mediates Alcohol-related Steatohepatitis Through Promoting Bacterial Translocation in Mice: Role of Zinc Deficiency. Hepatology, hep.30945. https://doi.org/10.1002/hep.30945

Zhong, Z., Ramshesh, V. K., Rehman, H., Liu, Q., Theruvath, T. P., Krishnasamy, Y., & Lemasters, J. J. (2014). Acute ethanol causes hepatic mitochondrial depolarization in mice: Role of ethanol metabolism. PloS One, 9(3), e91308. https://doi.org/10.1371/journal.pone.0091308

Zhou, Z., Xu, M.-J., & Gao, B. (2016). Hepatocytes: A key cell type for innate immunity. Cellular & Molecular Immunology, 13(3), 301–315. https://doi.org/10.1038/cmi.2015.97

Zimmermann, R., Strauss, J. G., Haemmerle, G., Schoiswohl, G., Birner-Gruenberger, R., Riederer, M., Lass, A., Neuberger, G., Eisenhaber, F., Hermetter, A., & Zechner, R. (2004). Fat mobilization in adipose tissue is promoted by adipose triglyceride lipase. Science (New York, N.Y.), 306(5700), 1383–1386. https://doi.org/10.1126/science.1100747